UILU-ENG 83-3601

FCP Report No. 45

THE FATIGUE OF WELDMENTS SUBJECTED TO COMPLEX LOADINGS

by

N.-J. Ho
Department of Metallurgy and Mining

and

F. V. Lawrence, Jr.
Professor of Civil Engineering and Metallurgy

A Report of the

FRACTURE CONTROL PROGRAM

College of Engineering, University of Illinois
Urbana, Illinois 61801-2983

January 1983

THE FATIGUE OF WELDMENTS SUBJECTED TO COMPLEX LOADINGS

ABSTRACT

Cruciform and double-strap lap weldments were fatigue tested under constant amplitude axial load and SAE Bracket Spectrum load conditions. For the cruciform weldments, fatigue cracks generally initiate at the root but may initiate at the toe if higher bending stresses are induced by joint distortion. For double strap lap weldments, the stress ratio (R) and weld shape are the major factors influencing the fatigue crack initiation site.

The fatigue test results were compared with predictions made using an initiation-propagation model, and good agreement between experiment and theory was observed. The model for the predictions assumes that the fatigue crack initiation period, which is the number of cycles for the initiation of a fatigue crack and its early growth and coalescence into a dominant fatigue crack, is the main portion of the total fatigue life at long lives.

ACKNOWLEDGEMENTS

Grateful acknowledgements are made to the University of Illinois Fracture Control Program which is funded by a consortium of midwest industries for providing financial support, and to Mr. R. A. Testin of General Motors Electro-Motive Division, Mr. B. N. Babu of Caterpillar Tractor Co., and Mr. H. D. Berns of Deere and Co. for providing specimens and data. Thanks are also extended to Professor D. F. Socie of Mechanical Engineering during the experimental portion of this study.

Special acknowledgements are made to Mr. S. D. Downing for his designing and constructing the function generator and to Mr. Glen Lafenhagen for his assistance in the operation of electronic and hydraulic testing apparatus.

TABLE OF CONTENTS

LIST OF SYMBOLS

a, a_I, a_f, a_{th},	Crack length, initial crack length, final crack length and threshold crack length
a	Peterson's material constant
α	Geometry coefficient
b	Fatigue strength exponent
C	Crack growth rate material constant
C	Half length of lack-of-penetration
D_i, D_{block}	Damage per histeresis loop and damage per block
$\Delta\varepsilon$, Δe	Range of local strain and remote strain
I	Crack growth integral constant
K_f, K_{fmax}	Fatigue notch factor and maximum fatigue notch factor
K_t	Theoretical stress concentration factor
ΔK, ΔK_{th}, K_{max} K_C	Range of stress intensity, threshold stress intensity, maximum stress intensity and fracture toughness
ℓ_o	Intrinsic crack length
ℓ	Weld leg length
m	Crack growth rate constant
M_s, M_t, M_k	Magnification factor for free surface, width size and stress concentration
N_T, N_I, N_P	Total, initiation and propagation fatigue life
ϕ_o	Crack shape correction factor
r	Notch root radius
S, S_b, S_n, S_{max}, S_a	Remote stress, remote surface stress, maximum remote stress and amplitude of remote stress
S_u	Ultimate tensile strength

σ'_f	Fatigue strength
$\sigma_{o,i}$	Initial mean stress
σ_r	Residual stress
$\Delta\sigma$	Range of local stress
t	Plate thickness
x	Ratio of bending stress to axial stress

1. INTRODUCTION

1.1 The Fatigue Resistance of Weldments

Because weldments are less fatigue resistant than the members they join, the fatigue resistance of welded joints has been extensively studied. Fatigue failures of weldments rarely occur in base metal; in most cases, fatigue cracks initiate at external discontinuities (undercut, overfill and reinforcement) or at internal discontinuities (porosity, slag inclusions, lack of fusion (LOF) and lack of penetration (LOP)). These discontinuities are always located in region which have material poperties different from base metal and cause local stresses higher than the nominal stress in the base metal.

Fatigue data for weldments often exhibit a large amount of scatter which is caused by uncertainty as to the magnitude of actual stresses because of the residual stresses and the induced stresses resulting from the weld joint's eccentricity and angular distortion. These stresses are very significant but difficult to measure and predict.

In the past few years, the effect of variable amplitude loading on the fatigue behavior of welded structure has begun to receive attention because most structures in service are subjected to complex, variable loadings.

This study attempts to interrelate the influence of material properties, geometry, stress state, and load history on the fatigue life of welds and to develop further the analytical methods for predicting the fatigue resistance of welds.

1.2 Role of Discontinuities in Weldment Fatigue

Fatigue cracks generally initiate and propagate from discontinuties in weldments. Many investigators have tried to predict when and where this will occur. Harrison [1], Gurney [2], Maddox [3] and Frank [4] assumed that all internal discontinuities were crack-like defects or that there were preexisting cracks at external discontinuities after fabrication; therefore, the fatigue crack initiation life (N_I) was said to be negligibly short or nonexistent. Under this assumption, the total fatigue life (N_T) of welds was considered to be the fatigue crack propagation life (N_P) of welds which could be estimated using linear elastic fracture mechanics (LEFM) concepts.

However, the work of Lawrence and Munse [5], and Lawrence and Burk [6] suggested that the fatigue life of butt welds with LOP (a crack like defect) could not be explained solely by crack propagation and that the initiation life was found to comprise as much as half the total fatigue life. Also, studies by Lawrence [7], and Burk and Lawrence [8] on A36 butt welds showed that a significant portion of fatigue life was spent in initiating a 0.01-in. fatigue crack at the weld toe and that unrealistically small values of initial crack length would be required, espically in the long life region, to account for total fatigue life. In addition, Smith and Smith [9] in their recent work measured fatigue cracks in the fillet weld by pontential drop methods and found that at stress ratio R= .17 initiation life occupied as much as 39% of total fatigue life (1.5×10^6 cycles). Thus, it does not seem proper to consider all discontinuities to be crack-like defects because the initiation life may be appreciable;

and neglecting it may be excessively conservative. Moreover, it is doubtful that there is always a preexisting crack in a sound weld.

1.3 Role of Material Properties in Weldment Fatigue

The base metal of a weld is seldom involved in the fatigue crack initiation process. Most fatigue cracks will initiate either at internal discontinuities in tempered weld metal or at the weld toe in the grain coarsened heat affected zone (HAZ) (high wetting angles) or in untempered highly diluted weld metal (low wetting angles). Thus, from the viewpoint of initiation, the fatigue properties of the weld metal and HAZ are more relevant than those of the base metal and must be determined from tests on smooth specimens.

Test data on weld metal and HAZ materials are generally unavailable and difficult to obtain experimentally [10]. However, Langraf [11] and Higashida [10] developed relationships between strain controlled fatigue properties and Brinell hardness that provide a very convenient means of determining the fatigue properties of HAZ and weld metal microstructures without having to do costly and time consuming tests. Hardness can be determined by microhardness measurements performed in the region where the fatigue crack is expected to initiate.

1.4 Role of State of Stresses in Weldment Fatigue

Bending Stresses

Seldom are welds subjected to either pure bending or pure axial loadings: most applications involve both. This situation requires that

welds under test be gauged on both sides of the plate so as to determine axial and bending strain components. Even situations seeming to be pure axial loading may involve considerable bending. Angular distortion and misalignment of the weld joint are more or less inevitable; so, cyclic bending stresses are induced during fatigue testing of a welded joint subjected to apparently pure axial loading. Burk et al. [8] found that the induced bending stresses were a function of the Young's modulus, distortion angle, applied axial load and the ratio of specimen's length to its thickness at $R > 0$ condition and had a significant effect on fatigue crack propagation life. The work of Berge and Myhre [12] showed that increasing joint misalignment increased induced bending stresses and decreased the fatigue strength of weldment. Lohne [13], also, observed a reduction in fatigue strength of butt and fillet welds as a result of joint misalignment. However, no analytical models have been proposed for estimating the fatigue crack initiation life considering the combination of axial and bending stresses.

Residual Stresses

When a weld deposit cools, contraction of the hot weld metal is restrained by adjacent parts that have not been heated to as high a temperature, and this contraction causes tensile residual stresses in the weld metal (and at weld toe) upon cooling. Normally, the residual stresses in the neighborhood of a weld will reach the magnitude of the yield point of the base metal.

It is currently accepted that residual stresses (whether they are introduced by the welding process or introduced during subsequent

treatment) may be treated as mechanical prestresses and thus can be considered to be additive to the applied stresses [14,15,16,17,18].

The influence of residual stressses on the fatigue life of weldments has been reviewed and summarized by Munse [19], Gurney [20], Pollard and Cover [21], Kelsey [22], and Reemsnyder [23]. Tensile residual stresses at the weld toe decreases the fatigue resistance of a weld. Stress relief (no residual stresses) improves weld fatigue resistance by reducing the tensile residual stresses. The compressive residual stresses improve the fatigue resistance [18,24,25]. Burk [18] found that, when A514 F butt welds were overloaded above 100 ksi. before fatiguing so as to induce compressive residual stress (-120 ksi. assumed), their fatigue strength was about two times more than that of as-welded welds. Lawrence and Ho [24] further found that overloading Tig dressed A514 F butt welds before fatiguing resulted in plain plate failure instead of weld toe failure. Also, Booth [25] studied shot peened, non load carrying fillet welds and found that plain plate failure occured. It seems possible, therefore, that compressive residual stresses may permit the recovery of the fatigue life lost through welding.

The influence of residual stress on weld fatigue life may be explained using the set-up-cycle analysis which predicts the established mean stress in the first few cycles of load application [15,18].

Variable-Amplitude Load Histories

Welded components are seldom subjected to constant amplitude loading, instead, variable load conditions are usually encountered. A

better understanding of the effect of variable load spectrum on fatigue crack initiation and propagation is essential for the successful prediction of the fatigue life of most welded structures. However, very few laboratory studies have been conducted on the fatigue behavior of welds under variable load histories.

Several methods have been proposed to predict variable amplitude fatigue behavior of notched members, and these have been applied to welds. The Palmgren Miner linear cumulative damage summation rule [26,27] was applied to the weld by Maddox [28] using LEFM. The statistical [29] and RMS [30] methods were proposed later by Munse and Barsom. However, neither of these methods took sequence effects and mean stress effects into consideration. A most promising method has been proposed by Dowling [31] who showed that the combination of the rain flow counting method, Palmgren Miner's linear cumulative damage summation rule and strain controlled fatigue data allowed sequence effects and mean stress to be considered and yielded better fatigue life estimates for smooth specimens. Subsequently, this approach has been applied and modified by Socie [32] to predict notched member fatigue crack initiation and propagation life.

1.5 Scope

The total fatigue life model developed by Lawrence, Mattos, Higashida and Burk [33] was modified for predicting the total fatigue life of welds and evaluating the severity of welds' discontinuities under the combination of axial and bending stresses and under constant and variable amplitude loadings.

A stress analysis of the critical region (discontinuity) was performed for several complex weld shapes including the cruciform and double strap lap weldments to determine the stress concentration factors and the variation of stress on the inward path along which the fatigue crack will propagate.

Fatigue tests of cruciform weldments with stress ratio R = 0, and -1 and SAE bracket loading spectrum were conducted. Fatigue tests of double strap lap joints with stress ratio R = 0, -1, -2, $-\infty$ and SAE bracket loading spectrum were also conducted. The results of these tests were compared with predictions made using the analytical metods developed.

2. METHOD FOR PREDICTING FATIGUE RESISTANCE OF WELDED COMPONENTS SUBJECTED TO COMPLEX LOADING

2.1 Stress Analysis of Weldments

The first step in a fatigue analysis of a weld joint is to identify the location(s) where a fatigue crack is most likely to initiate. Next, a stress analysis of that region must be performed to determine the elastic stress concentration factor (K_t) and the variation of stress on the inward path along which the fatigue crack will propagate. The finite element method (FEM) is particularly useful in this connection.

The finite element program used in this study is call Polo Finite [34], and was developed at the Civil Engineering System Laboratory of the Department of Civil Engineering at University of Illinois. The constant strain triangle element was chosen because of its simplicity. The finite element mesh was refined to an element size less than 1/30 of the notch root radius at the notch root in order to produce accurate results.

The peak stresses at a weld toe occur in an exceedingly small region which precludes their direct measurement using strain gage or other convenient strain measurement methods. The peak stresses decrease rapidly with distance along the surface of the weldment away from the weld toe (y/t) and with distance inward (x/t) along the path of the fatigue crack will take (Fig. 1) [35]. At (y/t) of 0.3 away from the weld toe, the stresses have decreased to the level of the nominal stresses in the plate and mounted strain gauges will not be influenced by

the stress concentration of the weld toe unless the size (scale) of the weldment is very large. Measurements of the nominal strain near the weld toe can be used in conjunction with the FEM analysis of the weld shape to determine the state of stress at the weld toe, the elastic stress concentration factor (K_t), and the inward variation of stress along the fatigue crack path.

2.1.1 Cruciform Weldment

In general, the elastic stress concentration factor (K_t) for a notch such as a weld toe can be expressed as [18]:

$$K_t = 1 + \alpha\,(t/r)^{1/2} \qquad (1)$$

where K_t is the ratio of the local stress to the remote stress, t is the plate thickness, r is the notch root radius and α is macrogeometry coefficient. The exponent has been found to be about one half for all cases studied [35]. Thus, it is possible to estimate K_t for any notch root radius from a single finite element analysis that can determine the value of coefficient (α) which is a function of the plate thickness (t), LOP length (c), weld leg length (ℓ) and the weld angle (θ) (see: Fig. 2A). Only a quarter of a cruciform joint need be analysed because of the two lines of symmetry. Both axial and bending loadings were considered.

The FEM analysis results for the weld toe are plotted in Fig. 3 and Fig. 4 for axial and bending loadings, respectively. The coefficient (α) can be determined at t/r equal to 1. Fig. 5 and Fig. 6 show the

relationships between α and c/ℓ and α and θ, respectively. Weld leg (ℓ) was varied from 2t to 1/2t and was found to have little influence on the value of α at the weld toe when no LOP exists

Fig. 7 and Fig. 8 show the results for the root of LOP under axial and bending loading conditions, respectively. K_t of LOP seems to have the same form as that of weld toe. In Fig. 9. K_t of LOP under axial loading was rearranged and could be expressed as:

$$K_t = 1 + \alpha \, (Ct/\ell r)^{1/2} \qquad (2)$$

2.1.2 Double Strap Lap Weldment

An attempt has been made to formulate the stress concentration factors of the double-strap lap joint using FEM analysis. Two different sizes of finite element mesh were used. A refined mesh was used to obtain the local notch root stress and a coarse one was used to obtain the nominal stress along the line from the toe to the root. One half of the double strap joint was analysed because one line of the symmetry exists (see Fig. 2B).

The FEM analysis results for the weld toe for axial and bending loadings are plotted in Fig. 10 and Fig. 11, respectively. Fig. 10 shows that the K_t for axial loading is not only a function of (t/r) but also a function of (t/ℓ_1):

$$K_t = 1 + \alpha \, (t/\ell_1)^{1/2} \, (t/r)^{1/2} \qquad (3)$$

where t is the main plate thickness and ℓ_1 is horizontal weld leg length. For both axial and bending loadings the coefficient (α) was found to be a function of weld angle (θ) as can be seen in Fig. 12.

Fig. 13 shows the non linear stress distribution around the weld root region. The normal stress which is high at the tip of the root has a direction perpendicular to the axial loading direction and has a sign opposite to the applied load (compressive stress at the root, when a tensile load is applied and vice versa). The results of the coarse mesh analysis for obtaining the norminal stress (S_n) can be formulated as:

$$S_n = 1.35\, S_b\, (t/\ell_1)^{0.45}\, (t/\ell_2)^{0.2} \tag{4}$$

where: S_b is the remote stress. Then, the K_t of the root could be approximately expressed as:

$$K_t = \frac{\sigma}{S} = 1 + \alpha\, (\ell_1/\ell_2)^{.12}\, (t/r)^{1/2} \tag{5}$$

All the equations for estimating Kt are listed in Table 1.

2.2 Fatigue Crack Initiation Life Estimates

For high cycle fatigue ($N_I >> N_{tr}$) cyclic hardening and softening effects can usually be ignored. N_I can be estimated using the Basquin equation and the linear damage summation rule [33]:

$$\int_1^{2N_I} \left[(\sigma_f'/\Delta\sigma/2)\ \ (1-\sigma_{o,i}\ (2N_i)^k/\sigma_f'\right]^{-1/b} dN_i = 1 \tag{6}$$

where: N_I = fatigue crack initiation life

σ_f' = the fatigue strength

b = the fatigue strength exponent

k = the mean stress relaxation exponent

$\sigma_{o,i}$ = the local initial mean stress

$\Delta\sigma$ = the local stress range

When test results are unavailable, it is possible to estimate roughly the fatigue properties and mean stress relaxation exponent from the hardness (Fig. 14) determined by micro-hardness measurements performed in the region where the fatigue crack is expected to initiate.

The notch root stress ($\Delta\sigma$), i.e. the stress at the critical region in the weld (weld toe or internal discontinuity) can be obtained using Neuber's rule [36] and a set up cycle analysis [15,18]:

$$\Delta\sigma\Delta\varepsilon = (K_f\Delta S)^2/E \qquad (7)$$

where: ΔS is the remote stress range which is in the elastic region and K_f is the fatigue notch factor which can be estimated using Peterson's Equation [37] (also K_{fmax}) and the known stress concentration factor (K_t) for the weld shape. For a weld, Lawrence el al. [33] have found that there is a maximum value (K_{fmax}) at notch root radius (r) equal to material parameter (a) ($\cong 0.001(300/S_u)^2$ for steel, ksi., inch in unit).

$$K_{fmax} = 1 + (\alpha/2)(t/a)^{1/2} \simeq 1 + .053\ \alpha\ S_u t^{1/2} \text{ (in steel)} \qquad (8)$$

2.2.1 Fatigue Crack Initiation Life with Complex Loadings

When a weld is subjected to axial stresses, bending stresses and residual stresses, a modification of Neuber's rule is necessary to simulate the notch root stress and strain. As is explained in Fig. 15, the notch root stress strain reponse at the end of the first reversal (0-1 in Fig. 15) can be obtained by solving Eq. 9

$$\sigma \varepsilon = (K^A_{fmax} S^A_{max} + K^B_{fmax} S^B_{max} + \sigma_r)^2/E \tag{9}$$

where the subscript A is for axial and the subscript B is for bending loading conditions. At the end of the second reversal (1-2):

$$\Delta\sigma\Delta\varepsilon = (\Delta S_A K^A_{fmax} + \Delta S_B K^B_{fmax})^2/E \tag{10}$$

the $\Delta\sigma$, $\Delta\varepsilon$ and initial mean stress $\sigma_{o,i}$, can be determined and N_I can be calculated using Eq. 6.

For the variable amplitude load history, the rule of linear cumulative fatigue damage was used to sum up the fatigue damage (D_i) of each closed hysteresis loop in one block of the load history:

$$D_{block} = \sum D_i = \sum \left[\frac{\sigma'_f - \sigma_o}{\Delta\sigma/2} \right]_i^{1/b} \tag{11}$$

Mean stress relaxation is a second order effect that can be neglected considering the uncertainty of stress-strain simulation and linear damage under variable amplitude loading. Then, N_I is the reciprocal of D_{block}:

$$N_I = 1/D_{block} \tag{12}$$

Although many cycle counting methods have been proposed in the past years, the "availability" concept developed by Wetzel [38] was considered to be most effective and easier to program for a digital computer. For a notched member without bending stresses and residual stresses, the load history was rearranged in such a manner that the largest absolute value of the history was made to be the first and the last value of the history. However, for a weld subjected to bending stresses and containing residual stress, one must consider the ith value (S_i) of the history having the largest absolute value of ($K^A_{fmax}S^A_i + K^B_{fmax}S^B_i + \sigma_r$) as the first and last values while performing the cycle counting.

2.3 Fatigue Crack Propagation Life Estimates

The fatigue propagation life (N_p) for a weld can be estimated by integrating Paris' Equation [39]:

$$da/aN = C(\Delta K)^m \tag{13}$$

$$N_p = \int_{a_I}^{a_f} da/C(\Delta K)^m \tag{14}$$

where: a_I and a_f are initial and final crack length, C and m are material constants, and

$$\Delta K = Y\Delta S\ (\pi a)^{1/2} \tag{15}$$

The geometry factor (Y) usually must be determined for each shape. Y may be considered to be the superposition of several effects [40]:

$$Y = \frac{M_s M_t M_k}{\phi_o} \tag{16}$$

M_s is a magnification factor for free sruface, M_t is a magnification factor for finite width (W):

for a center crack

$$M_t = (\sec \pi a/2w)^{1/2} \tag{17}$$

for a single edge crack

$$M_t = \mathrm{Sin}^2 (\pi a/2W) + \mathrm{Sec}^2 (\pi a/2w) \tag{18}$$

M_k is a magnification factor for stress concentration of the weld discontinuity in question and ϕ_o is a correction factor for crack shape. The biggest problem in applying Eq. 16 is determining M_k which is usually a function of crack length (a). A method proposed by Lawrence [7] is based on the principle of elastic superposition and Emery's solution [41] for an edge crack subject to any arbitary system of crack opening stress:

$$M_k = 1/S \left[1.12\, \sigma_a - \int_o^a f\,(x/a)\, \frac{d\sigma}{dx}\, dx \right] \tag{19}$$

where:

$$f(\tfrac{x}{a}) = 0.8(\tfrac{x}{a}) + 0.04\, (\tfrac{x}{a})^2 + 3.62 \times 10^{-6} \exp\,(11.18\, \tfrac{x}{a}) \tag{20}$$

σ_a = stress at x = a,

$d\sigma/dx$ = stress gradient.

Albrecht and Yamada [42] also has given an expression for f(x/a):

$$f(\frac{x}{a}) = 1.12 \frac{2}{\pi} \sin^{-1} (\frac{x}{a}) \quad (21)$$

2.3.1 Fatigue Crack Propagation Life under Complex Loading

The notch-root residual stresses were assumed to have no effect on the long crack growth because the crack was outside the plastic zone at the tip of the weld discontinuity. Since Bending stresses have a direction parallel to the axial load and normal to the crack surface, the stress intensity factor (ΔK_T) for combined axial and bending loads can be obtained using superposition methods [8]:

$$\Delta K_T = \Delta K_A + \Delta K_B \quad (22)$$

where: ΔK_A is the stress intensity factor for axial load and ΔK_B is the stress intensity factor for bending load. Substituting ΔK_T for ΔK into Eq. 14 the N_p can be calculated.

The method for calculating fatigue crack propagation life with variable load history developed by Socie [32] was used and extended. Spectrum was truncated at zero load and stress ratio effect was neglected. The crack growth rate per block ($\Delta a/\Delta B$) is calculated by considering the crack length being fixed at the initial crack size and by summing the incremental crack extension for each cycle:

$$\Delta a/\Delta B = \sum da_i \quad (23)$$

Combining Eq. 15 and Eq. 23, $\Delta a/\Delta B$ for axial loads is:

$$\Delta a/\Delta B = CY^m (\pi a)^{m/2} \sum S^m \tag{24}$$

The crack propagation life (N_p) in terms of blocks can be calculated.

$$N_P = \int_{a_I}^{a_f} \left(\frac{\Delta B}{\Delta a} \right) da \tag{25}$$

When a weld is subjected to both bending and axial loads, Eq. 24 should be:

$$\frac{\Delta a}{\Delta B} = CY_A^m (\pi a)^{m/2} \sum \Delta S_A^m (1 + Y_B \Delta S_B / Y_A \Delta S_A)^m \tag{26}$$

Using Eq. 26 rather than Eq. 24, N_p under combined axial and bending loadings can be obtained by performing the integration of Eq. 26.

3. EXPERIMENTAL PROCEDURES

3.1 Materials and Test Specimens

Three types of load-carrying mild steel fillet weldments were used in this study: MS4361 cruciform weldments donated by General Motors' Eelectro-Motive Division (EMD), 1E650 cruciform weldments in three groups donated by Caterpillar Tractor Co., and SAE 1020 HR double strap lap weldments donated by Deere and Co.

The cruciform weldments were fabricated with a nearly 45 degree weld angle (θ), weld size (ℓ) roughly equal to 0.5-in. plate thickness and LOP of various lengths (<0.2-in. for 1E650 Group A specimens, >0.35-in. for 1E650 Group B specimens, <0.4-in. for 1E650 Group C specimens < 0.35 -in. for MS4361 specimens). All specimens were cut to a 3-in. width after welding. The welding process for the MS4361 weldment provided by EMD was a FCAW process with 5/64-in. AWS E70T-1 wire 30 volts 40 amps DC for the final (main) pass (138 Kj/in). The welding process for 1E650 weldments provided by Research Department of Caterpillar Tractor Co. was a semiautomatic SAW process with Linclon LN9F/DC600 equipment and L50 wire, L980 flux.

The double-strap lap weldments of 1020 HR steel were fabricated with a 90 degree weld angle (θ). The main plate (t) was 0.5-in. thick and the cover plate was 0.375-in. thick. The horizontal weld leg length (ℓ) was 0.3-in. and vertical weld leg length was 0.25-in..

3.2 Heat-Affected-Zone and Weld Metal Specimens of MS4361 Steel

Both heat-affected-zone (HAZ) and weld metal (WM) specimens of MS4361 steel were made and donated by EMD. The HAZ specimens used in this study were artificially produced [43] by a programmable weld thermal simulator (Gleeble machine). The thermal cycle utilized to produce the specimens was determined at the toe of 1/2 inch FCAW process fillet weld [44]. The weld metal specimens were cut longitudinally from muti-pass U butt welds and, thereafter, were heat treated to obtain a hardness which was close to the hardness in MS4361 WM [45]. All the specimens were carefully machined and polished to the final dimensions of 0.25-in. in diameter and 0.4-in. gage length.

3.3 Test Programs

Test of Smooth Specimens

HAZ-simulated and WM-simulated smooth specimens were tested monotonically with 20 kips. MTS closed loop, servo-controlled axial hydraulic test system to obtain the monotonic properties. Strain was controlled before necking, then stroke was controlled to failure. Fatigue tests were conducted under strain control using the same equipment employed for monotonic tension test. A sine-wave function generation was employed to control the strain signal, and the test frequency was to 0.1 Hz to 10 Hz. Stress-strain hysteresis loops were stored in a digital computer for later analysis.

Test of Welded Specimens

All specimens were fatigue tested to failure under load control in a 100 kip MTS; haydraulic testing machine using frequencies ranging from 2 Hz to 5 Hz. Every cruciform weldment and some double strap lap weldments had four strain gauges mounted 0.5-in. inch away from weld toes so that nominal secondary bending stresses could be recorded just outside the influence of the weld toe.

For constant load amplitude fatigue tests of cruciform weldments, the stress ratios (considering axial load only) R=0 and R=-1 were set. Stress levels were chosen to give fatigue lives from 10^4 to 10^7 cycles. The stress ratios, R=0, R=-1, R=-2 and R=-∞ were used for double strap lap weldments to study the effect of stress ratio on the fatigue crack initiation site.

For variable amplitude fatigue test, the SAE bracket load history was recorded into a special function generator that was connected to the MTS machine. This function generator which were designed and donated by S. Downing of Deere and Co. can store all kinds of load histories and reproduces these at various frequencies. A signal is sent to the MTS cycle counter to count lives as blocks when the end of the history (one block) was encountered. SAE 1020 HR double strap lap weldments and 1E650 Group B cruciform weldments were fatigue tested using the SAE bracket load history without any imposed average mean stress.

4. RESULTS AND PREDICTIONS

4.1 Properties of MS4361 HAZ and E70-T1 Weld Metal

The monotonic and cyclic stress-strain properties for both the MS4361 HAZ and E70T-1 weld metal are listed in Table 2 and Table 3, respectively. Monotonic and cyclic true stress strain response are reproduced in Fig. 16. Comparison of the monotonic and cyclic reponse of the HAZ and weld metal shows that the weld metal is stronger and more ductile. The weld metal cyclically hardens, but the HAZ cyclically softens.

The results of strain controlled fatigue tests are plotted in Fig. 17 and Fig. 18 for MS4361 HAZ and E70T-1 weld metal, respectively. The fatigue strength coefficient (σ_f') and exponent (b) and fatigue ductility coefficient (ε_f') and exponent (c) were calculated by a least square fit to the elastic or plastic strain life results. Comparison of the total strain-life curves shows that the two materials are almost identical.

4.2 Predictions of Weldment Fatigue Life

The total fatigue lives of the weldments studied were estimated using the method discussed in Chapter 2. The value of K_{fmax} for each specimen was calculated based on its weld geometry. If the specimen failed at the LOP, the largest LOP length measured on the fracture surface was used; otherwise, the LOP length observed at the polished end of the specimen was used. Nominal bending stresses measured using strain gages were taken into consideration. For all specimens, estimation of

their fatigue crack initiation life was based on the properties of MS4361 HAZ and E70T-1 WM.

Crack growth rate for HAZ was obtained from Barsom's work [46]. Crack growth rate for WM were obtained from Maddox's work [47] by matching the hardness and tensile strength. The crack growth rates for HAZ and WM are listed in Table 5. The notch root radii (r) equal to Peterson's material constant (a) (K_{fmax} condition) was used in calculating the M_k. For simplicity, Albrecht's equation was used to calculate the M_k instead of Emery's equation. The comparison of Albrecht's and Emery's equations is shown in Fig. 19. Emery's Equation gives f(x/a) about 5% higher than Albrecht's. The M_k for a cruciform weldment can be calculated by knowing stress distribution [35] and for axial loading can be expressed approximately as:

$$M_k = 1 + (K_t - 1) \exp\left[(K_t - 1)^{.85} \frac{a}{t}\right] \tag{27}$$

for bending loading

$$M_k = 1 + (K_t - 1) \exp\left[(K_t - 1)^{.65} \frac{a}{t}\right] \tag{28}$$

For cruciform weldments, the method for predicting total fatigue life was applied to both the toe and the LOP. It was assumed that the LOP was not a crack-like defect but a sharp notch; thus a fatigue crack initiation life was calculated for the LOP, also.

To calculate the fatigue crack propagation life of the LOP, the stress intensity factor (K) was obtained from Frank's work [4].

$$\Delta K = (A_1+A_2/w)\ (\pi a)^{1/2}\ \mathrm{Sec}^{1/2}\ \left(\frac{\pi a}{2w}\right) \qquad (29)$$

$$A_1 = .528+3.287\left(\frac{\ell}{t}\right)-4.361\left(\frac{\ell}{t}\right)^2+3.696\left(\frac{\ell}{t}\right)^2-1.874\left(\frac{\ell}{t}\right)^4+0.415\left(\frac{\ell}{t}\right)^5$$

$$A_2 = .218+2.717\left(\frac{\ell}{t}\right)-10.171\left(\frac{\ell}{t}\right)^2+13.122\left(\frac{\ell}{t}\right)^3-7.755\left(\frac{\ell}{t}\right)^4+1.785\left(\frac{\ell}{t}\right)^5$$

For double strap lap weldments, the method was applied to both the toe and the root. The induced bending stresses in the weld, which can not be measured experimentally were estimated using FEM and are shown in Fig. 13. It is difficult to formulate the stress distribution for the double strap lap weldment; thus a_I could not be estimated analytically and an a_I of 0.01-in. was assumed for calculating the fatigue crack propagation life. This point will be discussed further in Secs. 5.1 and 5.2.

Computer programs are listed in the Appendix.

4.3 Fatigue Life of the Cruciform Weldment

Results for the constant amplitude fatigue tests on cruciform weldments are listed in Table 6 to Table 8 with predictions, and graphed in Figs. 20 to 25. The vertical axis represents the applied axial stress. The number associated with each point is the measured bending stresses. Solid lines are predictions for toe failure for different bending stresses. The dotted line is the prediction for LOP failure. All the predictions shown in figures are based on the same weld geometry.

For MS4361 cruciform weldments, two of eight specimens under R = -1 condition and six of eleven under R = 0 conditions failed at the toe. The remainder of the specimens failed at the LOP. Most of the toe

failures occured at higher applied loads and in specimens which had greater bending stresses. Those specimens which failed at the LOP experienced lesser bending stresses.

For 1E650 cruciform weldments, only one of the specimens in Group A failed at the toe with higher axial and bending stresses in short life region. All specimens of Group B with longer LOP contained fatigue cracks initiating at the LOP. The results also show that shorter LOP lengths improve the fatigue resistance by factor two to three in the long life region, but none were sufficiently short to avoid LOP failures.

The total fatigue life of the toe and the LOP was estimated. The location giving the shortest life was assumed to be the failure site and the predicted total fatigue life associated with it was considered to be the predicted total fatigue life of the specimen. In Tables 6 to 8, one can see that the actual failure site was correctly predicted in each case. Comparisons of the predicted total fatigue lives with the observed total fatigue lives were shown in Fig. 26. The predictions of the total life agree with the experimental results within a factor of two.

4.4 Fatigue Life of the Double-Strap Lap Weldments

Fatigue test results for the double strap lap weldments are listed in Table 9 with coresponding predictions and are graphed in Figs. 27 to 30. Induced bending stresses in the main plate were neglected in the prediction because they were small in comparison with the applied axial stresses.

For the R=0 condition, toe failures were observed and fatigue cracks propagated either through thickness (at low stress levels)

or through weld (at high stress levels). None of these specimens were found to have cracks which initiated at the root. For the R=-∞ (zero to compression) condition, cracks initiated at the root and propagated through weld to the weld toe. There was no sign of cracks initiating at the weld toe on the other side of the specimen. However, for the R=-1 and R=-2 conditions, cracks initiated at both toe and root.

For R=-1 and R=-2 conditions, the shortest predicted total fatigue life (the toe or the root) was considered to be the predicted total fatigue life for the specimen. In Table 9 and Figures 27 to 30, the predicted life assuming toe failure and predicted life assuming root failure are shown. One can see that for R=-1 conditions, the toe has a lesser fatigue resistance than the root; and for R=-2 conditions, the root has a lesser fatigue resistance than the toe. The comparison of the predicted and observed total fatigue lives is shown in Fig. 31. Most of the predictions are within the factor of two scatter band.

4.5 Fatigue Life for Variable Amplitude Loading

The SAE bracket load history fatigue test results for 1E650 Group B cruciform weldments and 1020 HR double strap lap weldments are listed in Table 10 and Table 11 with predictions and are graphed in Figs. 32 and 33, respectively. The nominal stresses shown in the figures were the largest absolute value of the load history, and the life was represented as blocks (5937 reversals in one block).

For 1E650 Group B cruciform weldments, all fatigue cracks occured at the LOP. As can be seen in Table 10, the total fatigue life predictions were shorter for the LOP than for the toe. Comparison of the

predicted and the observed total fatigue lives in Fig. 34 shows that the predictions were slightly nonconservative.

For 1020 HR double strap lap weldments, the fatigue cracks initiated at both the toe and the root. The shortest predicted total fatigue life was chosen as the predicted total fatigue life and is plotted in Fig. 35 against the actual fatigue life.

5. DISCUSSION

5.1 The Relative Importance of Crack Initiation

According to the model of Lawrence et al. [33], the total fatigue life of a weldment (N_T) may be considered to be the sum of the fatigue crack initiation life (N_I) and the crack propagation life (N_P):

$$N_T = N_I + N_P \tag{30}$$

N_I is defined as the number of cycles for initiation of a fatigue crack and its early growth and coalescence into a dominant fatigue crack (of length (a_I)); and N_P is the number of cycles to propagate the crack, thereafter, to final fracture. It is controversal whether N_T is appreciable or whether N_P donimates N_T of a weldment. There is mounting evidence [5,6,7,8,9] that a significant portion of N_T is spent in fatigue crack initiation (as defined above), particularly at long lives.

The predicted percentage of N_T spent in crack initiation for the cruciform weldment is plotted as a function of total fatigue life in Fig. 36 in which it is seen that, for fatigue failure at the toe, crack initiation should dominate at lives greater than 10^5 cycles. However, for failure at the LOP, fatigue crack propagation should dominate at lives less than $5x10^5$ cycles. These findings are also clearly shown in Figs. 37 and 38 in which the predicted N_I and N_P are compared with the observed N_T. In Fig. 37, the predicted N_I for fatigue failure at the toe and the LOP, lie within the factor of two scatter band for observed N_T

greater than 10^5 cycles and $5x10^5$ cycles, respectively. In Fig. 38 the predicted N_P for failure at the weld toe only occupied a small portion of the observed N_T, and the predited N_P for failure at the LOP crack propagation dominate only for observed N_T less than $5x10^5$ cycles.

The predicted percentage of N_I as a function of N_T for the double-strap lap weldments is shown in Fig. 39 from which it is apparent that N_P should dominate at total fatigue lives less than 10^6 cycles. The predicted N_I and N_P are compared with observed N_T in Figs. 40 and 41. Fatigue crack propagation dominates at lives less than 10^6 cycles for all conditions except $R = -\infty$ for which a larger percentage of the total fatigue life was spent in crack initiation.

As discussed above, a significant portion of N_T appears to be spent in crack initiation for all weld geometries studied. Neglecting N_I would give conservative fatigue life estimates. Even for welds which contain LOP and fail at the LOP, N_P cannot entirely account for N_T. In general, N_I is the main portion of N_T in the long life region; however, N_P is the main portion of N_T for lives less than 10^6 cycles.

5.2 Estimating the Initiated Crack Length (a_I)

When initiation occurs at an obvious defect such as a pore, slag or LOP, the size of the initiated crack length (a_I) may be taken as the dimension of the defect. However, a discontinuity such as a weld toe at which fatigue failure often occurs is not a deep notch, and the value of a_I is not obvious. It has been past practice of Lawrence et al. [7,8] to assume arbitarily that a_I was 0.01-in. regardless of the stress level or

the material. The British Welding Institute researchers have back calculated values of a_I for some materials assuming N_T to be entirely devoted to fatigue crack propagation; while this is a convenient ex post facto method, it does not seem entirely reasonable and leads to rather small estimated values of a_I.

An alternative strategy for the definition of a_I was suggested by Chen and Lawrence [48] and applied to the weld toe by Lawrence et al. [35]. Using this strategy, a_I can be expressed as:

$$a_I = x\Big|_{K_t = K_f} = \frac{0.198\ t}{K_t - 1} = 0.1878\ t^{1/2}/(\alpha\ S_u) \qquad (31)$$

Hence, a_I should depend upon the weld geometry (α), the scale of the weldment (t) and the strength of the material (S_u). For 1-in. mild steel single-V butt weld, a_I is about 0.01-in.

One can see from Eq. 14 that different a_I will give different N_p. Fig. 42 shows the variation of calculated $\Delta K/\Delta S$ with crack length for a weld toe. Surprisingly, $\Delta K/\Delta S$ seems nearly constant in the range of crack length from 0.003-in. to 0.01-in. for values of K_t between 2 to 5. Thus, while the crack propagates from a_I (which is generally greater than 0.003-in. and less than 0.01-in. for mild steel) to 0.01-in. the difference of N_p can be estimated as:

$$\Delta N_p = 1.0 \times 10^{10}\ (3.3 + 2.4x)^{-3.3}\ (\Delta S)^{-3.3}\ (0.01 - a_I) \qquad (32)$$

where x is the ratio of bending stress to axial stress. For a cruciform

weldment (G-76 in Table 6) subjected to 22 ksi. axial stress and 7 ksi. bending stress, the ΔN_P is about 4.6×10^4 cycles which is about 35% of the calculated propagation life (1.61×10^5 cycles) which is in turn 34% of the total life. So if a_I was unknown and one was, therefore, forced to assume a value of 0.01-in., the fatigue crack propagation life would yield a N_P which would give a N_T of 5.6×10^5 cycles, a value which is very close to a N_T of 6.1×10^5 cycles (obtained using a_I estimated using Eq. 31) and which underestimates N_P only by about 10% of N_T. This small difference may be the reason why the predictions for the double strap lap weldments which were made using 0.01-in. for a_I agree as well as they do with the experimental results.

5.3 The Influence of Bending on Fatigue Resistance

Most of the cruciform weldments tested in this study experienced some bending stresses which were measured using strain gauges. In Table 1, one can see that the bending stress concentration is much larger for the weld toe than for the LOP (which lies close to the neutral axis). Consequently, bending stresses lower the fatigue resistance of the weld toe but only slightly diminish the fatigue resistance of the LOP. The principal influences of bending stresses on N_I of welds are to change the sign and magnitude of the initial mean stress and to change the local stress range ($\Delta\sigma$). N_P is also influenced by bending stress as was explained by Burk et al. [8].

If the bending stresses act in the direction opposite to the applied axial load, N_T should be improved. However, for cruciform

weldments, bending stresses always have a negative effect on fatigue resistance because they will always increase the local stresses at one or the other of the opposing weld toes. However, as pointed out by Chang [49] for single-V butt welds, properly controlling the angle of distortion could induce bending stresses at the weld toe which are compressive and which, therefore, improve the fatigue resistance.

The influence of bending stresses on N_T of the cruciform weldment which failed at the weld toe can be seen in Fig. 43. The open symbols are estimates made neglecting the bending stresses: the predicted lives are greater than the observed lives. When bending stresses are considered in the estimates, the predictions agree well with the observed life.

The presence or absence of bending apparently influences the location of failure. The predicted LOP life and predicted toe life in the absence of bending are clearly shown that:

Life(Toe,no bending) > Life(LOP) > Life(Toe,bending)

Thus, LOP failure may be expected if the specimens are straight and the induced bending stresses are small. This observation explains why more LOP failures were observed for 1E650 Group A cruciform weldments which exhibited very low bending stresses due to weldment straightening under load. The magnitude of bending stresses necessary to change the failure site from LOP to toe can be deduced from the curves of Figs. 20-25 for various weld geometries and stress ratios.

It seems that bending stresses decrease the fatigue crack propagation life more than the fatigue crack initiation life. Thus,

bending stresses cause the initiation life to increase in dominance: see Fig. 44.

5.4 The Influence of Weldment Geometry

The influence of the several weldment geometries studied on their fatigue resistance is shown in Fig. 45. For mild steel at a stress ratio (R) equal to zero, a transverse butt weldment has the highest fatigue strength and a double strap lap weldment has the lowest. This difference can be explained by comparing the value of K_{fmax} of these three weldments: 2.51 for the butt weldment, 3.57 for the cruciform weldment (LOP=0.2-in.) and 4.5 for double strap lap weldment. According to Eq. 7 decreasing the K_f (or decreasing K_t) will increase the fatigue strength The fatigue test results for mild steel cruciform butt weldments with weld angle of 20 and 50 degrees showed that at 10^7 cycles, the weld with a 20 degree weld angle had fatigue strength of 20 ksi.-a value which is higher than the fatigue strength for the 50 degree weld angle (14 ksi.) [50]. The calculated K_{fmax} values are 4.78 and 6.0 for 20 and 50 degrees, respectively. Thus, K_{fmax} (or K_t) seems to be an effective index of the fatigue strength of different geometry weldments. In other words, for the same material, the geometry coefficients (α) of weldments will determine which weldment has the better fatigue resistance.

Weldments are often divided into classes by experimental determination of their fatigue strength. There were seven classes in the old British fatigue design rule BS 153 [51] and nine classes in the revised design rule BS 5400 [52]. A summary of these classifications is given in Table 12. Typical examples are followed by the available stress

concentration factors and their weld classes. Also for most examples, the K_{fmax} values for mild steel were calculated. Eight of nine classes of BS 5400 design rule refer essentially to weldments involving toe failure; and only one (class W) refers to root failure, i.e. the load carrying cruciform weldment.

Actually, class A refers to a polished surface (not a weld) and has the greatest fatigue strength of all classes. Classes B, C and D of BS 5400 design rule may be considered members having different kinds of notches at their surfaces. From Chang's work [49], K_{fmax} of an as rolled surface (class B) is about 1.47. The K_{fmax} for classes C and D can be calculated from the surface roughness of flame cut and flame gouged (similar to the start/stop in a weld) surfaces [53] and have the values 1.32 and 1.59, respectively. For weldments other than classes A, B, C and D, the following conditions were assumed for estimating K_{fmax}: the notch root radius (r) was equal to the material constant (a) which is 0.01-in. for mild steel, the plate thickness (t), weld leg (ℓ) and LOP length (2C) were equal to 1 in., and the weld angle (θ) was 45 degree. In Table 12, it seems that the values of K_{fmax} correlate well with the British classifications.

The K_{fmax} (or K_t) of a weldment varies with changes in its macrogeometry and microgeometry. If the weld angle (θ) of transverse butt weld (class E) varies from 20 to 60 degrees, the K_{fmax} varies from 2.05 to 2.6. For similar variation in the weld angle of a cruciform butt (class F) weld, the K_{fmax} varies from 2.32 to 3.02. Thus, overlap between the classes E and F must exist. It is clear then, that a lower class does not necessarily have a poorer fatigue performance than a

higher class when variations in weld shape are considered. Moreover, it is difficult to classify the load carrying cruciform weldment (class W) which has two potential failure sites. If the LOP length is short, the fatigue failure may occur at the toe, and the weldment is classified as class F2; otherwise, it is classified as class W. However, British classifications do not clearly describe the condition under which the load carrying cruciform weldment is in class W or class F2.

For the double-strap lap weldment (class F2), the loading conditions will change the failure locations and the weldment's fatigue strength. This study showed that for zero to tension conditions, fatigue failure occured at the toe; and for zero to compression loading, fatigue failure occured at the root. The root has a lesser fatigue strength than the toe. This phenomenon of stress ratio dependent failure site was not dealt with in the British classification system.

Another important factor which was not considered by British classification system for classifying weldments is the bending stresses induced by joint distortion and misalignment. As discussed in the previous section, the bending stresses may drastically decrease (or increase) the fatigue strength of a weldment and alter the fatigue failure site. The available bending stress concentration factors for weldments are compared with the British classifications in Table 13. Again, there is a reasonable agreement between the K_{fmax} for bending and the British classification system since K_{fmax} for bending is proportiona to K_{fmax} for axial loading (for external notches).

Although usually useful and roughly correct, the current British classification system does not seem to describe completely the fatigue

strength of different kinds of weldments and their severity under all conditions. A case by case estimation of weldments' fatigue strength through comparison of their K_{fmax} values for axial and bending loadings seems preferable and will not mislead. A further discussion of K_{fmax} as an index of fatigue severity will be found in the next section.

5.5 Fatigue Severity of Weldment

For long life fatigue, the present model predicts that the crack initiation life (N_I) will dominate the total fatigue life. N_I can be estimated using the Basquin equation substituting $K_f \Delta S/2$ for the local stress $\Delta\sigma$.

$$2 N_I = \left(\frac{\sigma_f' - \sigma_o}{K_f \frac{\Delta S}{2}} \right)^{-1/b} \tag{33}$$

σ_f' and b may be estimated from Fig. 14 which shows the variation in fatigue properties with hardness. Equation 33 can be rewritten as:

$$2 N_I = \left(\frac{S_u + 50 - \sigma_o}{K_f \frac{\Delta S}{2}} \right)^{\frac{6}{\text{Log } 2\ (1 + 50/S_u)}} \tag{34}$$

For R=-1 conditions σ_o can be considered equal to the residual stress σ_r. For a cruciform weldment, the presence of bending must be taken into account and Eq. 34 should be:

$$2 N_I = \left(\frac{S_u + 50 - \sigma_r}{(K_f^A + xK_f^B) \frac{\Delta S}{2}} \right)^{\frac{6}{\text{Log } 2\ (1 + 50/S_u)}} \tag{35}$$

where x is the ratio of bending stress to the axial stress. Thus, a rational approach to rating the severity of an internal discontinuity in fatigue would be to compare the expected N_I ($=N_T$) due to fatigue failure at the internal discontinuity with the expected N_I due to the external discontinuity (weld toe etc.). An internal discontinuity causing failure before external discontinuity must be considered detrimental. From the K_{fmax} concept and the model used here, it is clear that the relative severity of an internal discontinuity will depend on the material properties, the scale of the weldment, the geometry of the weldment and type of loading. For example, the relative severity of a cruciform weldment subjected to axial loading, the ratio of $2N_I$ of the toe to $2N_I$ of the LOP may be written as Eq. 36 assuming the same fatigue exponent (b).

$$\left\{ \frac{(2\,N_I)^{Toe}}{(2\,N_I)^{LOP}} \right\}^b = \left(\frac{K_f^A + K_f^B\,x}{S_u + 50 - \sigma_r} \right)^{Toe} \Big/ \left(\frac{K_f^A + K_f^B\,x}{S_u + 50 - \sigma_r} \right)^{LOP} \qquad (36)$$

Thus, a LOP in a cruciform weldment should become the more serious fatigue failure site when the value of Eq. 36 is less than 1. The critical weld size which is the smallest weld size to avoid the LOP failure may be determined from Eq. 36. In Fig. 46, 45 degree weld angle cruciform weldments are considered. The S_u for the notch root materials of toe and LOP are 90 ksi. and 110 ksi., respectively; σ_r is assumed to be 36 ksi., the yield stress for the mild steel; the plate thickness is 0.5-in. The region to the right of the lines is the region of LOP failure, and the region to the left is the region of the toe failure.

The present model shows that the fatigue failure site depends on

the magnitude of bending stresses and the geometry of the weldments. For 1E650 Group A specimens (R=-1), unless bending stresses are above 25% of the axial stresses, LOP failures are expected; while for the MS4361 specimens (R=-1), bending stresses should be about 50% of the axial stresses to cause toe failures. For 1E650 Group B specimens, bending stresses should be more than 100% of the axial stresses to avoid LOP failure. As can be seen in Table 7 and 8, all 1E650 specimens (R=-1) failed at LOP; but the measured bending stresses were not more than 15% of the axial stresses. For MS4361 specimens (R=-1) only two specimen with bending stresses larger than 50% of the axial stresses failed at the toe. For R=0 conditions, even though the weld toe is subjected to a higher tensile mean stress which reduces its fatigue life, only those specimens with sufficient bending stresses experienced toe failure. Only one of 1E650 Group A specimens which was subjected to bending stresses 50% of the axial stresses had a toe failure rather than an LOP failure.

For practical design purposes, the toe failure is probably more desireable because it is easier to detect and to repair. The present model shows the toe failure can be favored by increasing the weld angle (θ) in addition to increasing the bending stresses. In Fig. 47 the weld angle is increases to 60 degree and the predicted lines which separate the toe and the LOP failures are shifted to the right.

The effect of the plate thickness can be seen in Fig. 48. The predictions are made for three different plate thickness and show that by increasing the plate thickness and keeping the same weld geometry, a weldment in the toe-failure region may shift to the LOP-failure region. Bending stresses will amplify this effect.

Maddox [3,54] of the British Welding Institute (BWI) used linear elastic fracture mechanics (LEFM) concepts to predict and compare the fatigue strength of cruciform weldments. The a_I of the weld toe was back calculated from the experimental S-N diagrams and is therefore an adjustable parameter. For axially loaded cruciform weldments, the critical weld size was determined [54]:

$$I/W^{1/2} = 0.189 \tag{37}$$

where I is an integral constant dependent on the weld size and LOP length, and W is the sum of the weld leg length (ℓ) and half of the plate thickness (t). The resulting relation for different LOP length (c) and weld leg length (ℓ) is replotted from Maddox's work [54] and shows that by increasing the plate thickness a weldment in the toe failure region could be shifted to the LOP failure region (Fig. 49). One can see that according to Maddox's work all specimens tested in this study should have had toe failures except the 1E650 Group B specimens; see Fig. 49. But the fatigue results showed that only those weldments having larger bending stresses failed at the toe, while weldments with lesser bending stresses failed at the LOP. Note particularly that ten of eleven 1E650 Group A specimens had LOP failures which were not predicted by the LEFM approach of the BWI.

In the BWI's method, induced bending stresses which are usually more than 50% of axial stresses were not considered in the calculation; but, without a doubt, they lower the fatigue resistance of the toe. This underestimation of the fatigue resistance of the toe under axial loading conditions leads to the larger estimates of allowable LOP length.

5.6 Comparison with Other Prediction Methods

El Haddad, Topper and Smith [55] developed an elasto-plastic fracture mechanics method (which will be termed the ETS method) which includes the behavior of short cracks. The ETS method is based upon the assumption that the fatigue crack initiation life (N_I) is small and negligible compared with the total fatigue life (N_T). The ETS method considers the threshold crack length (ℓ_o) of a smooth specimen at fatigue limit to be the initiated fatigue crack length (a_I) of the weld toe. The ETS method is summarized below:

(1) In the highly strained region, the strain intensity factor or ΔJ integral are substituted for ΔK. [56,57]

(2) An ℓ_o is introduced into ΔK:

$$\Delta K = Y \Delta S \left[\pi (a + \ell_o)\right]^{1/2} \tag{38}$$

and ℓ_o can be estimated by

$$\ell_o = \left(\frac{\Delta K_{th}}{\Delta \sigma_e}\right)^2 \left(\frac{1}{\pi}\right) \tag{39}$$

where ΔK_{th} is the threshold stress intensity which is assumed 5.5 ksi.(in.)$^{0.5}$ for mild steel and σ_e is the fatigue limit which can be calculated from the strain controlled fatigue data at 10^7 cycles.

(3) McEvily's crack propagation equation [58] was substituted for the Paris law [39]

$$da/dN = A(\Delta K - \Delta K_{th})^M (K_C/K_C - K_{max}) \tag{40}$$

Where K_C is the fracture toughness (assumed to be 70 ksi.(in.)$^{0.5}$ for mild steel.

In addition, the effect of nominal mean stresses or stress ratios are taken into consideration for lives greater than 10^5 - $3x10^5$ substituting an equivalent stress (ΔS_e) [17] for nominal stress (ΔS) in Eq. 38:

$$\Delta S_e = 2 (S_a S_{max})^{1/2} \quad (41)$$

where S_{max} is the maximum peak stress and S_a is the stress amplitude.

Bending stresses were neglected by ETS method. However, in this work, bending stresses have been seen to influence the total fatigue life of the weld toe, and were therefore introduced in the prediction of the fatigue lives of the cruciform weldments using the ETS method. The comparison of the predicted and observed N_T for the specimens failing at the weld toe are shown in Fig. 50. The solid symbols are predictions made assuming the effect of the imposed mean stresses. The predictions are a factor of two to four less than observed total fatigue lives. However, the predictions made using the ETS method and neglecting mean stresses are in good agreement with the observed N_T and are within the factor of two scatter band.

The ETS method was also used to predict the total fatigue life of the cruciform weldments failing at LOP. Since bending is insignificant at the root of the LOP, the predictions for R = -1 conditions for which the mean stress are zero agree well with the observed total fatigue lives (Fig. 51). For R = 0 conditions, the ETS method predictions which

consider the imposed mean stress effects show the factor of two to three underestimation. The predictions without mean stresses are within the a factor of two scatter band (Fig. 52).

It is clear,then, that the ETS method predicts well the fatigue life of a weldment not having induced bending stresses and/or imposed mean stresses. For weldments with significant bending or mean stresses, the ETS method underestimate the total fatigue life.

A similar method which considers the fatigue crack propagation life to be the total fatigue life was proposed by Smith and Smith [59] (which will be termed the SS method). The SS method is:

(1) The Hartman and Schijve's propagation equation [60] was used:

$$da/dN = C(\Delta K - \Delta K_{th})^m \qquad (42)$$

(2) There is no evidence of faster growth rate due to plasticity or short crack effects [61]. It was not necessary therefore to use the ℓ_o and the strain intensity factor concept.

(3) The preexisting initial crack at the weld toe was found to have a 45um (0.0017-in.) average length using the potential drop measurements [9,62].

The SS method gave good predictions for longitudinal cruciform weldments for stress ratios larger than zero. However, the influence of stress ratios less than zero, the influence of the tensile and compressive residual stresses, the influence of induced bending stresses on the predictions made using the SS method were not studied and from the results of this study would seem to warrant further attention.

6. CONCLUSIONS

1. Bending stresses induced by the joint distortion and misalignment significantly influence the fatigue crack initiation and crack propagation life of external discontinuities (weld toe etc.) but only slightly diminish the fatigue resistance of internal discontinuities. Therefore, a weld which should fail at an internal discontinuity may because of bending stresses fail at an external discontinuty.
2. The present study showed that crack initiation (as defined herein, i.e. crack initiation plus early growth and coalescence) dominated the total fatigue life in the long life region.
3. The critical weld size of the load-carrying cruciform weldment which avoids failure at the LOP, is more accurately predicted using the proposed initiation propagation method than by LEFM method of Maddox (propagation only).
4. The comparison of the values of K_{fmax} for both axial and bending loadings leads to a more accurate and versitile classification of the weldments than the current British standard.
5. The El Haddad, Topper and Smith method reliably predicts the total fatigue life of a weldment not having induced bending stresses and/or imposed mean stresses; however, for weldments with significant bending or mean stresses, their method underestimates the total fatigue life. The method of Smith and Smith gives good predictions for weldments subjected to stress ratios larger than zero; however, the influences of bending stresses, residual stresses

and stress ratios less than zero were not studied; whereas, the initiation propagation method does accurately predict the total fatigue life in these circumstances.

TABLES

Table 1

THEORETICAL STRESS CONCENTRATION FACTORS (K_t) FOR VARIOUS WELDED JOINTS

Welded Joint	Site	K_t	Condition
Butt Welds	Toe	$1+0.27(\tan\theta)^{1/4}(t/r)^{1/2}$	Axial
	Toe	$1+0.165(\tan\theta)^{1/6}(t/r)^{1/2}$	Bending
Load-Carrying Fillet Weld Cruciform Joint	Toe	$1+0.35(\tan\theta)^{1/4}[1+1.1(c/L)^{1.65}](t/r)^{1/2}$	Axial
	Toe	$1+0.21(\tan\theta)^{1/6}(t/r)^{1/2}$	Bending
	LOP	$1+1.15(\tan\theta)^{-1/4}(c/L)^{1/2}(t/r)^{1/2}$	Axial
	LOP	$1+3.22(c/t)^{.12}(t/r)^{1/2}$*	Bending
Load-Carrying Filet Weld Douple Strap Lap Joint	Toe	$1+0.6(\tan\theta)^{1/4}(t/L_1)^{1/2}(t/r)^{1/2}$	Axial
	Toe	$1+0.24(\tan\theta)^{1/6}(t/r)^{1/2}$	Bending
	Root	$1+0.50(L_1/L_2)^{.12}(t/r)^{1/2}$	Axial

*Definition of K_t is shown in Fig. 8.

Table 2

MECHANICAL PROPERTIES OF GM MS4361 HEATED-AFFECTED AND AWS E70-1 WELD METAL

Property	MS4361 HAZ	E70T-1 WM
Hardenss, NHN/DPH	136/190	196/200
Young's Modulus, E (ksi)	28,700.00	30,740.00
.2% Offset Yield Strength, S_y (ksi)	60.00	67.00
Tensile Strength, S_u (ksi)	90.50	110.00
Reduction in Area, RA%	60.60	48.20
True Fracture Strength, σ_f (ksi)	133.00	212.00
True Fracture Ductility, ε_f	.745	.928
Strain Hardening Exponent, n	---	---
Strength Coefficient, K (ksi)	---	---

Table 3

CYCLIC AND FATIGUE PROPERTIES OF GM MS4361 HAZ AND E70T-1 WM

Property	MS4361 HAZ	E70T-1 WM
Cyclic Yield Strength, S_y (ksi)	50.00	71.00
Cyclic Strength Coefficient, K' (ksi)	148.00	200.00
Strain Hardening Exponent, n'	.175	.170
Fatigue Strength Coefficient, σ_f' (ksi)	120.00	156.00
Fatigue Ductility Coefficient, ϵ_f'	.28	.37
Fatigue Strength Exponent, b	-0.082	-0.083
Fatigue Ductility Exponent, c	-0.52	-0.548
Transition Fatigue Strain, ϵ_{tr}	.0036	.0050

Table 4

RESULTS FOR STRAIN CONTROLLED FATIGUE TESTS OF MS4361 HAZ AND E70T-1 WM

Material	Total Strain Amplitude ε_a	Elastic Strain $\Delta\varepsilon_E/2$	Plastic Strain $\Delta\varepsilon_p/2$	Reversals to Failure $2N_f$
MS4361 HAZ	0.0085	0.0023	0.0062	1,892
	0.0065	0.0020	0.0045	4,684
	0.0050	0.0018	0.0032	8,373
	0.0030	0.0017	0.0013	53,084
	0.0022	0.0015	0.00072	151,160
	0.0016	0.0013	---	1,710,000
E70T-1 WM	0.010	0.0030	0.0070	1,400
	0.0070	0.0027	0.0043	35,100
	0.0040	0.0024	0.0016	21,776
	0.0025	0.0020	0.00050	187,500

Table 5

ASSUMED CRACK GROWTH RATE CONSTANTS
FOR MATERIALS AT THE CRACK INITIATION SITE

Initiation Site Material	C in/cycle	m
Mild Steel HAZ	1.0×10^{-10}	3.3
Soft Weld Metal	3.0×10^{-10}	3.0
Hard Weld Metal	2.54×10^{-9}	2.4

Table 6

FATIGUE RESULTS FOR MS4361 CRUCIFORM JOINTS

Spec.	S_A max. / S_B min (ksi.)	S_B max. / S_A min (ksi.)	c (in.)	L_1 / L_2 (in.)	Site	$K^A_{fmax.}$	$K^B_{fmax.}$	N_I predicted cycles	N_P predicted cycles	N_T predicted cycles	N_T observed cycles
G-81	+20 / -20	8.0 / 3.4	.17	.65 / .50	Toe / LOP	2.35 / 3.81	1.71 / 0.33	150,000 / 34,000	93,000 / 217,000	243,000 / 251,000	***** / 220,000
G-99	+20 / -20	10.7 / 5.9	.153	.5 / .45	Toe / LOP	2.45 / 3.95	1.74 / 0.37	116,000 / 31,000	73,000 / 195,000	189,000 / 227,000	***** / 130,000
G-44	+14 / -14	16.1 / 1.43	.147	.55 / .43	Toe / LOP	2.36 / 3.83	1.72 / 0.38	250,000 / 249,000	100,000 / 511,000	350,000 / 731,000	400,000 / *****
G-83	+16 / -16	8.0 / 5.0	.175	.7 / .5	Toe / LOP	2.32 / 3.78	1.70 / 0.34	450,000 / 143,000	158,000 / 404,000	608,000 / 547,000	***** / 550,000
G-36	+16 / -16	8.0 / 0.5	1.75	.5 / .42	Toe / LOP	2.47 / 4.18	1.73 / 0.50	210,000 / 70,000	164,000 / 270,000	374,000 / 340,000	***** / 300,000
G-16	+16 / -16	10.1 / 1.5	.16	.55 / .45	Toe / LOP	2.38 / 3.93	1.73 / 0.39	210,000 / 102,000	96,000 / 356,000	307,000 / 458,000	413,000 / *******

Table 6 (continued)

Spec.	$S_{A_{max.}}$ / $S_{A_{min.}}$ (ksi.)	$S_{B_{max.}}$ / $S_{B_{min.}}$ (ksi.)	c (in.)	L_1 / L_2 (in.)	Site	$K^A_{fmax.}$	$K^B_{fmax.}$	N_I predicted cycles	N_P predicted cycles	N_T predicted cycles	N_T observed cycles
G-53	+25 / 0	13.4 / 13.0	.15	.6 / .44	Toe	2.33	1.71	900,000	110,000	1,010,000	******
					---	---	---	---	---	---	---
					LOP	3.77	0.37	271,000	283,000	554,000	710,000
G-47	24 / 0	8.7 / 5.6	.16	.58 / .44	Toe	2.36	1.71	850,000	179,000	1,030,000	******
					---	---	---	---	---	---	---
					LOP	3.89	.40	304,000	298,000	600,000	700,000
G-64	24 / 0	13.2 / 6.97	.145	.55 / .45	Toe	2.38	1.72	480,000	124,000	614,000	410,000
					---	---	---	---	---	---	---
					LOP	3.79	0.35	400,000	352,000	752,000	******
G-82	24 / 0	2.5 / 0	.17	.65 / .55	Toe	2.39	1.73	1,150,000	100,000	1,250,000	******
					---	---	---	---	---	---	---
					LOP	3.76	.27	360,000	470,000	830,000	650,000
G-76	+22 / 0	12.4 / 5.4	.145	.65 / .55	Toe	2.35	1.73	750,000	161,000	911,000	610,000
					---	---	---	---	---	---	---
					LOP	3.55	.23	1,000,000	724,000	1,724,000	******
G-85	+22 / 0	3.4 / 1.63	.17	.70 / .51	Toe	2.32	1.71	3,045,000	376,000	3,420,000	******
					---	---	---	---	---	---	---
					LOP	3.74	0.31	750,000	512,000	1,260,000	1,000,000
G-71	20 / 0	7.9 / 6.57	.175	.5 / .45	Toe	2.50	1.74	3,050,000	317,000	3,370,000	******
					---	---	---	---	---	---	---
					LOP	4.15	.44	660,000	475,000	1,135,000	710,000

Table 6 (continued)

Spec.	$S_{A_{max.}}$ / $S_{A_{min}}$ (ksi.)	$S_{B_{max.}}$ / $S_{B_{min.}}$ (ksi.)	c (in.)	L_1 / L_2 (in.)	Site	$K^A_{fmax.}$	$K^B_{fmax.}$	N_I predicted cycles	N_P predicted cycles	N_T predicted cycles	N_T observed cycles
G-15	+12 / -12	8.0 / 1.5	.16	.55 / .45	Toe	2.40	1.72	1,250,000	235,000	1,480,000	******
					LOP	3.93	0.39	540,000	840,000	1,380,000	1,370,000
G-35	+12 / -12	8.0 / 3.0	.16	.45 / .45	Toe	2.54	1.76	1,100,000	243,000	1,340,000	******
					LOP	4.18	0.40	415,000	840,000	1,250,000	936,000
G-73	34 / 0	13.6 / 4.77	.16	.55 / .48	Toe	2.42	1.74	97,500	53,500	140,000	135,000
					LOP	3.89	0.34	52,000	124,000	176,000	******
G-45	30 / 0	26.6 / 13.7	.155	.55 / .47	Toe	2.41	1.74	97,500	34,000	132,000	140,000
					LOP	3.86	0.34	86,000	173,000	259,000	******
G-46	30 / 0	23.1 / 8.7	.15	.55 / .43	Toe	2.38	1.72	96,000	40,000	136,000	120,000
					LOP	3.86	0.39	86,000	150,000	240,000	******
G-17	26.7 / 0	13.4 / 6.77	.147	.55 / .45	Toe	2.38	1.72	270,000	96,000	366,000	390,000
					LOP	3.81	0.35	185,000	251,000	436,000	******

Table 7

FATIGUE RESULTS FOR 1E 650 CRUCIFORM JOINTS (GROUP A)

Spec.	$S_{A_{max.}}$ / $S_{A_{min.}}$ (ksi.)	$S_{B_{max.}}$ / $S_{B_{min.}}$ (ksi.)	c (in.)	L_1 / L_2 (in.)	Site	$K^A_{fmax.}$	$K^B_{fmax.}$	N_I predicted cycles	N_P predicted cycles	N_T predicted cycles	N_T observed cycles
A-26	30 / 0	1.64 / .6	.085	.45 / .36	Toe --- LOP	2.31 --- 3.37	1.72 --- 0.29	322,000 ------- 162,000	173,000 ------- 147,000	494,000 ------- 310,000	***** ------- 329,000
A-15	30 / 0	10.1 / 7.0	.085	.46 / .37	Toe --- LOP	2.31 --- 3.34	1.72 --- 0.28	350,000 ------- 126,000	89,000 ------- 150,000	438,000 ------- 276,000	***** ------- 283,000
A-59	30.0 / 0	14.8 / 7.2	.085	.4 / .42	Toe --- LOP	2.42 --- 3.38	1.77 --- 0.22	210,000 ------- 111,000	67,000 ------- 180,000	277,000 ------- 291,000	260,000 ------- *****
A-27	26 / 0	1.65 / -.4	.085	.48 / .4	Toe --- LOP	2.31 --- 3.28	1.73 --- 0.24	960,000 ------- 350,000	84,000 ------- 246,000	1,050,000 ------- 595,000	***** ------- 540,000
A-49	22 / 0	8.77 / 7.9	.105	.41 / .41	Toe --- LOP	2.44 --- 3.64	1.76 --- 0.30	1,610,000 ------- 540,000	227,000 ------- 311,000	1,840,000 ------- 850,000	***** ------- 550,000
A-31	22 / 0	8.4 / 3.8	.10	.42 / .4	Toe --- LOP	2.39 --- 3.57	1.76 --- 0.29	960,000 ------- 580,000	233,000 ------- 313,000	1,200,000 ------- 894,000	***** ------- 490,000

Table 7 (continued)

Spec.	$S_{A_{max.}}$ / $S_{A_{min.}}$ (ksi.)	$S_{B_{max.}}$ / $S_{B_{min.}}$ (ksi.)	c (in.)	L_1 / L_2 (in.)	Site	$K^A_{fmax.}$	$K^B_{fmax.}$	N_I predicted cycles	N_P predicted cycles	N_T predicted cycles	N_T observed cycles
A-45	20 / 0	6.5 / 5.8	.115	.42 / .45	Toe LOP	2.46 3.61	1.77 0.28	3,180,000 960,000	364,000 378,000	3,550,000 1,340,000	***** 1,000,000
A-41	+24 / -24	3.3 / 0.0	.105	.45 / .41	Toe LOP	2.38 3.57	1.75 0.29	52,400 17,500	93,000 110,000	154,000 127,000	***** 75,000
A-13	+18 / -18	5.9 / 2.8	.10	.4 / .4	Toe LOP	2.37 3.37	1.74 0.263	210,000 75,000	157,000 219,000	366,000 288,000	***** 220,000
A-6	+16 / -16	6.8 / 4.0	.095	.45 / .42	LOP LOP	2.36 3.43	1.74 0.262	430,000 171,000	186,000 326,000	616,000 498,000	***** 330,000
A-21	+12 / -12	4.81 / 2.76	.105	.38 / .42	Toe LOP	2.38 3.69	1.75 0.30	1,485,000 690,000	522,000 357,000	2,000,000 1,290,000	***** 730,000
A-8	+10.5 / -10.5	4.54 / 1.47	.09	.42 / .42	Toe LOP	2.4 3.27	1.76 0.24	5,300,000 3,500,000	743,000 941,000	6,000,000 4,440,000	***** 1,600,000

Table 8

FATIGUE RESULTS FOR 1E650 CRUCIFORM JOINTS (GROUP B)

Spec.	$S_A^{max.}$ / $S_A^{min.}$ (ksi.)	$S_B^{max.}$ / $S_B^{min.}$ (ksi.)	c (in.)	L_1 / L_2 (in.)	Site	$K^A_{fmax.}$	$K^B_{fmax.}$	N_I predicted cycles	N_P predicted cycles	N_T predicted cycles	N_T observed cycles
B-4	+24 / -24	+2.44 / -1.9	.2	.38 / .4	Toe	2.79	1.77	27,300	112,000	110,000	*****
					LOP	4.74	0.67	3,500	48,000	53,000	51,000
B-11	+14 / -14	9.0 / 7.5	.20	.45 / .38	Toe	2.58	1.73	580,000	200,000	780,000	*****
					LOP	4.6	0.71	75,000	150,000	225,000	294,000
B-8	+12 / -12	+3.2 / -1.6	.2	.45 / .4	Toe	2.60	1.74	890,000	712,000	1,600,000	*****
					LOP	4.56	0.65	163,000	262,000	424,000	467,000
B-6	+10 / -10	+6.0 / 3.0	.18	.44 / .4	Toe	2.57	1.74	2,660,000	664,000	3,360,000	*****
					LOP	4.58	0.66	471,000	389,000	860,000	560,000
B-17	30 / 0	9.45 / 4.77	.2	.4 / .4	Toe	2.59	1.74	170,000	104,000	274,000	*****
					LOP	4.69	0.66	27,300	61,800	89,000	87,000
B-3	20 / 0	3.4 / 2.0	.2	.39 / .42	Toe	2.78	1.78	1,400,000	560,000	2,980,000	*****
					LOP	4.68	0.61	185,000	198,000	382,000	345,000

Table 8 (continued)

Spec.	S_A max. / S_B min. (ksi.)	S_B max. / S_A min. (ksi.)	c (in.)	L_1 / L_2 (in.)	Site	$K^A_{fmax.}$	$K^B_{fmax.}$	N_I predicted cycles	N_P predicted cycles	N_T predicted cycles	N_T observed cycles
B-24	16 / 0	11.4 / 2.0	.2	.42 / .42	Toe LOP	2.7 4.60	1.76 0.60	1,150,000 610,000	380,000 319,000	1,530,000 927,000	***** 587,000
B-5	13.5 / 0	1.67 / -1.3	.2	.43 / .4	Toe LOP	2.65 4.6	1.75 0.66	46,000,000 4,600,000	1,440,000 471,000	47,400,000 5,140,000	***** 1,600,000

Table 9

FATIGUE RESULTS FOR SAE 1020 DOUBLE STRAP LAP JOINT

Spec.	max. S_A / min. (ksi.)	max. S_B / min. (ksi.)	c (in.)	L_1 / L_2 (in.)	Site	$K^A_{fmax.}$	$K^B_{fmax.}$	N_I predicted cycles	N_P predicted cycles	N_T predicted cycles	N_T observed cycles
D-1	+30 / 0	** / **	**	.30 / .25	Toe --- Root	4.5 ---- **	2.1 ---- **	8,600 ------- ***	22,000 ------- ***	31,000 ------- ***	25,800 ------- ***
D-12	+26 / 0	** / **	**	.30 / .25	Toe --- Root	4.5 ---- **	2.1 ---- **	22,000 ------- ***	35,000 ------- ***	57,000 ------- ***	54,500 ------- ***
D-11	+20 / 0	** / **	**	.30 / .25	Toe --- Root	4.5 ---- **	2.1 ---- **	75,000 ------- ***	84,000 ------- ***	160,000 ------- ***	288,000 ------- ***
D-5	+17 / 0	** / **	**	.30 / .25	Toe --- Root	4.5 ---- **	2.1 ---- **	150,000 ------- ***	140,000 ------- ***	293,000 ------- ***	262,000 ------- ***
D-7	+14 / 0	** / **	**	.30 / .25	Toe --- Root	4.5 ---- **	2.1 ---- **	350,000 ------- ***	271,000 ------- ***	620,000 ------- ***	680,000 ------- ***
D-6	+12 / 0	** / **	**	.30 / .25	Toe --- Root	4.5 ---- **	2.1 ---- **	690,000 ------- ***	450,000 ------- ***	1,140,000 ------- ***	1,320,000 ------- ***

Table 9 (continued)

Spec.	max. S_A / min. (ksi.)	max. S_B / min. (ksi.)	c (in.)	L_1 / L_2 (in.)	Site	$K^A_{fmax.}$	$K^B_{fmax.}$	N_I predicted cycles	N_P predicted cycles	N_T predicted cycles	N_T observed cycles
D-33	+12 / −12	** / **	**	.30 / .25	Toe / Root	4.5 / **	2.1 / 3.72	35,000 / 35,000	138,000 / 239,000	174,000 / 274,000	--- / 197,980 / ---
D-4	+10 / −10	** / **	**	.30 / .25	Toe / Root	4.5 / **	2.1 / 3.72	86,300 / 90,000	254,000 / 370,000	340,000 / 460,000	--- / 400,000 / ---
D-38	+9 / −9	** / **	**	.30 / .25	Toe / Root	4.5 / **	2.1 / 3.72	150,000 / 163,000	360,000 / 477,000	510,000 / 640,000	--- / 695,000 / ---
D-3	+8 / −8	** / **	**	.30 / .25	Toe / Root	4.5 / **	2.1 / 3.72	280,000 / 350,000	530,000 / 630,000	810,000 / 980,000	--- / 900,000 / ---
D-40	+7 / −14	** / **	**	.30 / .25	Toe / Root	4.5 / **	2.1 / 3.72	75,000 / 58,000	180,000 / 165,000	250,000 / 224,000	--- / 285,000 / ---
D-18	+6 / −12	** / **	**	.30 / .25	Toe / Root	4.5 / **	2.1 / 3.72	170,000 / 130,000	290,000 / 240,000	460,000 / 370,000	--- / 345,600 / ---
D-39	+5 / −10	** / **	**	.30 / .25	Toe / Root	4.5 / **	2.1 / 3.72	479,000 / 360,000	530,000 / 370,000	1,000,000 / 740,000	--- / 909,410 / ---

Table 9 (continued)

Spec.	S_A max. / S_B min. (ksi.)	S_B max. / S_A min. (ksi.)	c (in.)	L_1 / L_2 (in.)	Site	$K^A_{fmax.}$	$K^B_{fmax.}$	N_I predicted cycles	N_P predicted cycles	N_T predicted cycles	N_T observed cycles
D-30	0 / -30	** / **	**	.30 / .25	Toe / Root	** / **	** / 3.72	*** / 5,200	*** / 26,000	*** / 31,000	*** / 12,000
D-37	0 / -20	** / **	**	.30 / .25	Toe / Root	** / **	** / 3.72	*** / 47,000	*** / 70,000	*** / 118,000	*** / 63,470
D-23	0 / -16	** / **	**	.30 / .25	Toe / Root	** / **	** / 3.72	*** / 143,000	*** / 120,000	*** / 263,000	*** / 252,000
D-14	0 / -14	** / **	**	.30 / .25	Toe / Root	** / **	** / 3.72	*** / 307,000	*** / 165,000	*** / 472,000	*** / 334,820
D-20	0 / -12	** / **	**	.25 / .25	Root / Root	** / **	** / 3.72	*** / 1,100,000	*** / 240,000	*** / 1,250,000	*** / 640,000

Table 10

FATIGUE RESULTS FOR 1E650 CRUCIFORM JOINTS (GROUP B) UNDER SAE BRACKET HISTORY

Spec.	$S_{A_{max.}}$ / $S_{A_{min.}}$ (ksi.)	$S_{B_{max.}}$ / $S_{B_{min.}}$ (ksi.)	c (in.)	L_1 / L_2 (in.)	Site	$K^A_{fmax.}$	$K^B_{fmax.}$	N_I predicted blocks	N_P predicted blocks	N_T predicted blocks	N_T observed blocks
B-x	26.57 / -36.0	** / **	.20	.4 / .4	Toe --- LOP	2.59 --- 4.69	1.74 --- 0.66	333 --- 73	487 --- 171	821 --- 244	**** --- 191
B-20	23.62 / -32.0	** / **	.20	.42 / .42	Toe --- LOP	2.7 --- 4.6	1.76 --- 0.6	984 --- 182	752 --- 248	1,740 --- 430	**** --- 197
B-19	22.14 / -30.0	** / **	.20	.40 / .38	Toe --- LOP	2.75 --- 4.72	1.77 --- 0.65	992 --- 222	806 --- 235	1,800 --- 457	**** --- 297
B-23	20.62 / -28.0	** / **	.20	.45 / .43	Toe --- LOP	2.6 --- 4.56	1.74 --- 0.64	2,470 --- 411	1,130 --- 345	3,600 --- 756	**** --- 547
B-Y	29.52 / -40	** / **	.20	.4 / .4	Toe --- LOP	2.59 --- 4.69	1.74 --- 0.66	169 --- 58	418 --- 127	587 --- 185	**** --- *171
B-Z	25.1 / -34	** / **	.20	.4 / .4	Toe --- LOP	2.59 --- 4.69	1.74 --- 0.66	528 --- 156	791 --- 193	1,320 --- 348	**** --- 700

Table 11

FATIGUE RESULTS FOR SAE 1020 DOUBLE STRAP LAP JOINTS UNDER SAE BRACKET HISTORY

Spec.	S_A max. / S_B min. (ksi.)	S_B max. / S_A min. (ksi.)	c (in.)	L_1 / L_2 (in.)	Site	$K^A_{fmax.}$	$K^B_{fmax.}$	N_I predicted blocks	N_P predicted blocks	N_T predicted blocks	N_T observed blocks
D-18	+30 / -22.2	** / **	**	0.3 / .25	Toe	4.5	2.1	27	67	93	---
					---	---	---	---	---	---	42
					Root	**	3.72	29	73	102	---
D-19	+24 / -17.8	** / **	**	.30 / .25	Toe	4.5	2.1	105	140	245	---
					---	---	---	---	---	---	146
					Root	**	3.72	122	129	251	---
D-13	+22 / -16.3	** / **	**	.30 / .25	Toe	4.5	2.1	176	206	382	---
					---	---	---	---	---	---	160
					Root	**	3.72	183	153	336	---
D-21	20 / -14.8	** / **	**	.30 / .25	Toe	4.5	2.1	281	280	561	---
					---	---	---	---	---	---	460
					Root	**	3.72	412	198	610	---
D-29	+18 / -13.3	** / **	**	.30 / .25	Toe	4.5	2.1	580	355	935	---
					---	---	---	---	---	---	538
					Root	**	3.72	911	253	1,164	---
D-9	+18 / -13.3	** / **	**	.30 / .25	Toe	4.5	2.1	580	355	935	528
					---	---	---	---	---	---	---
					Root	**	3.72	911	253	1,164	---

Table 12

THEORETICAL STRESS CONCENTRATION FACTOR (K_t), FATIGUE NOTCH FACTOR (K_f) AND CLASSIFICATIONS OF VARIOUS WELDS UNDER AXIAL LOADING CONDITIONS

Weld Type	K_t	K_{fmax}* Ref.	class	
			BS 5400	BS 153
Machined Surface	1		A	A
As-Rolled Surface Weld with Reinforcement Removed	$1+2(d/r)^{1/2}$	1.47	B	A
Flame-Cut Surface Longitudinal Weld	$1+2(d/r)^{1/2}$	1.31	C	B
Above with Start/Stop	$1+2(d/r)^{1/2}$	1.59	D	C
Transverse Butt Weld	$1+.27(t/r)^{1/2}$	2.35	E	D
Butt Weld with Backing Strip Cruciform Butt Weld	$1+.35(t/r)^{1/2}$	2.7	F	E
Lap Weld (Toe Failure)	$1+.6(t/L)^{1/2}(t/r)^{1/2}$	4	F2	F
Load-Carrying Cruciform Weld (Toe Failure)	$1+.35[1+1.1(c/L)^{1.65}](t/r)^{1/2}$	3.25	F2	G
Weld on or Adjacent to Plate Edge	------	---	G	G
Load-Carrying Cruciform Weld (Root Failure)	$1+1.15(c/L)^{1/2}(t/r)^{1/2}$	6.7	W	G

*Calculated at t=L=2c=1-in., θ=45° and θ=a=0.01-in.

Table 13

THEORETICAL STRESS CONCENTRATION FACTOR (K_t), FATIGUE NOTCH FACTOR (K_f) AND CLASSIFICATIONS OF VARIOUS WELDS UNDER BENDING LOADING CONDITIONS

Weld Type	K_f	K_{fmax}* Ref.	class	
			BS 5400	BS 153
Machined Surface	1	1	A	A
As-Rolled Surface Weld with Reinforcement Removed	$1+1.8(d/r)^{1/2}$	1.38	B	A
Flame-Cut Surface Longitudinal Weld	$1+1.8(d/r)^{1/2}$	1.25	C	B
Above with Start/Stop	$1+1.8(d/r)^{1/2}$	1.49	D	C
Transverse Butt Weld	$1+.165(t/r)^{1/2}$	1.83	E	D
Butt Weld with Backing Strip Cruciform Butt Weld	$1+.21(t/r)^{1/2}$	2.1	F	E
Lap Weld (Toe Failure)	$1+.24(t/r)^{1/2}$	2.2	F2	F
Load-Carrying Cruciform Weld	$1+.21(t/r)^{1/2}$	2.1	F2	G
Weld on or Adjacent to Plate Edge	----	---	G	G

*Calculated at t=L=2c=1-in., $\theta=45°$ and r=a=0.01-in.

FIGURES

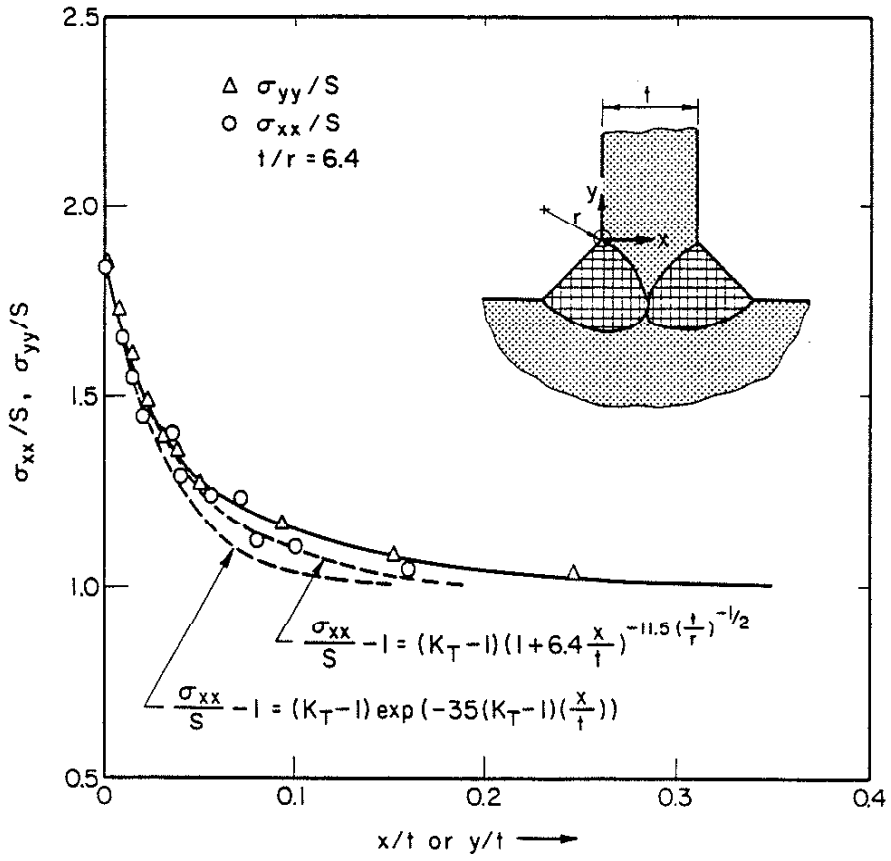

Fig. 1 VARIATION OF STRESS WITH DISTANCE AWAY FROM THE WELD TOE (σ_y/S) AND DISTANCE INWARD ALONG THE PATH THE FATIGUE CRACK WILL FOLLOW (σ_{xx}/S). TWO MATHEMATICAL APPROXIMATIONS TO THE FINITE ELEMENT STRESS ANALYSIS RESULTS ARE INDICATED [35].

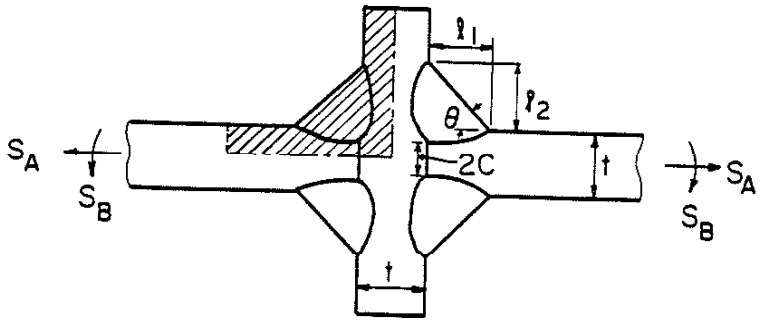

(A)

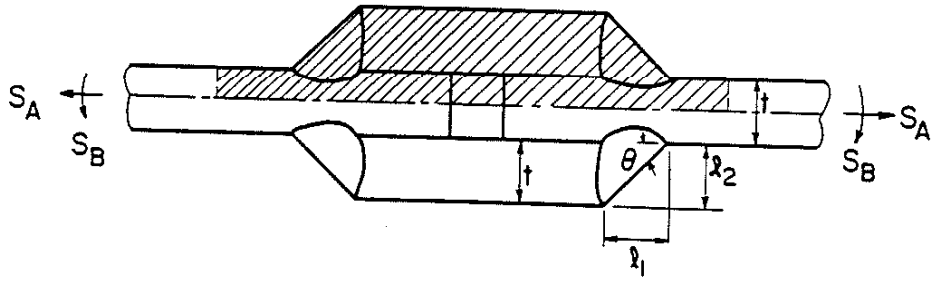

(B)

Fig. 2 CRUCIFORM WELDMENT (A) AND DOUBLE-STRAP LAP WELDMENT (B).

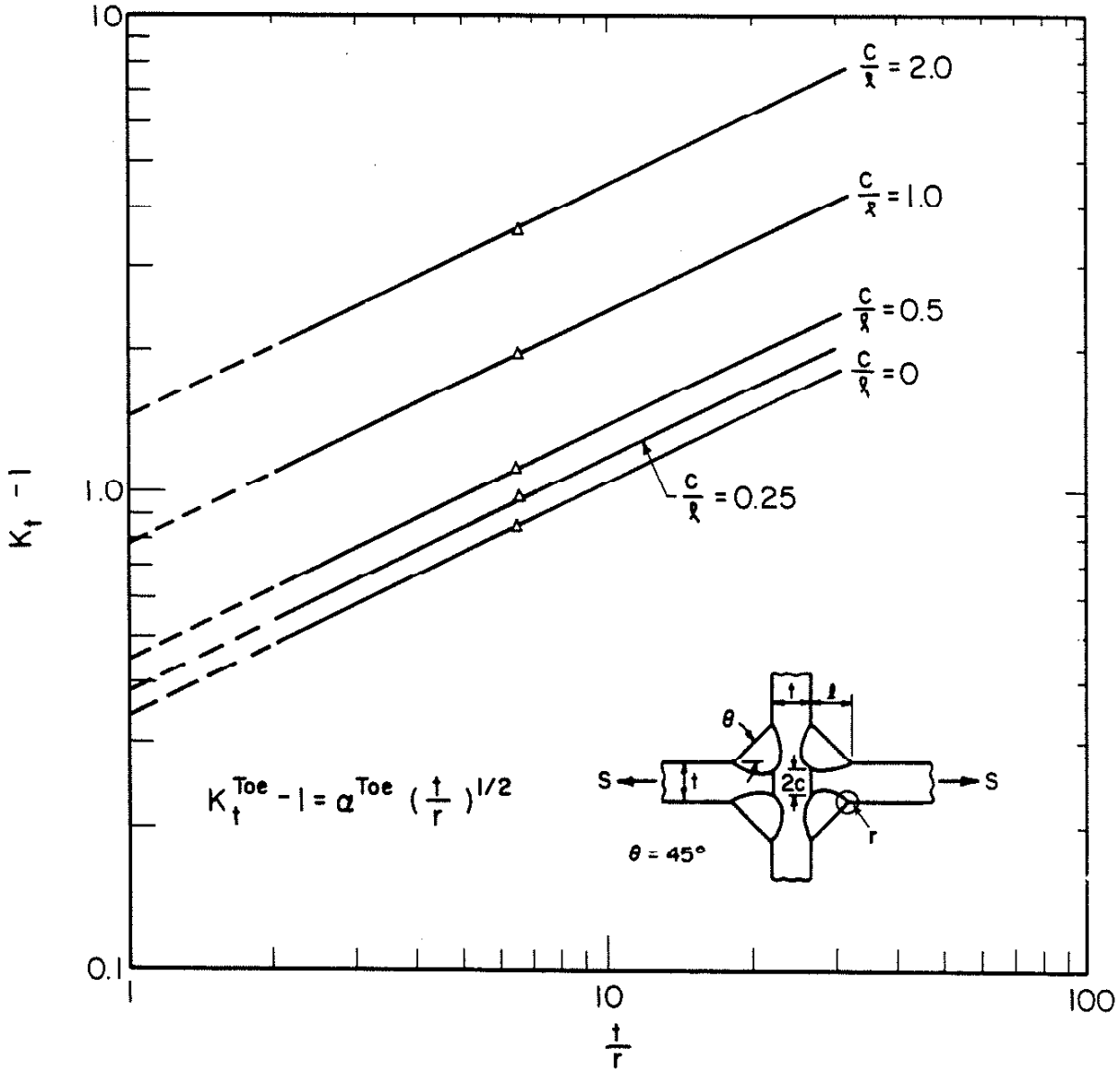

Fig. 3 VARIATION OF K_{t-1} VERSUS t/r FOR THE WELD TOE OF CRUCIFORM WELDMENTS AT DIFFERENT VALUES OF C/ℓ UNDER AXIAL LOADING CONDITIONS.

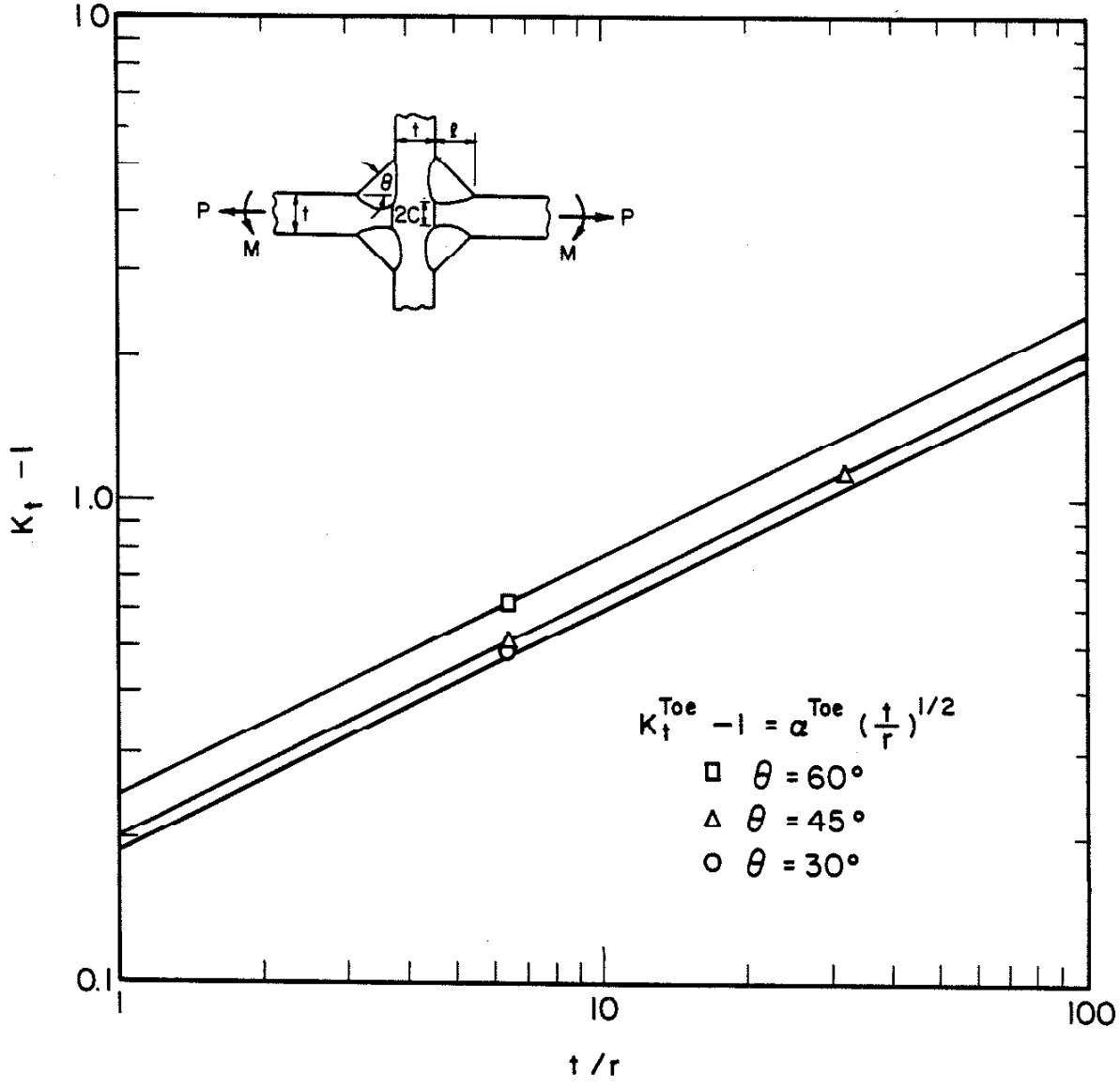

Fig. 4 VARIATION OF K_t-1 VERSUS t/r FOR THE WELD TOE OF CRUCIFORM WELDMENTS UNDER BENDING LOADING CONDITIONS.

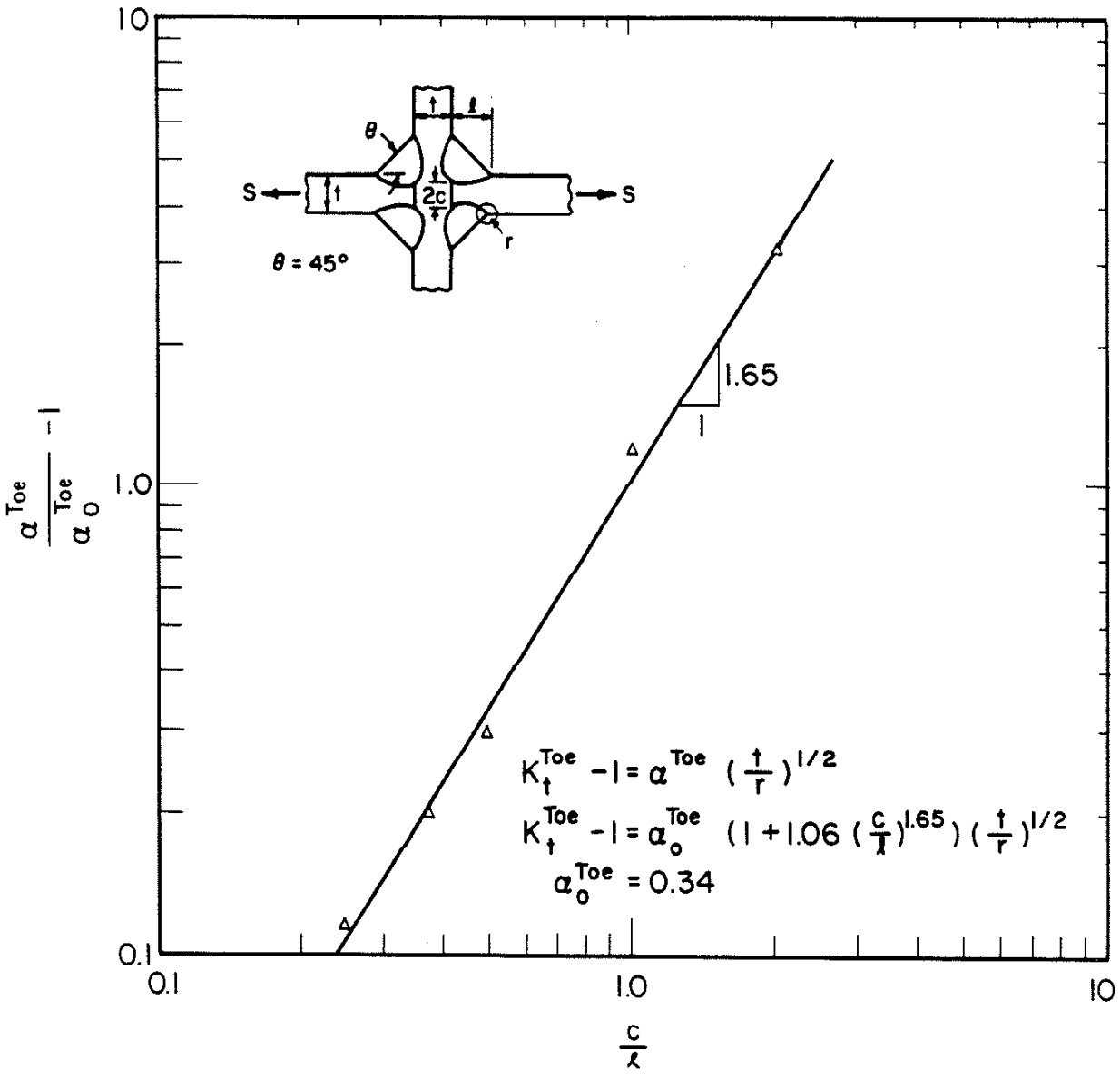

Fig. 5 GEOMETRY COEFFICIENT (α) AS A FUNCTION OF c/ℓ FOR THE WELD TOE OF CRUCIFORM WELDMENTS ($\theta = 45^{\circ}$).

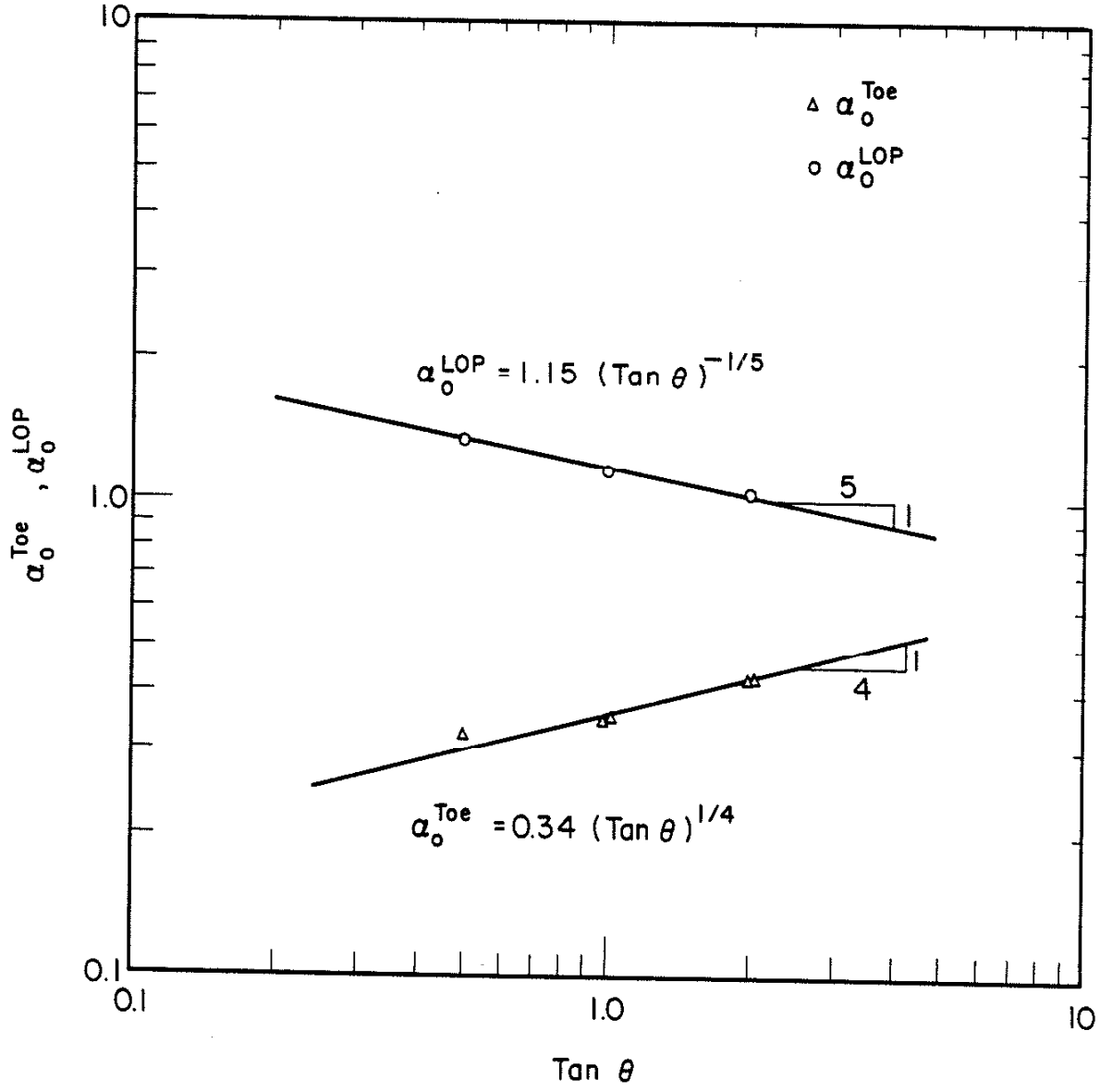

Fig. 6 GEOMETRY COEFFICIENT (α) AS A FUNCTION OF WELD ANGLE (θ) FOR THE WELD TOE AND LOP OF CRUCIFORM WELDMENT.

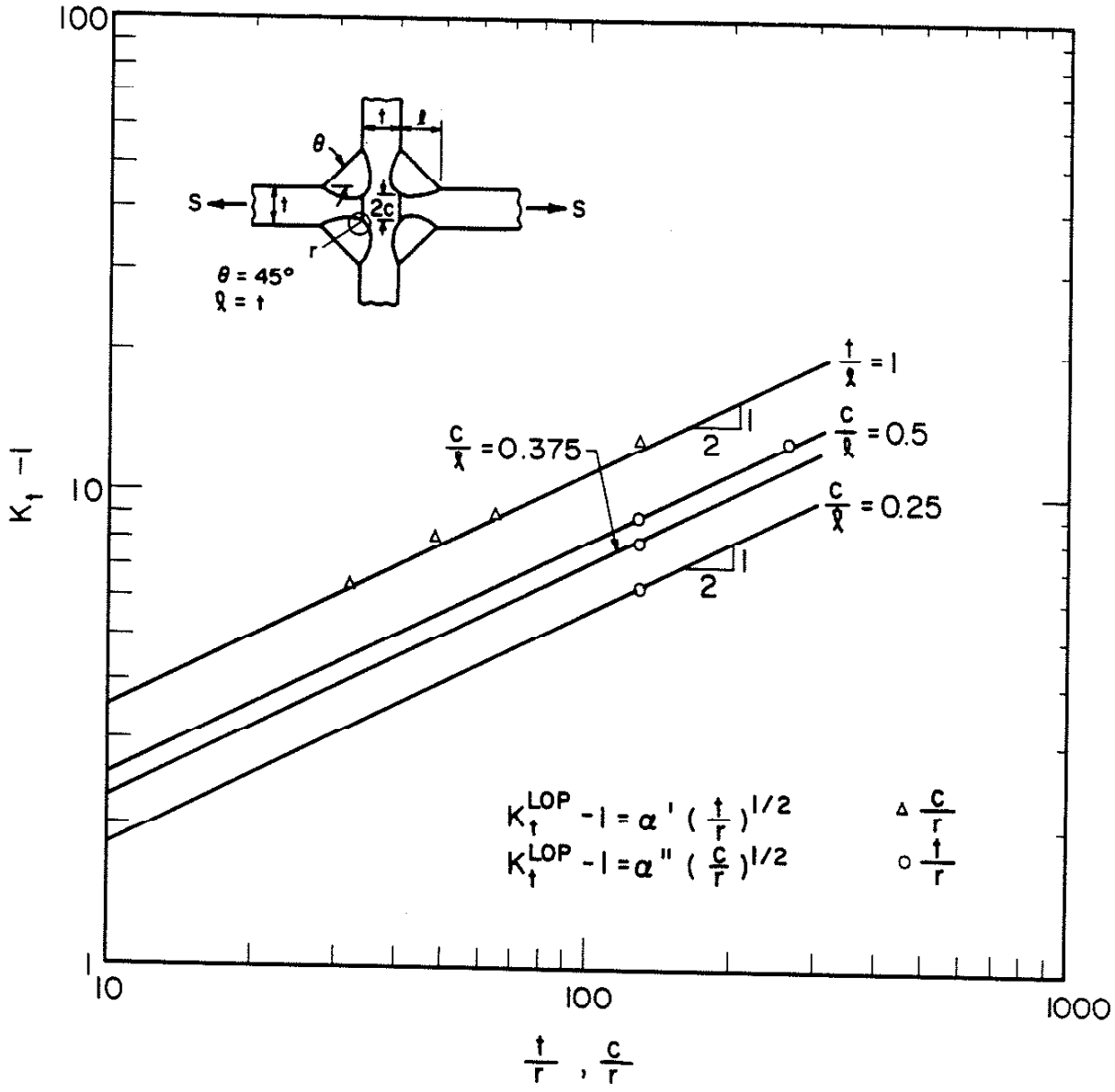

Fig. 7 VARIATION OF $K_t - 1$ VERSUS t/r OR c/r FOR LOP OF THE CRUCIFORM WELDMENT UNDER AXIAL LOADING CONDITIONS.

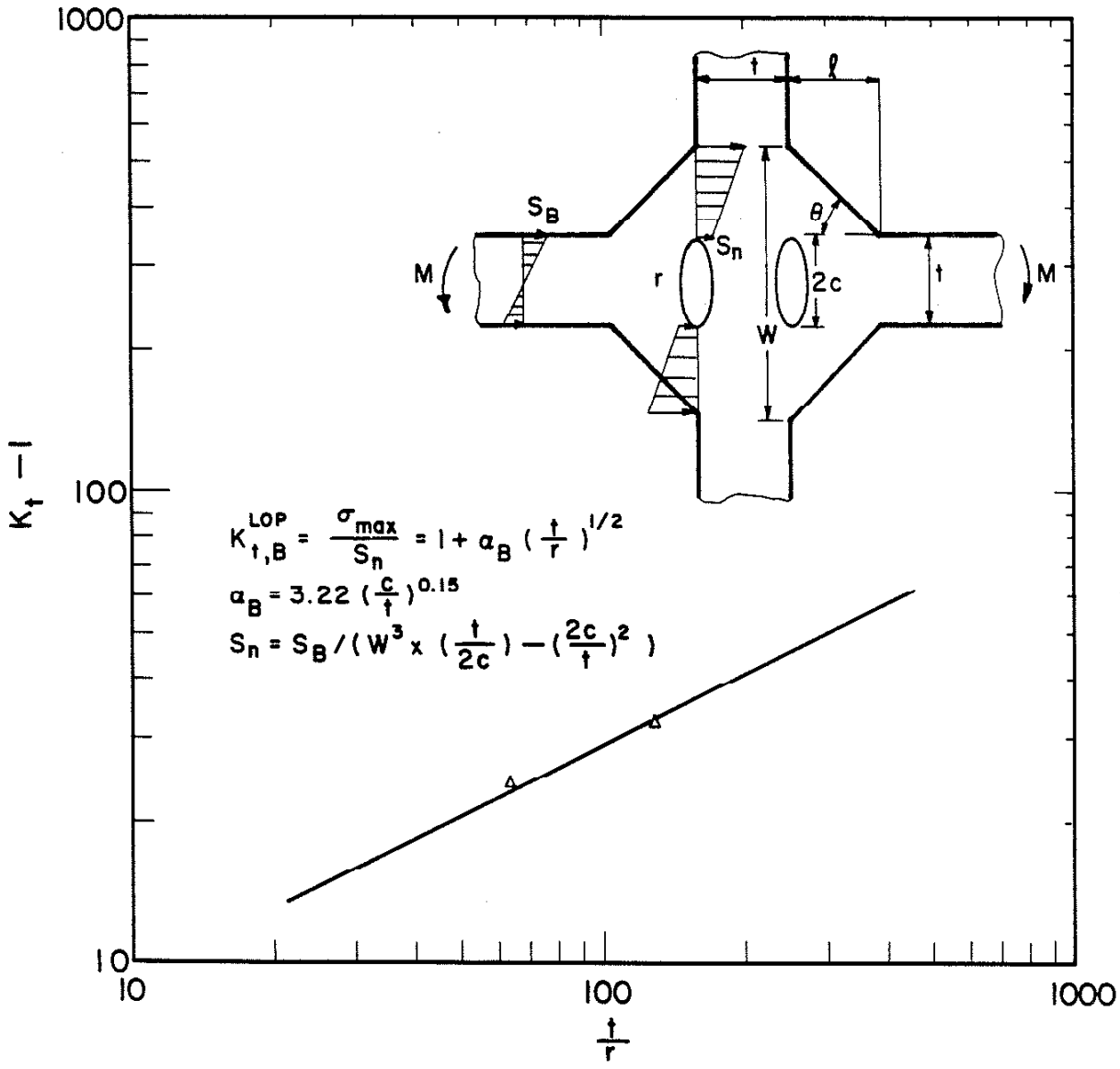

Fig. 8 THEORETICAL STRESS CONCENTRATION FACTOR (K_t) VERSUS t/r FOR LOP OF THE CRUCIFORM WELDMENT UNDER PURE BENDING CONDITIONS.

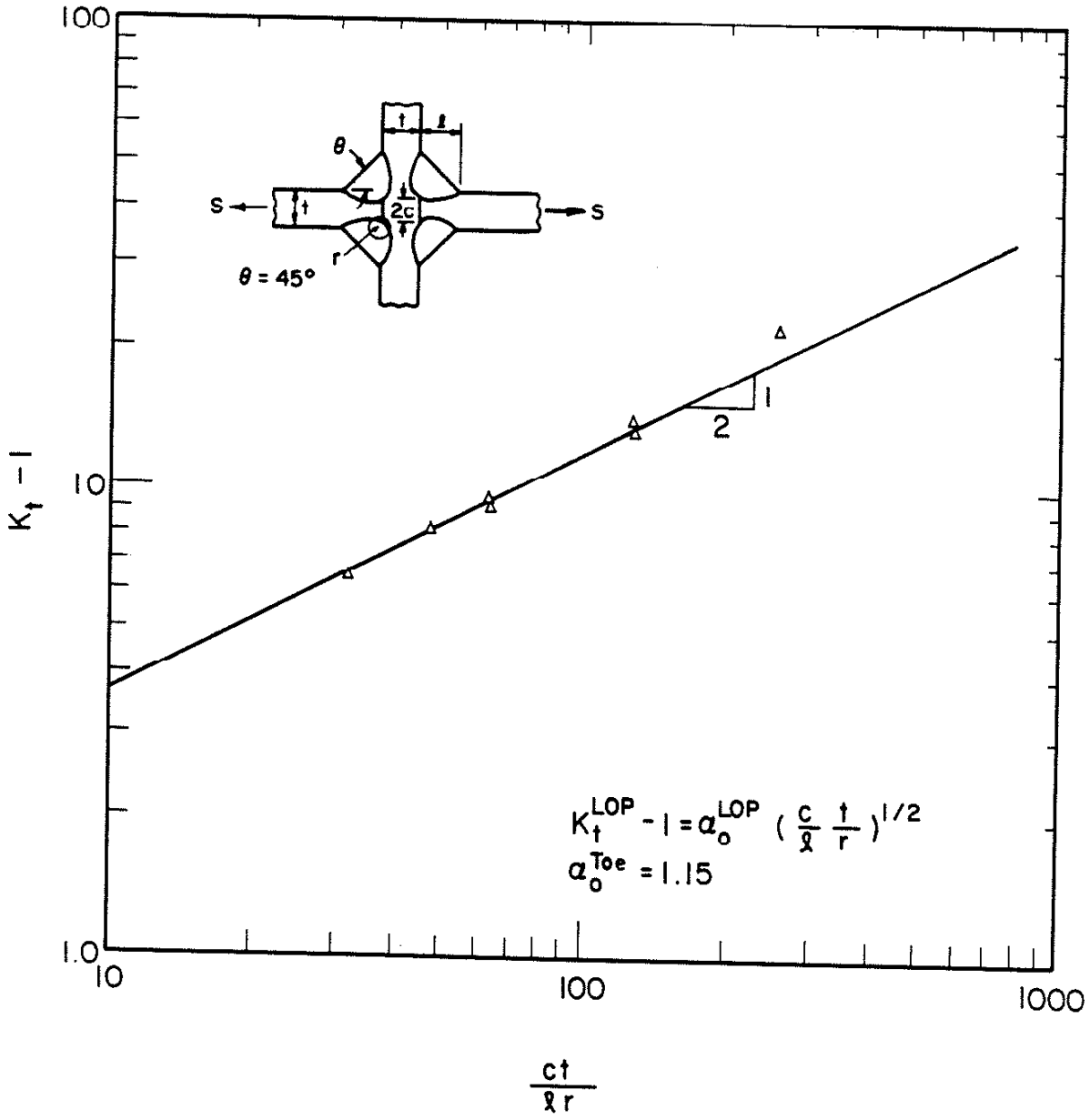

Fig. 9 THEORETICAL STRESS CONCENTRATION FACTOR (K_t) VERSUS $(t/r)(c/\ell)$ FOR LOP OF THE CRUCIFORM WELDMENT UNDER AXIAL LOADING CONDITIONS.

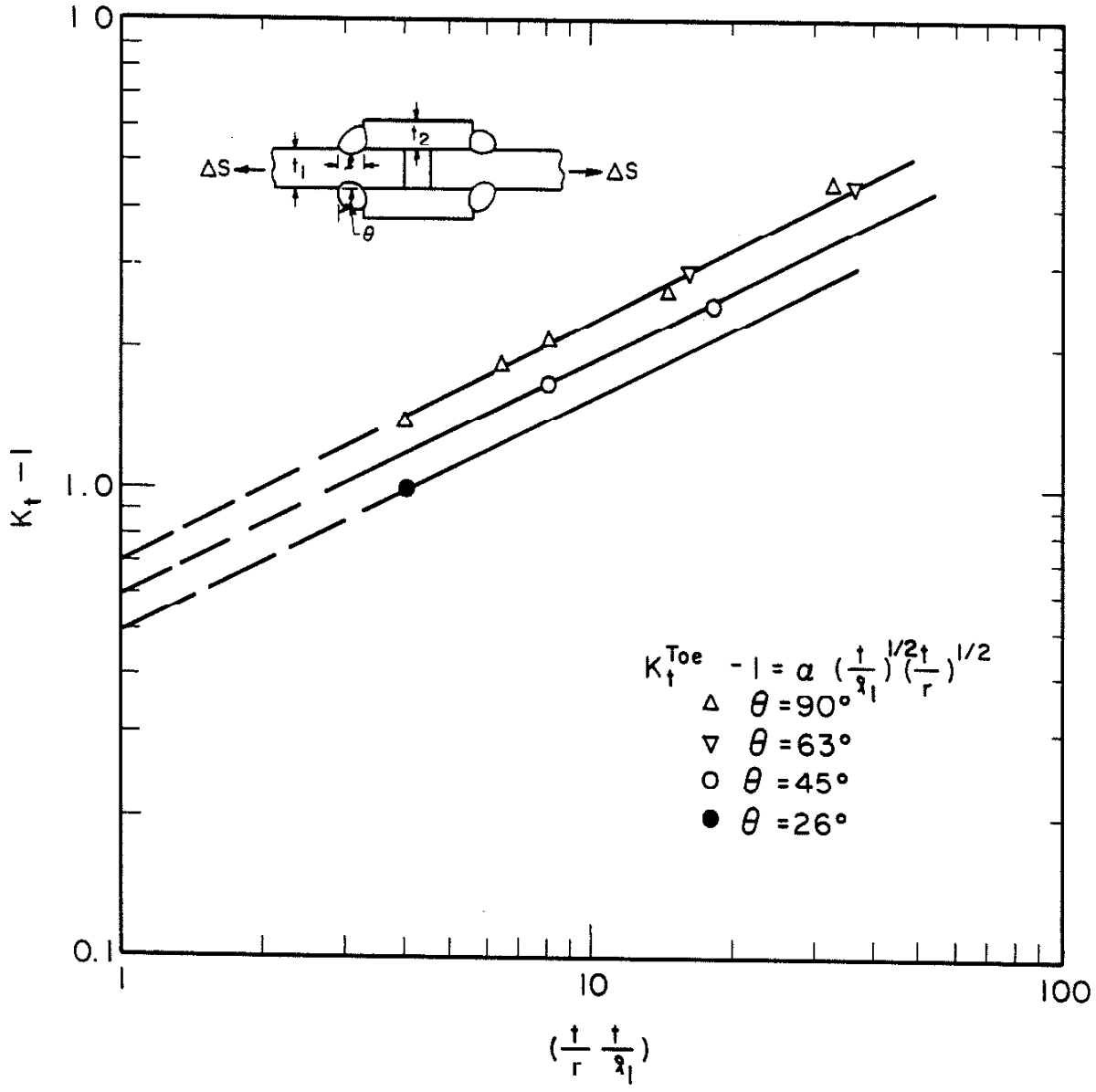

Fig. 10 VARIATION OF K_t-1 VERSUS (t/r)(t/ℓ) FOR THE WELD TOE OF DOUBLE STRAP LAP WELDMENT WITH VARIOUS WELD ANGLES (θ) UNDER AXIAL LOADING CONDITIONS.

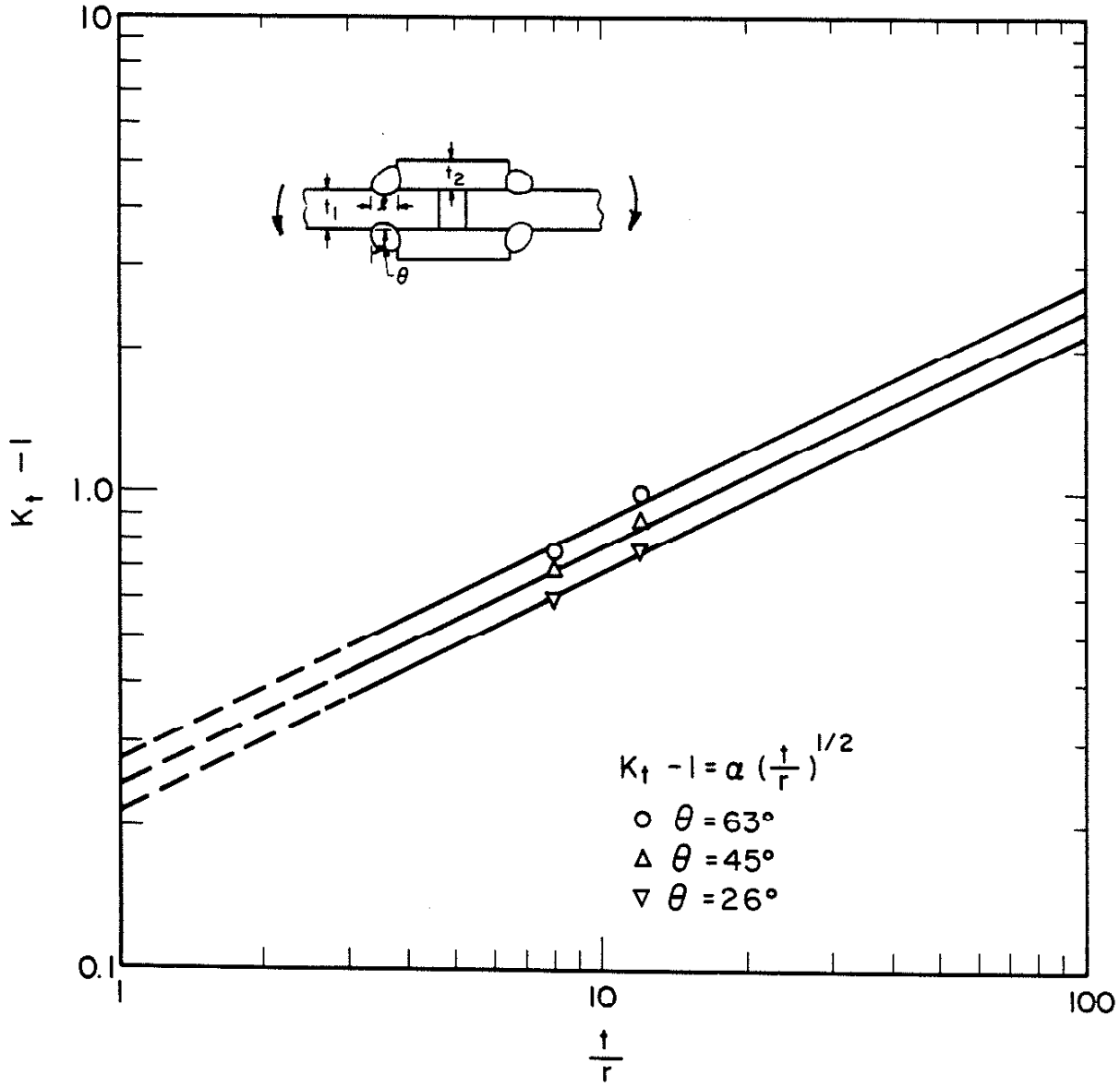

Fig. 11 VARIATION OF $K_t - 1$ VERSUS t/r FOR THE WELD TOE OF DOUBLE STRAP LAP WELDMENT WITH VARIOUS WELD ANGLES (θ) UNDER PURE BENDING CONDITIONS.

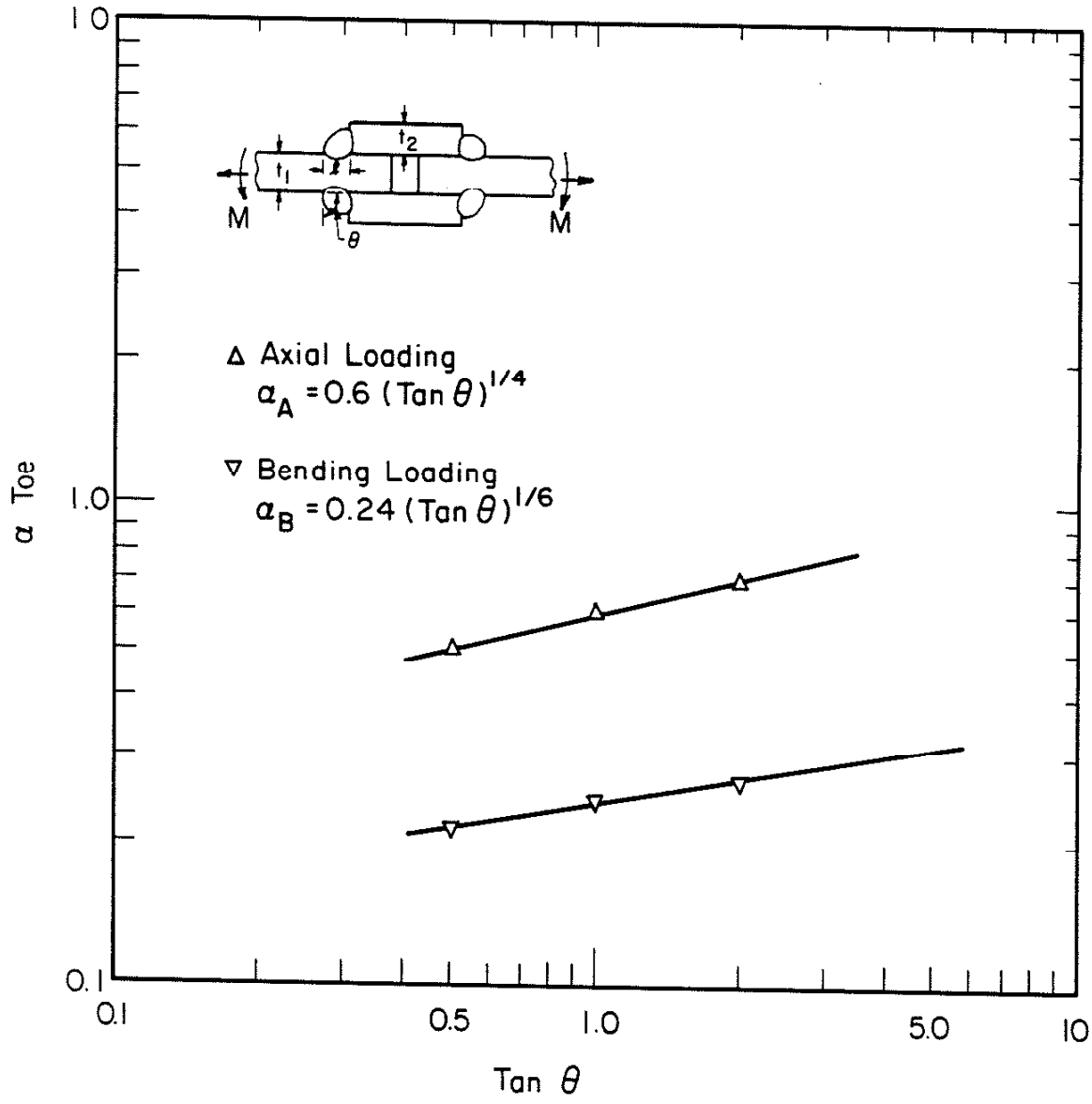

Fig. 12 GEOMETRY COEFFICIENT (α) AS A FUNCTION OF WELD ANGLE (θ) FOR DOUBLE-STRAP LAP WELDMENT UNDER AXIAL OR PURE BENDING LOADING CONDITIONS.

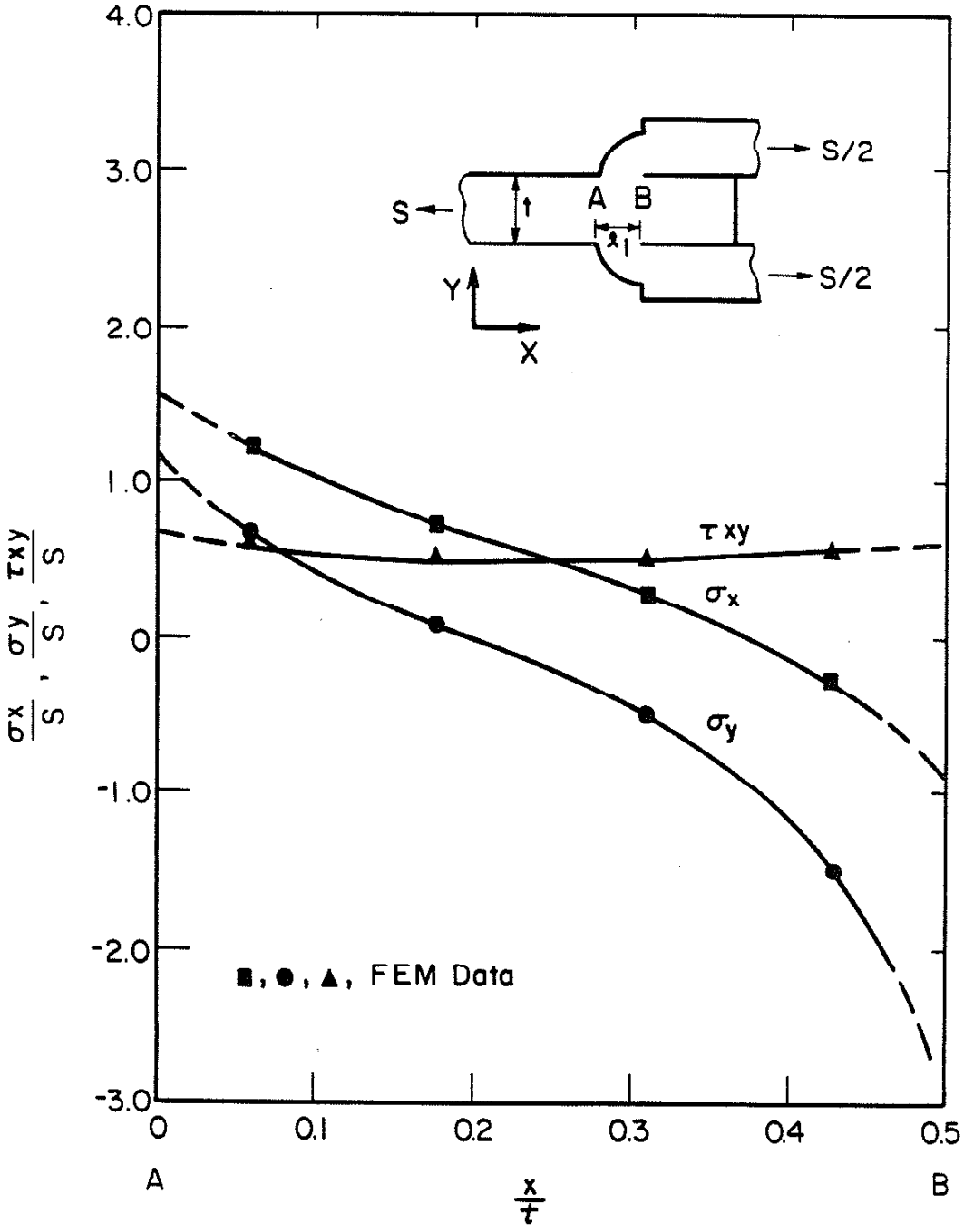

Fig. 13 VARIATION OF NORMAL STRESS (σ_y) ALONG THE PATH FROM THE TOE TO THE ROOT FOR DOUBLE-STRAP LAP WELDMENT.

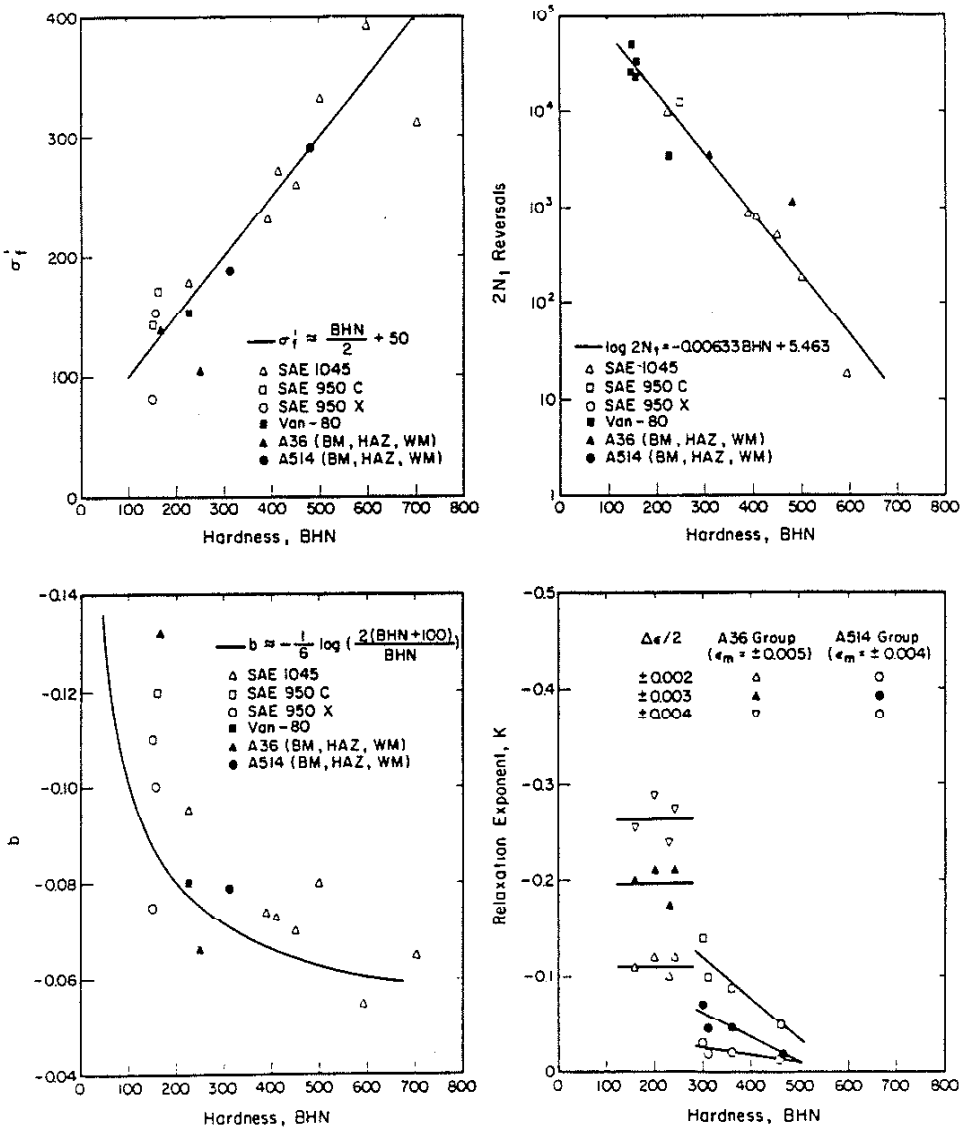

Fig. 14 VARIATION OF σ_f', b, $2N_t$, AND k WITH BRINNEL HARDNESS (BHN) [10].

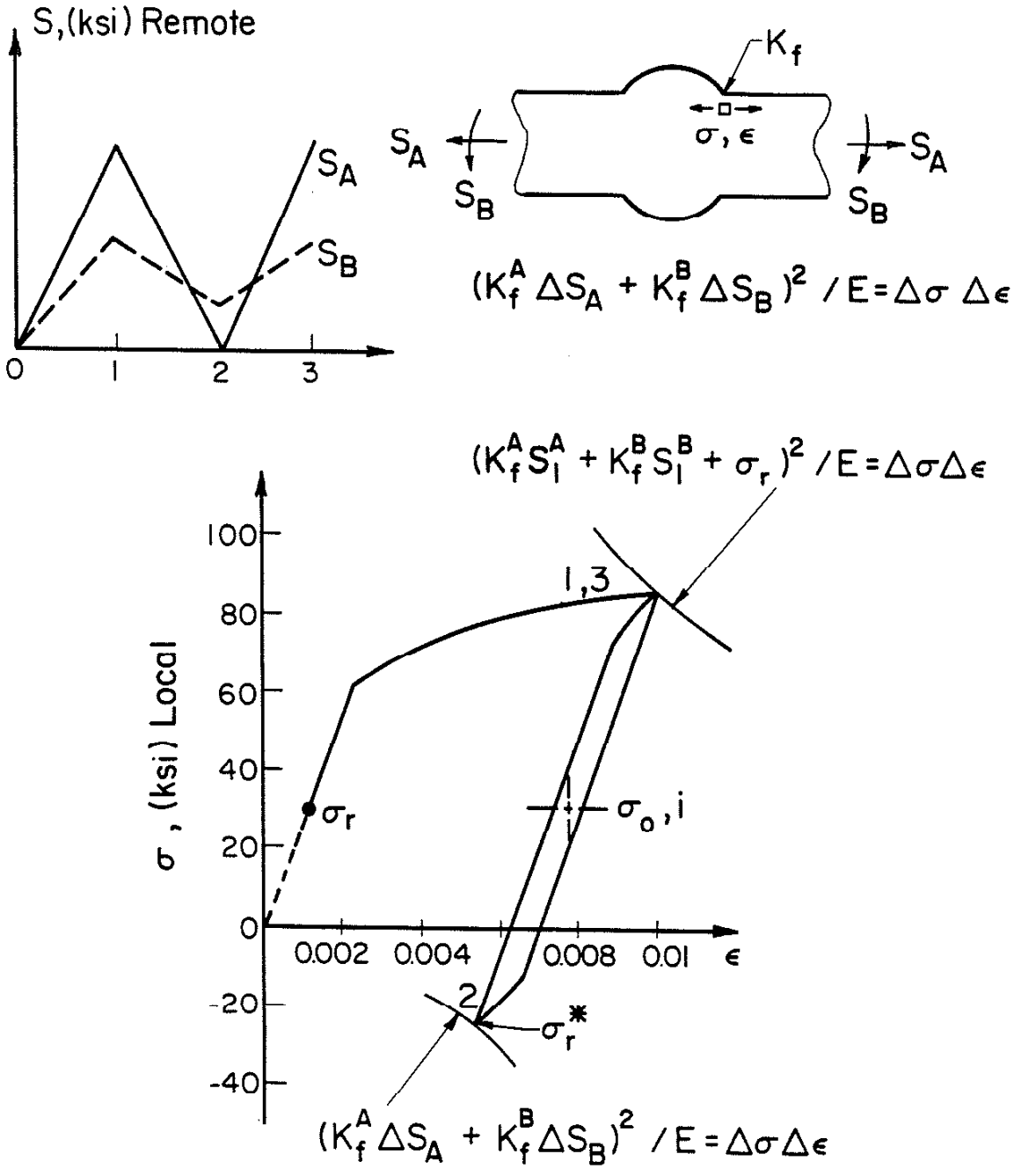

Fig. 15 COMPUTER SIMULATED LOCAL STRESS-STRAIN RESPONSE AT THE WELD TOE WITH TENSILE RESIDUAL STRESSES.

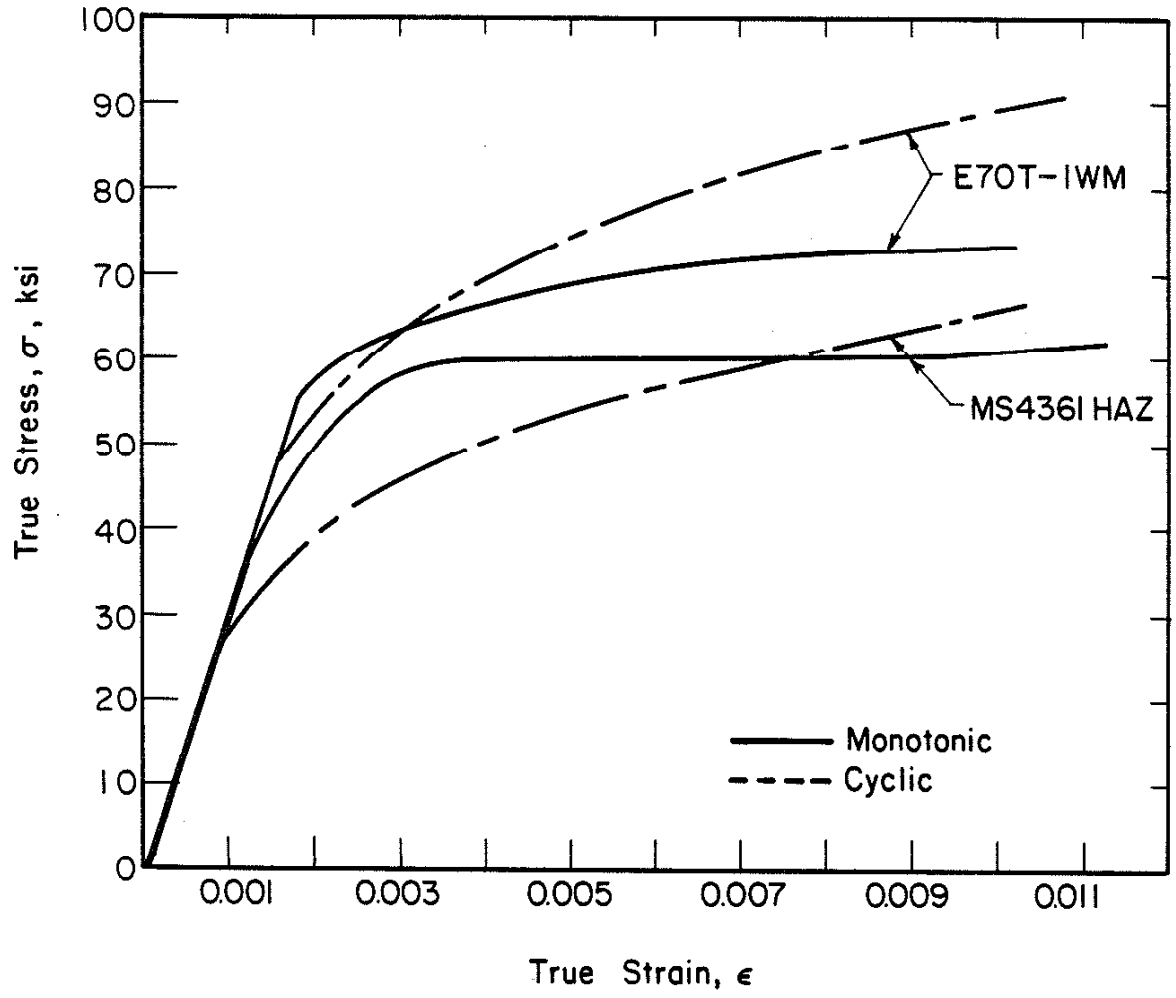

Fig. 16 MONOTONIC AND CYCLIC TRUE STRESS-STRAIN BEHAVIOR OF MS4361 HAZ AND E70T-1 WELD METAL.

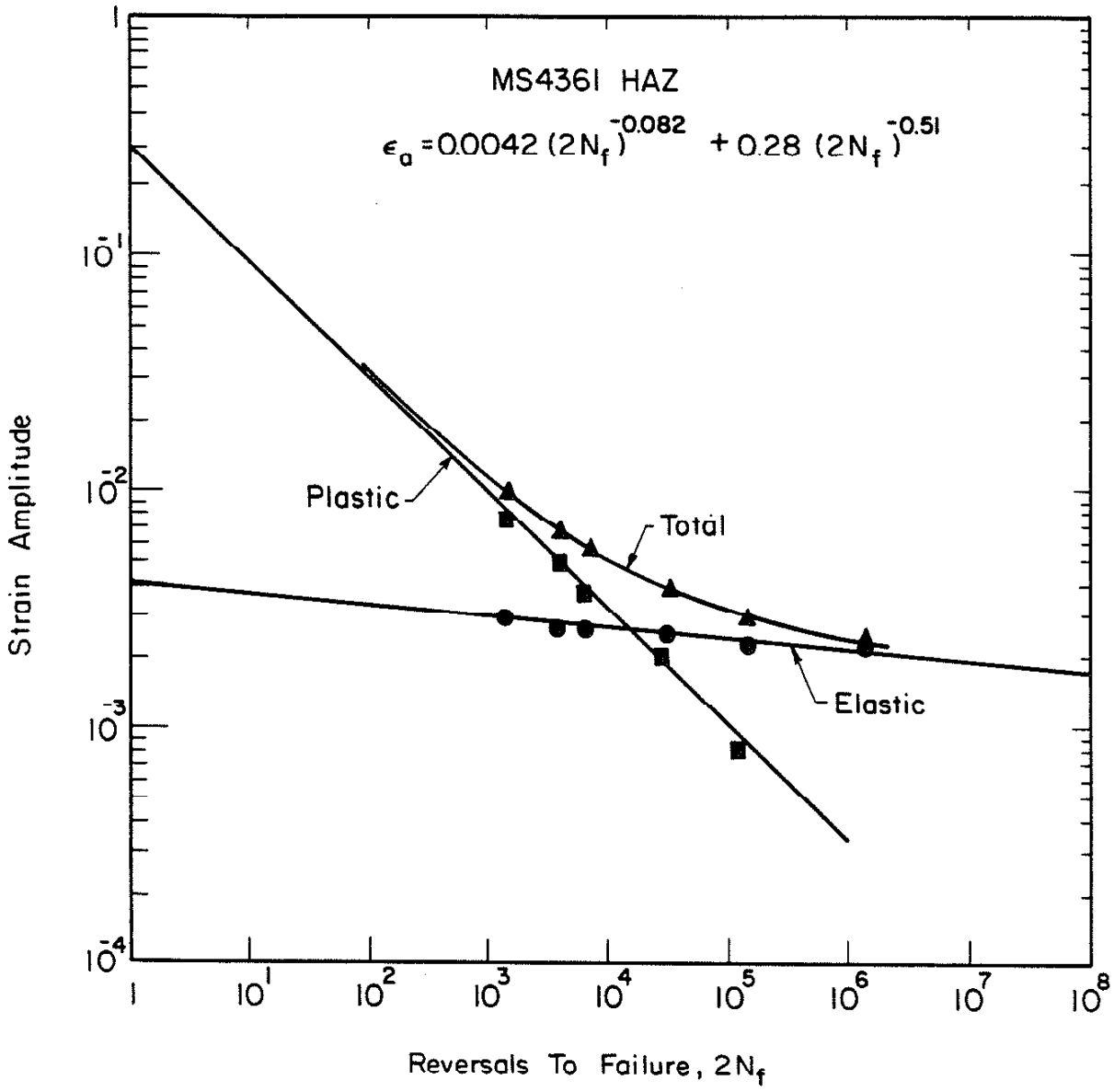

Fig. 17 STRAIN-LIFE PLOT FOR MS4361 HAZ MATERIAL.

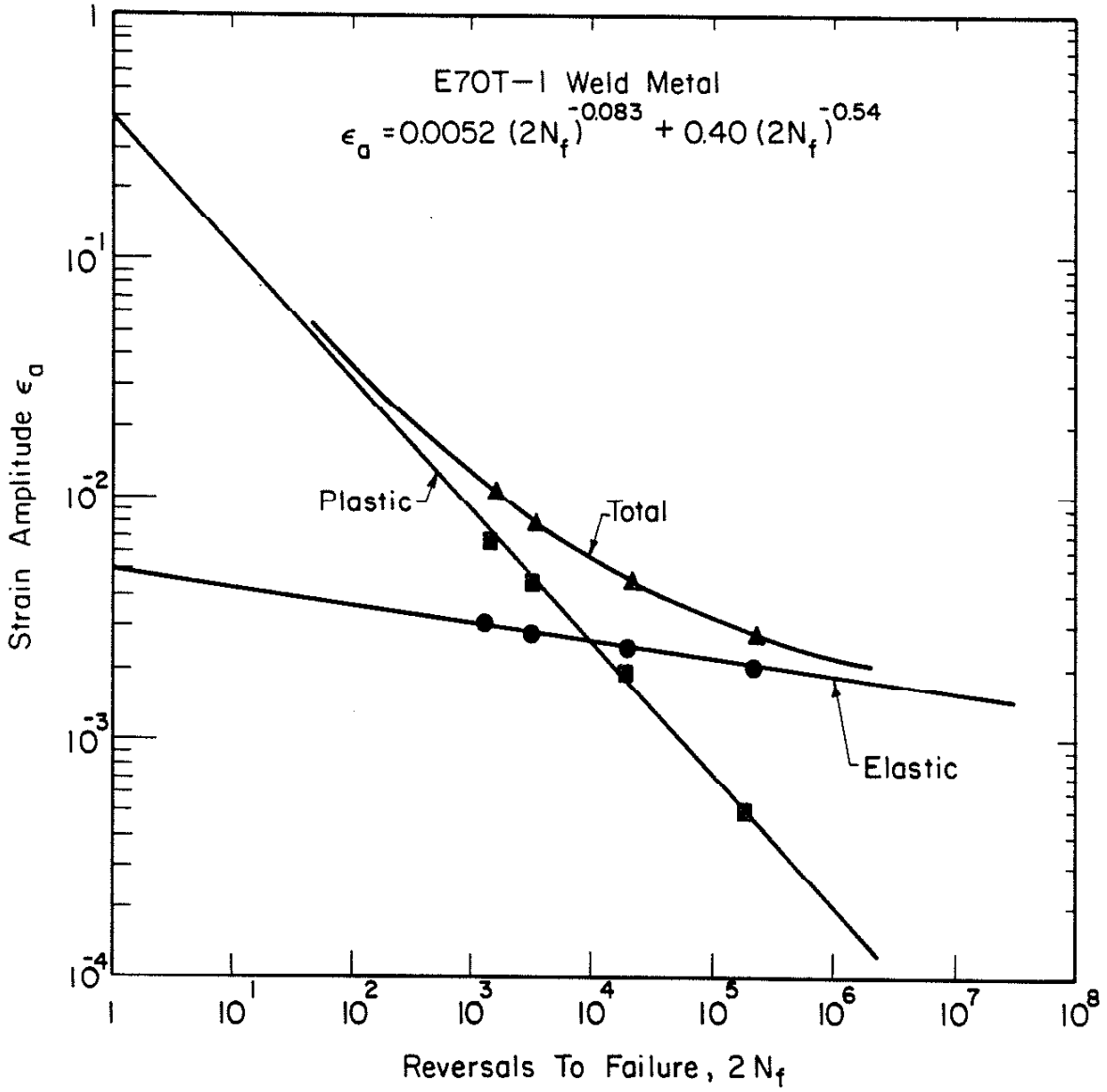

Fig. 18 STRAIN-LIFE PLOT FOR E70T-1 WELD METAL.

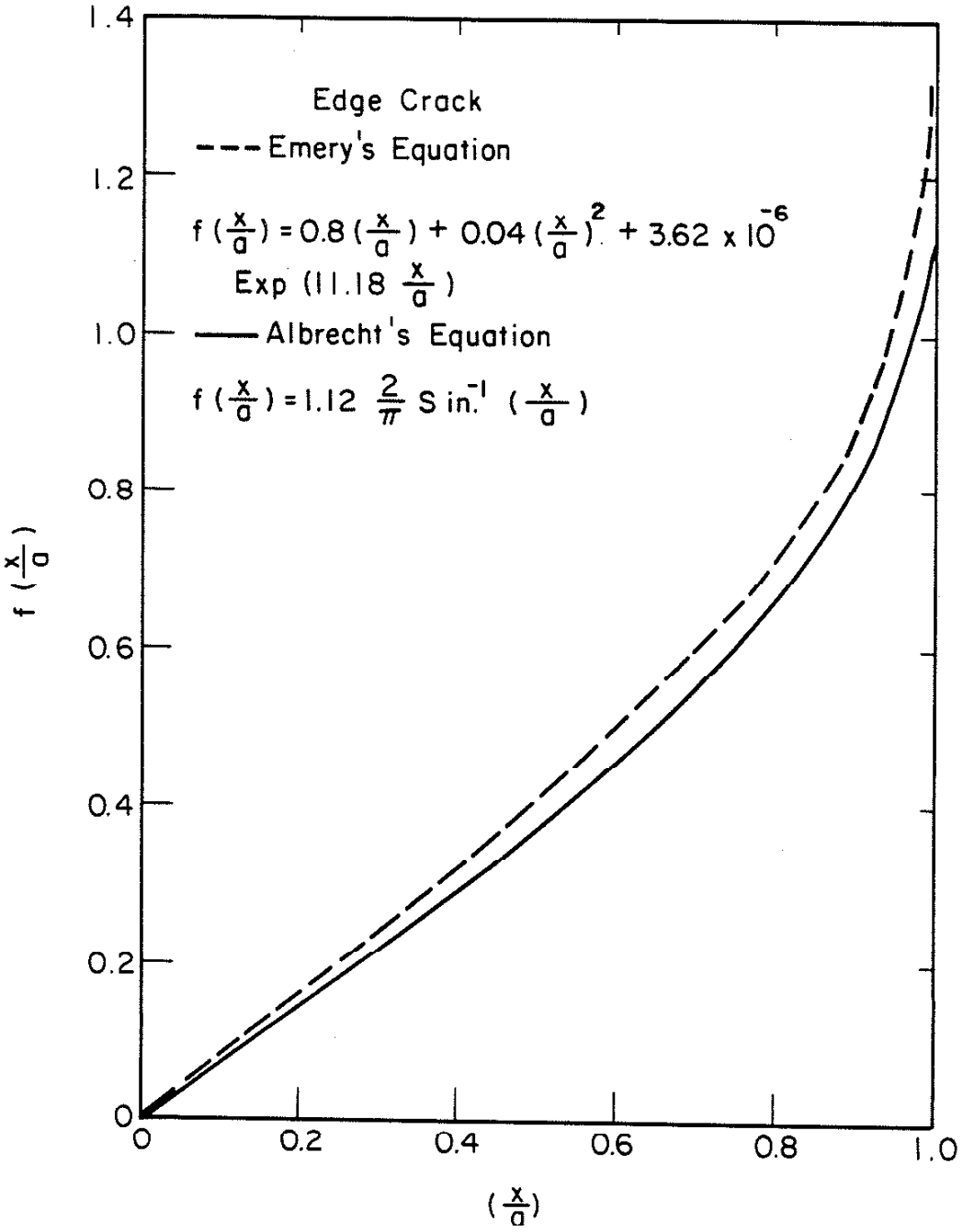

Fig. 19 COMPARISON OF EMERY'S AND ALBRECHT'S EQUATIONS.

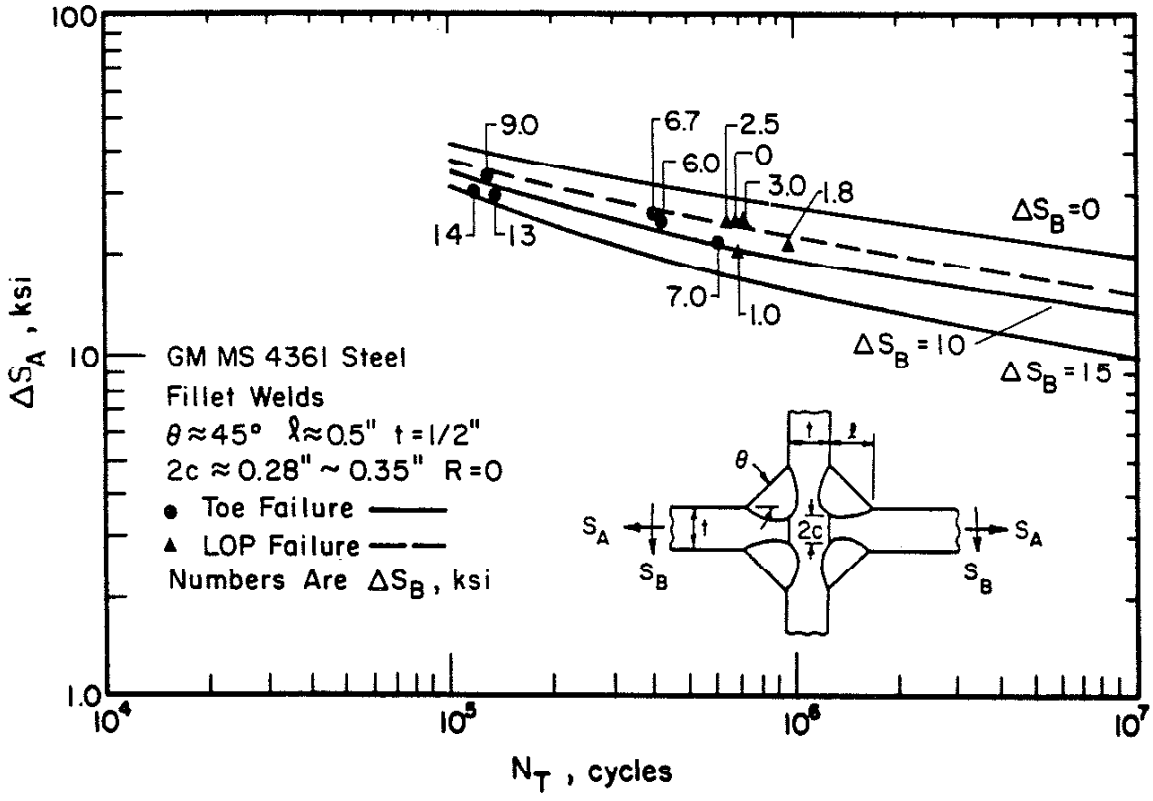

Fig. 20 TOTAL FATIGUE LIFE PREDICTIONS AND EXPERIMENTAL RESULTS FOR MS4361 CRUCIFORM WELDMENTS AT A STRESS RATIO OF R = 0.

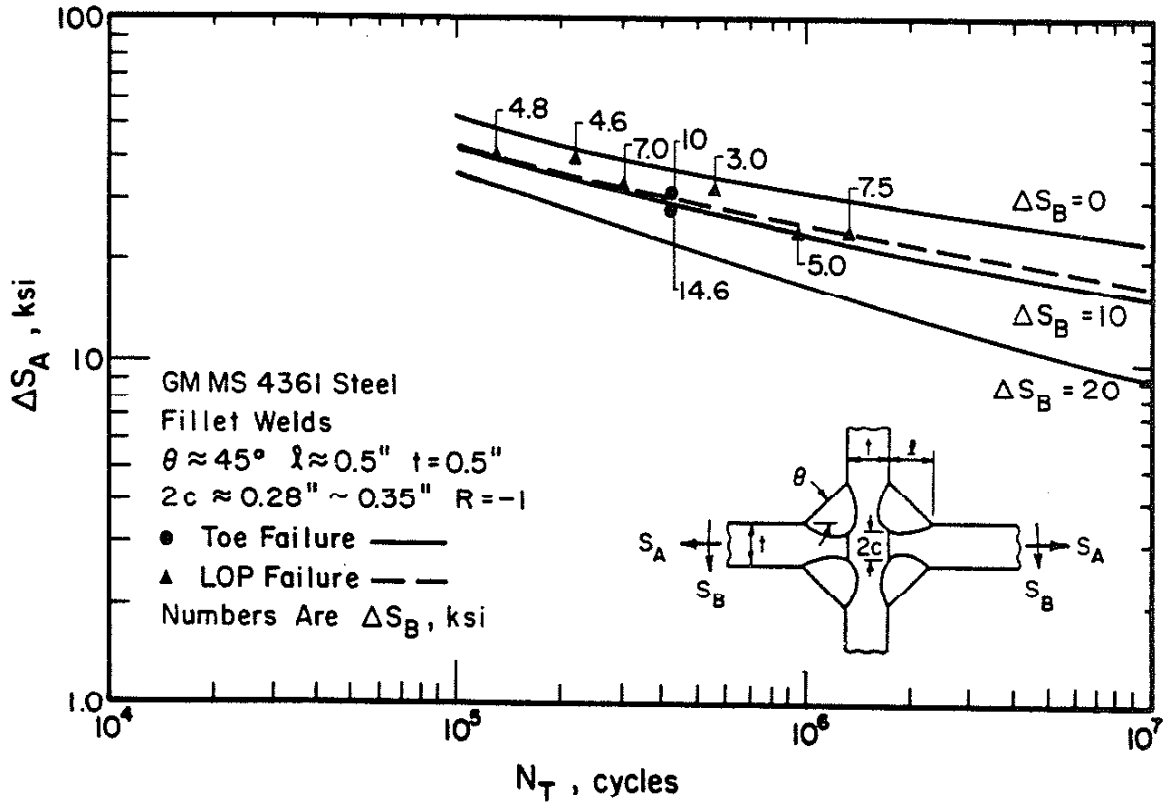

Fig. 21 TOTAL FATIGUE LIFE PREDICTIONS AND EXPERIMENTAL RESULTS FOR MS4361 CRUCIFORM WELDMENTS AT A STRESS RATIO OF R = -1.

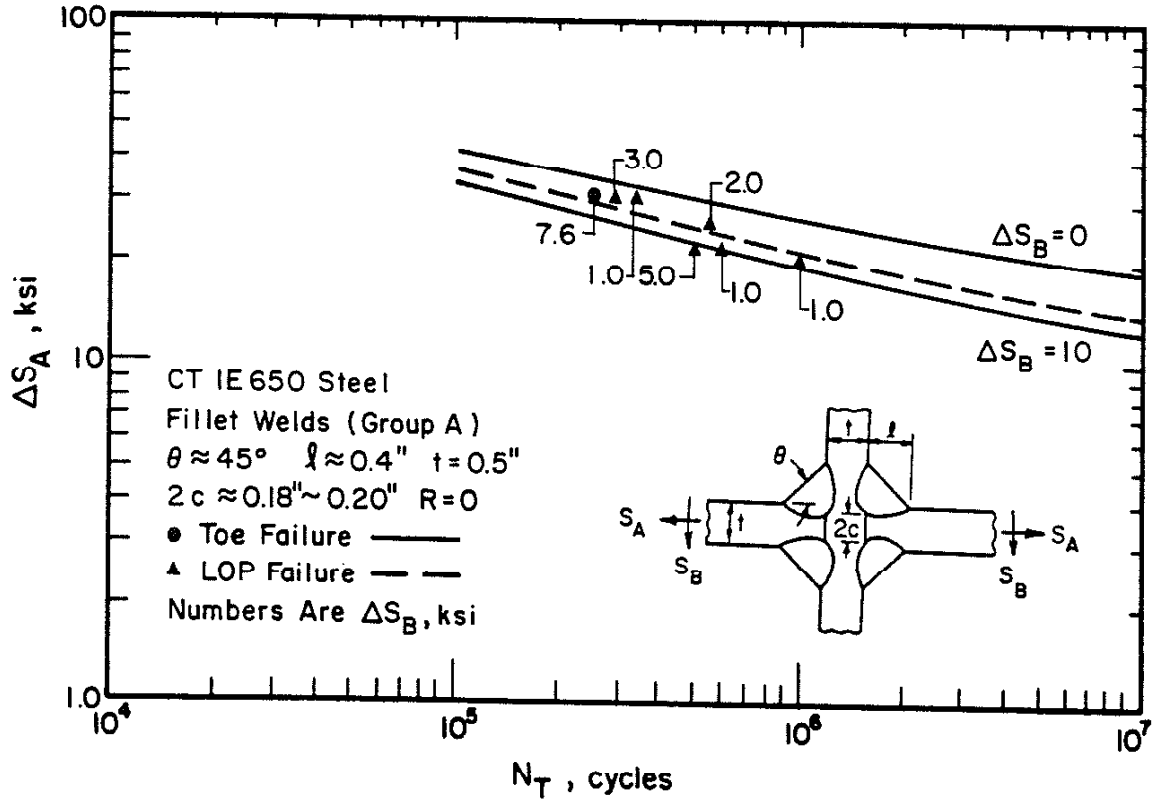

Fig. 22 TOTAL FATIGUE LIFE PREDITIONS AND EXPERIMENTAL RESULTS FOR 1E650 CRUCIFORM WELDMENTS (GROUP A) AT A STRESS RATIO OF R = 0.

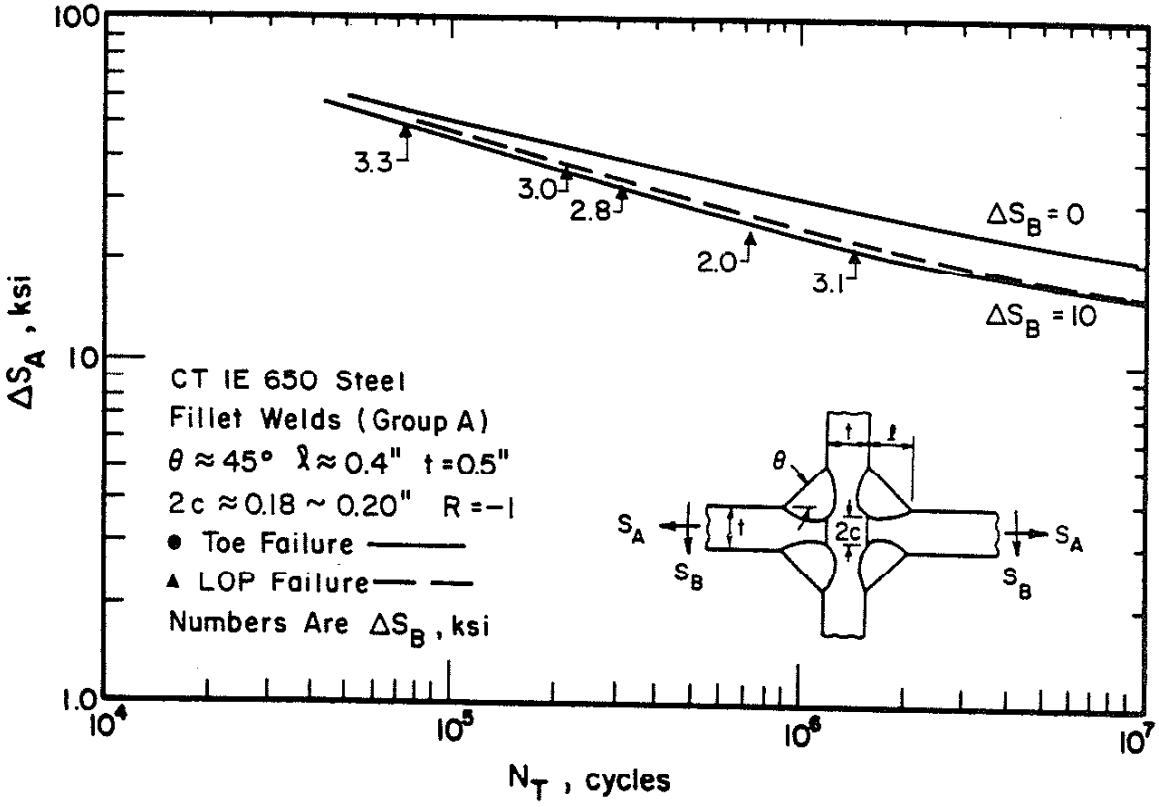

Fig. 23 TOTAL FATIGUE LIFE PREDICTIONS AND EXPERIMENTAL RESULTS FOR 1E650 CRUCIFORM WELDMENTS (GROUP A) AT A STRESS RATIO OF R =-1.

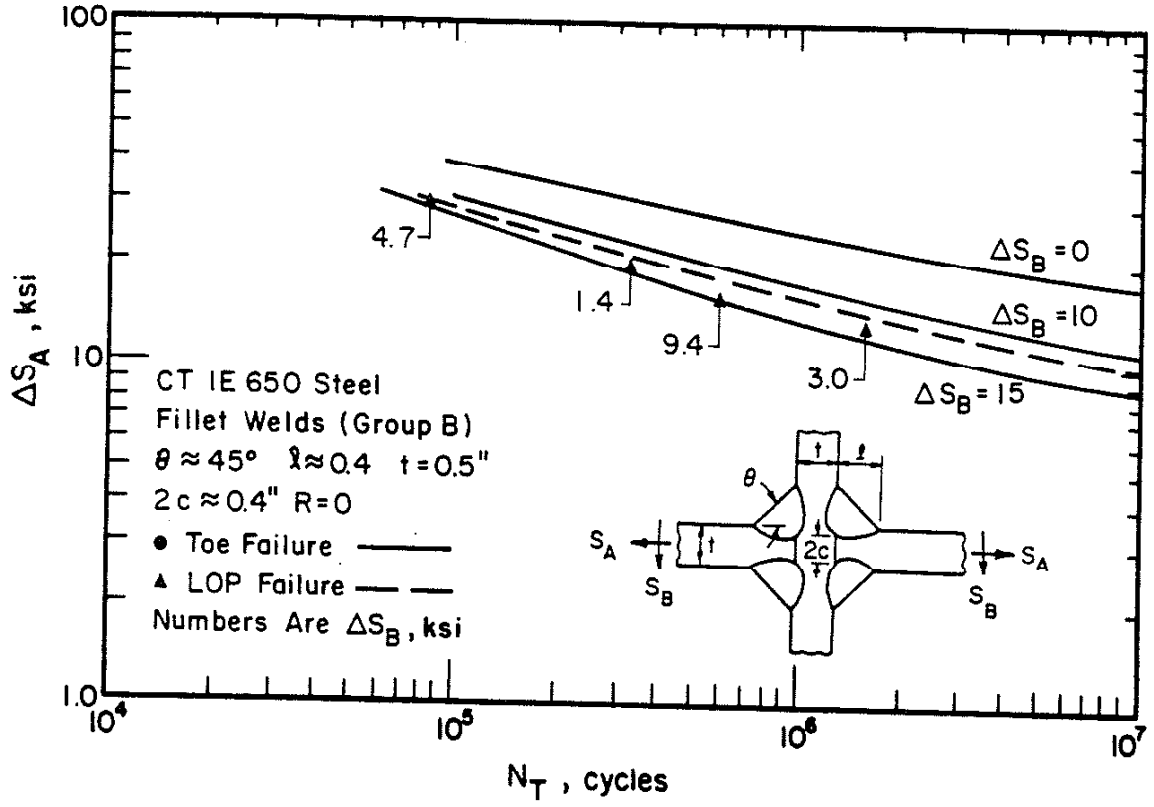

Fig. 24 TOTAL FATIGUE LIFE PREDICITONS AND EXPERIMENTAL RESULTS FOR 1E650 CRUCIFORM WELDMENTS (GROUP B) AT A STRESS RATIO OF R = 0.

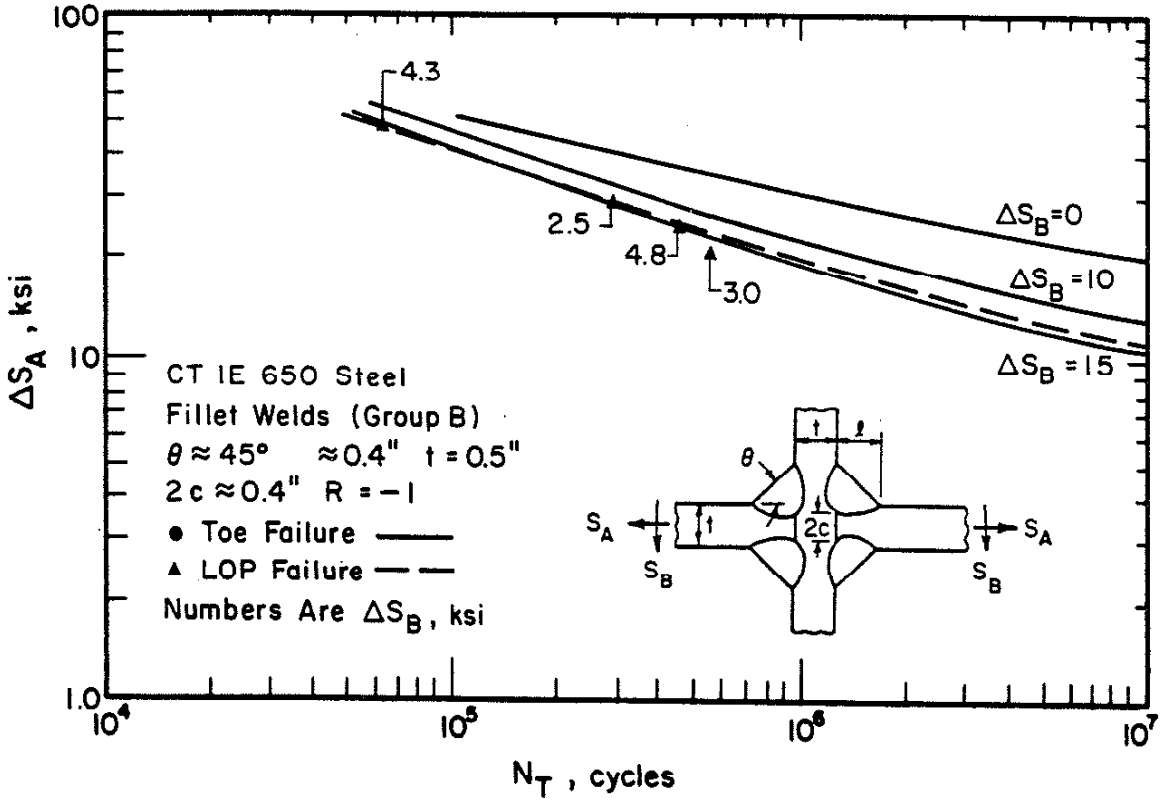

Fig. 25 TOTAL FATIGUE LIFE PREDICTIONS AND EXPERIMENTAL RESULTS FOR 1E650 CRUCIFORM WELDMENTS (GROUP B) AT A STRESS RATIO OF R =-1.

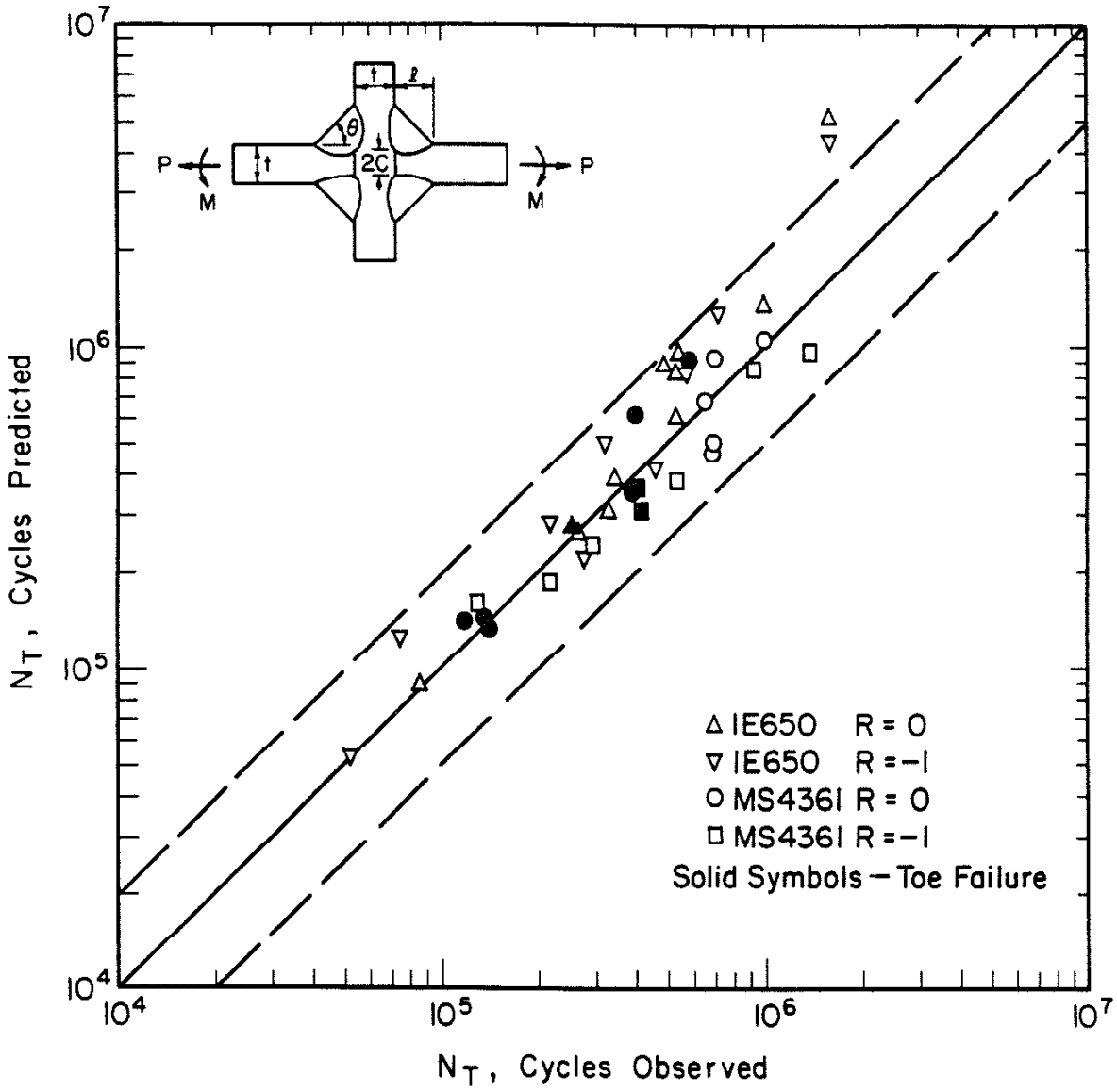

Fig. 26 COMPARISON OF PREDICTED AND OBSERVED TOTAL FATIGUE LIFE FOR VARIOUS CRUCIFORM WELDMENTS.

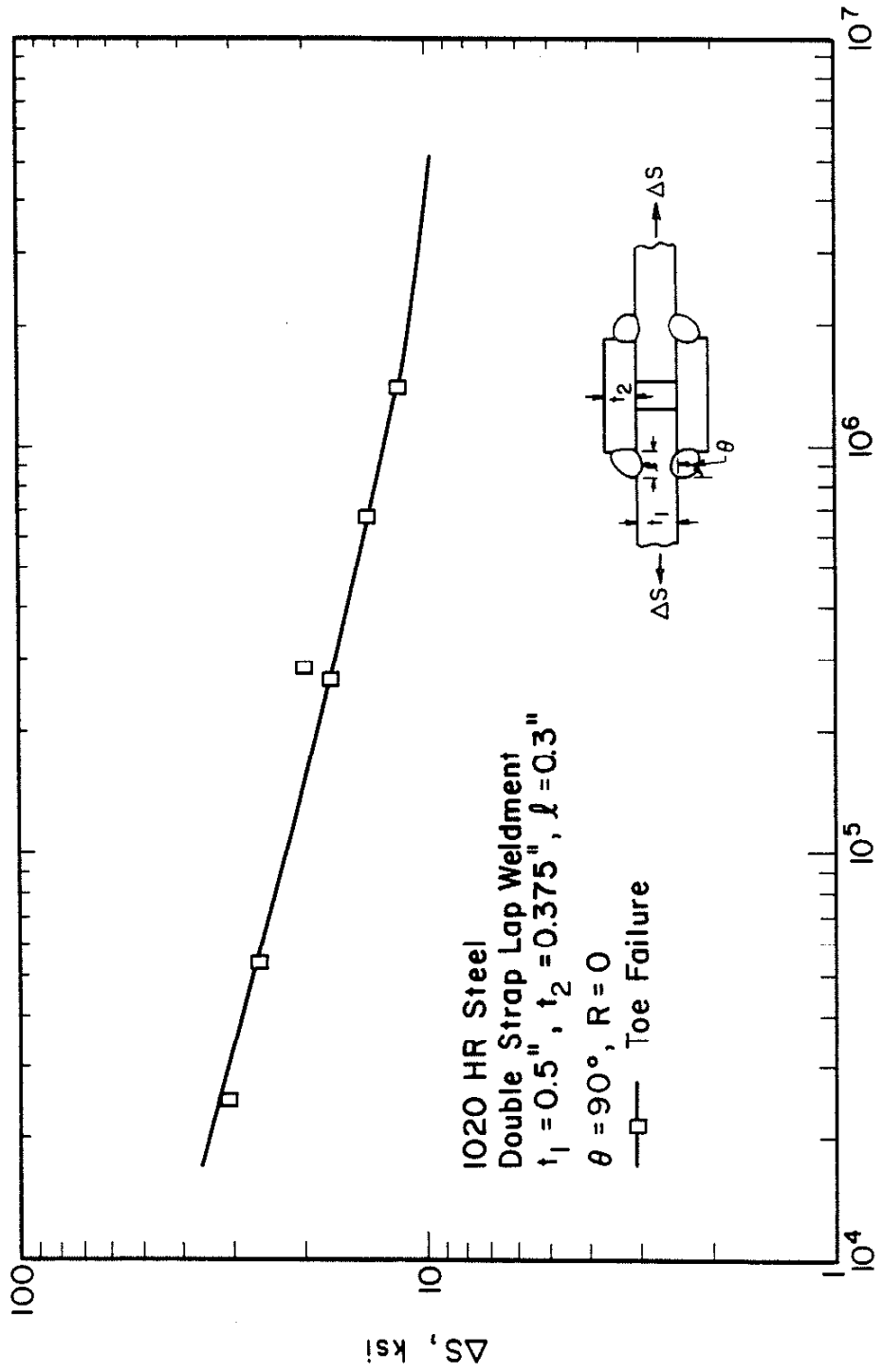

Fig. 27 TOTAL FATIGUE LIFE PREDICTIONS AND EXPERIMENTAL RESULTS FOR DOUBLE-STRAP LAP WELDMENTS AT A STRESS RATIO OF R = 0.

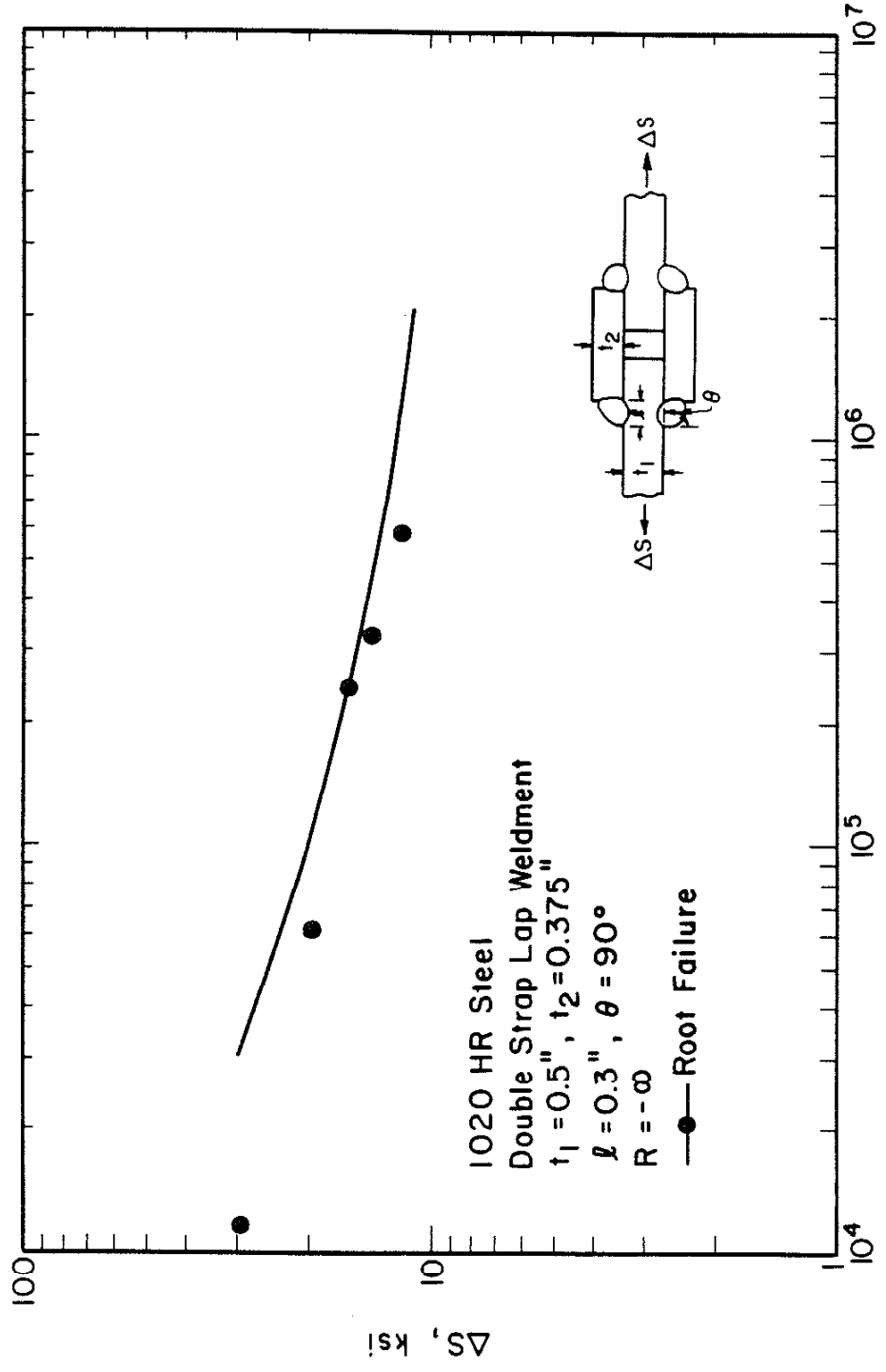

Fig. 28 TOTAL FATIGUE LIFE PREDICTIONS AND EXPERIMENTAL RESULTS FOR DOUBLE-STRAP LAP WELDMENTS AT A STRESS RATIO OF R = - ∞.

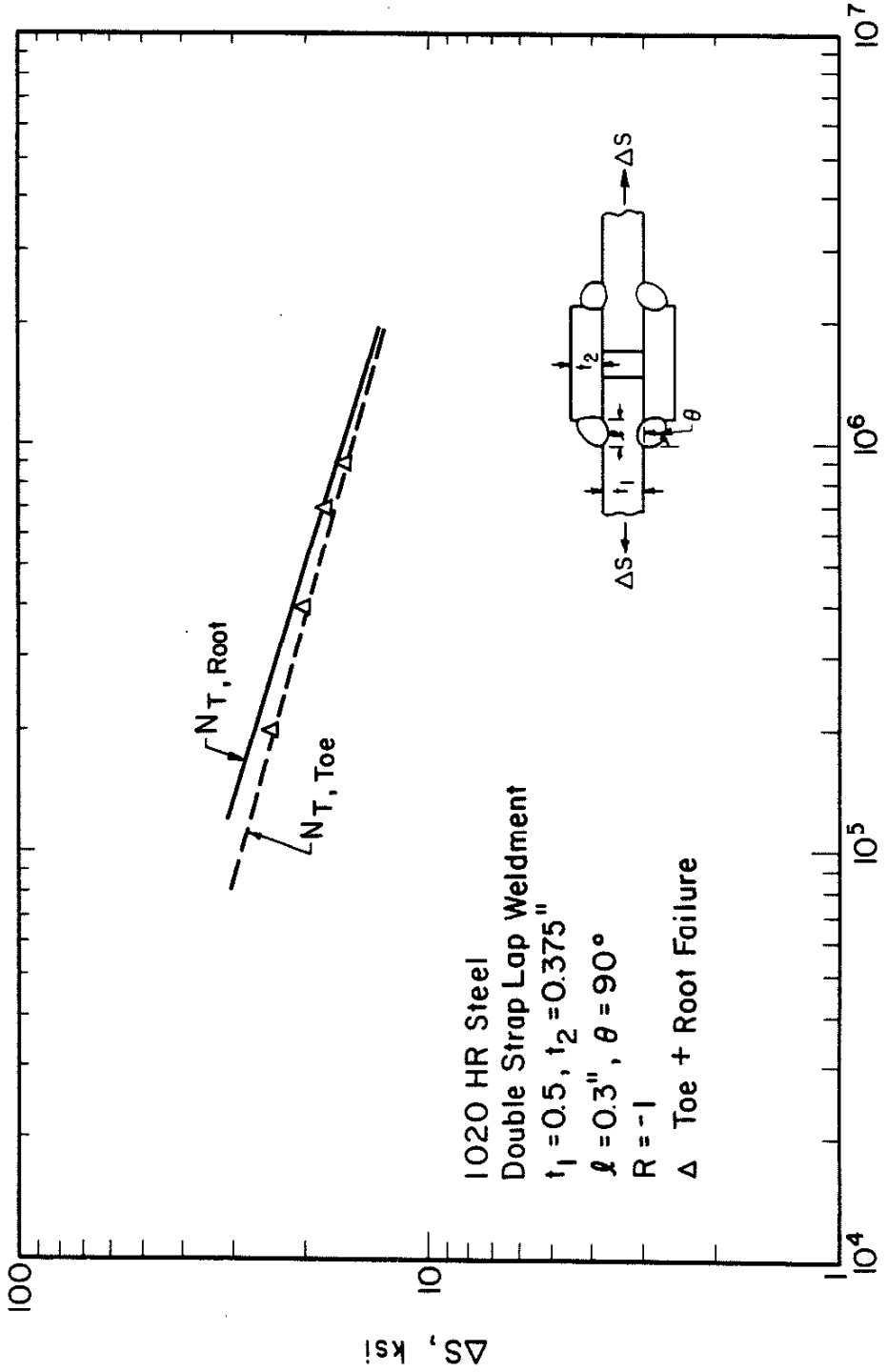

Fig. 29 TOTAL FATIGUE LIFE PREDICTIONS AND EXPERIMENTAL RESULTS FOR DOUBLE-STRAP LAP WELDMENTS AT A STRESS RATIO OF R = -1.

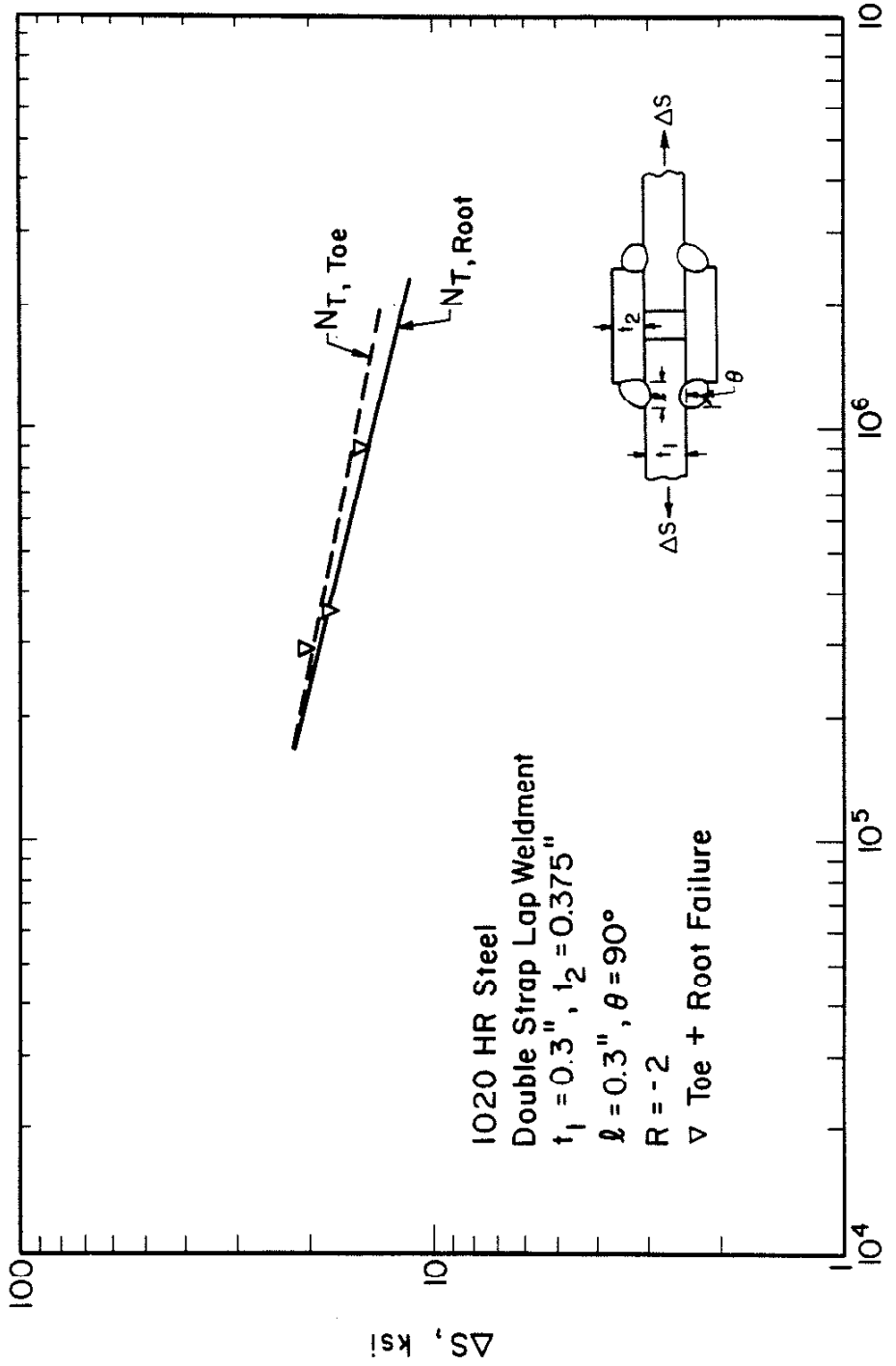

Fig. 30 TOTAL FATIGUE LIFE PREDICTIONS AND EXPERIMENTAL RESULTS FOR DOUBLE-STRAP LAP WELDMENTS AT A STRESS RATIO OF R = -2.

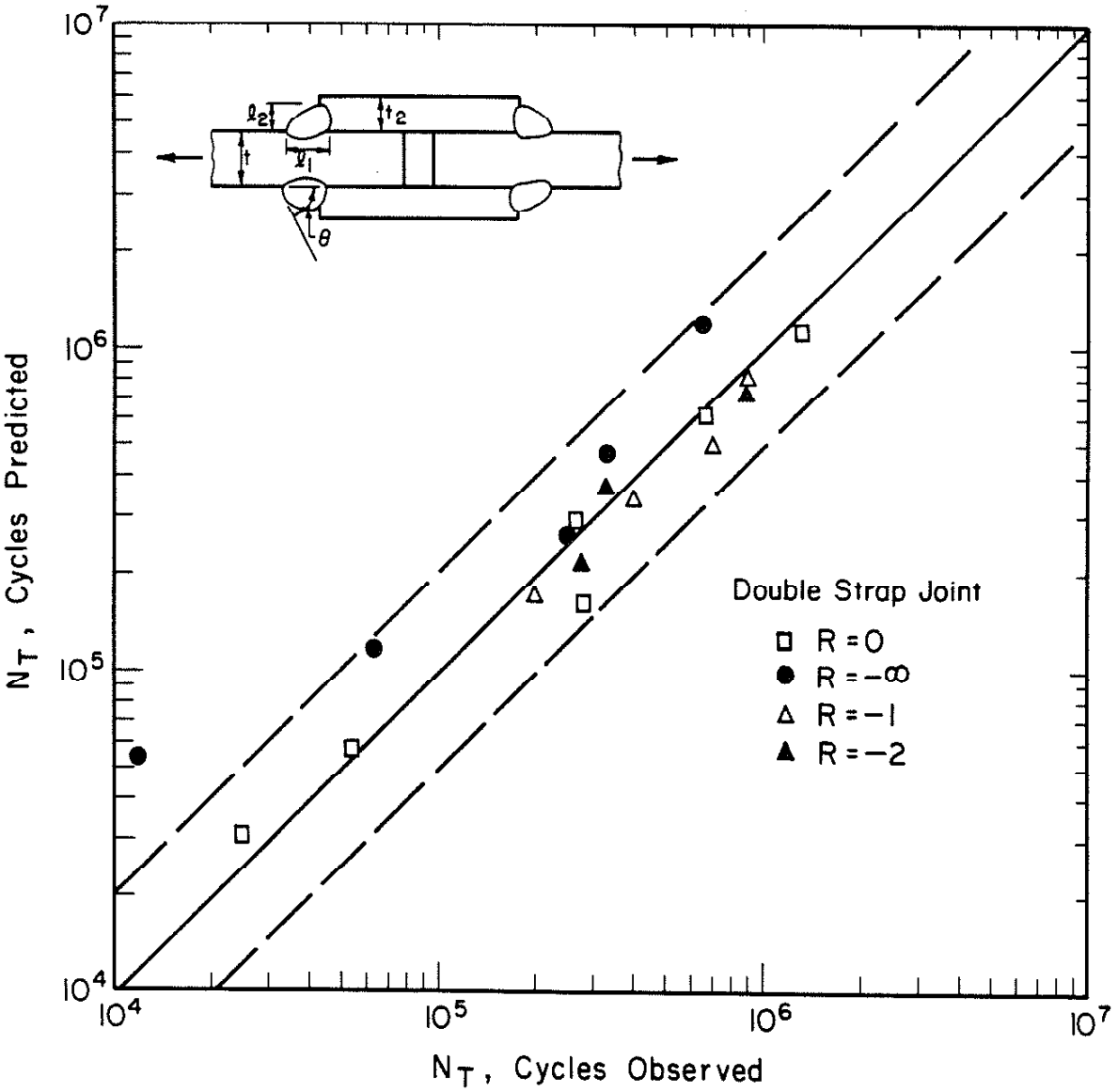

Fig. 31 COMPARISON OF PREDICTED AND OBSERVED TOTAL FATIGUE LIFE FOR DOUBLE STRAP LAP WELDMENTS AT VARIOUS STRESS RATIOS.

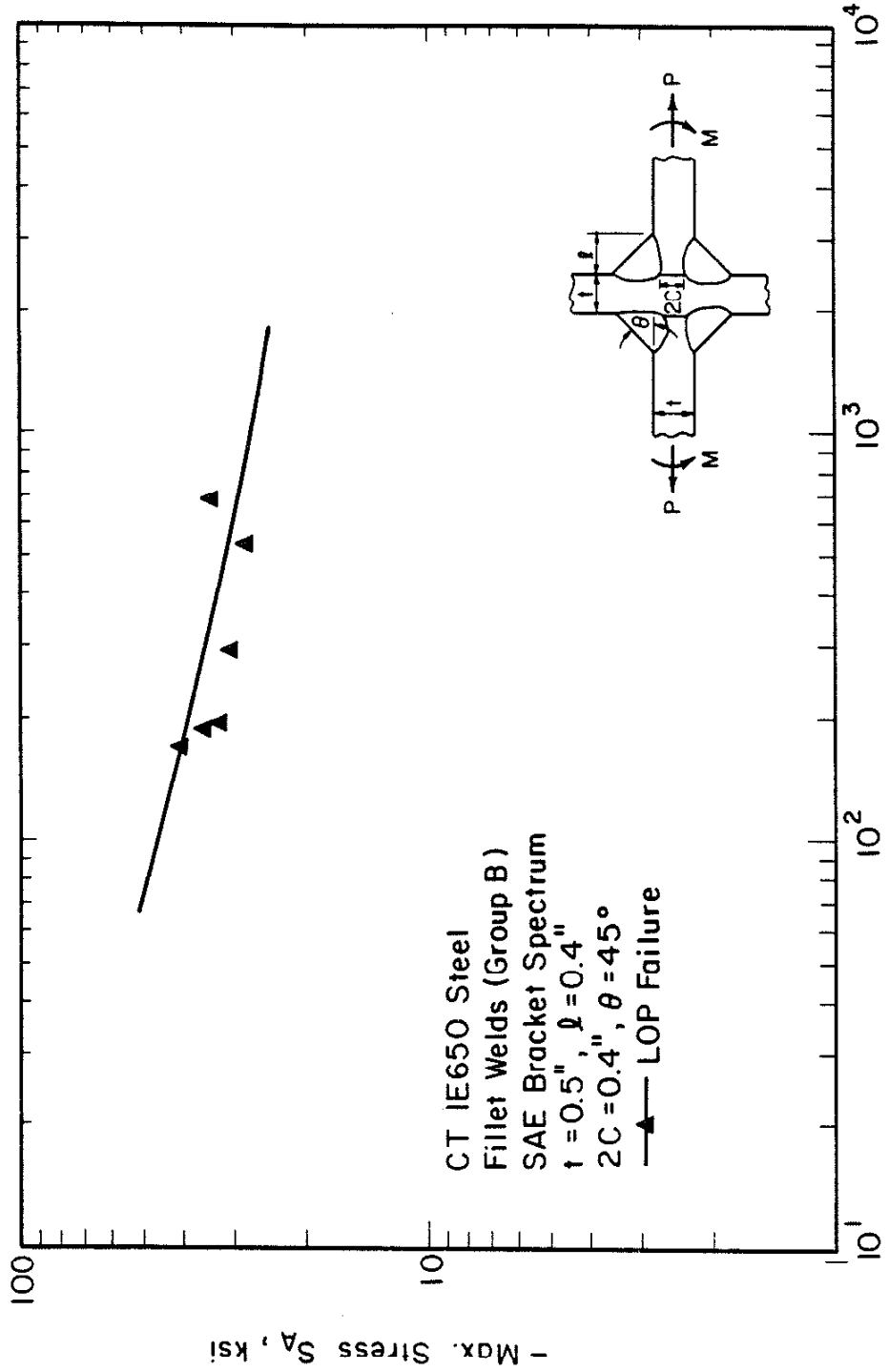

Fig. 32 TOTAL FATIGUE LIFE PREDICTIONS AND EXPERIMENTAL RESULTS FOR 1E650 CRUCIFORM WELDMENTS (GROUP B) UNDER SAE BRACKET LOADING HISTORY.

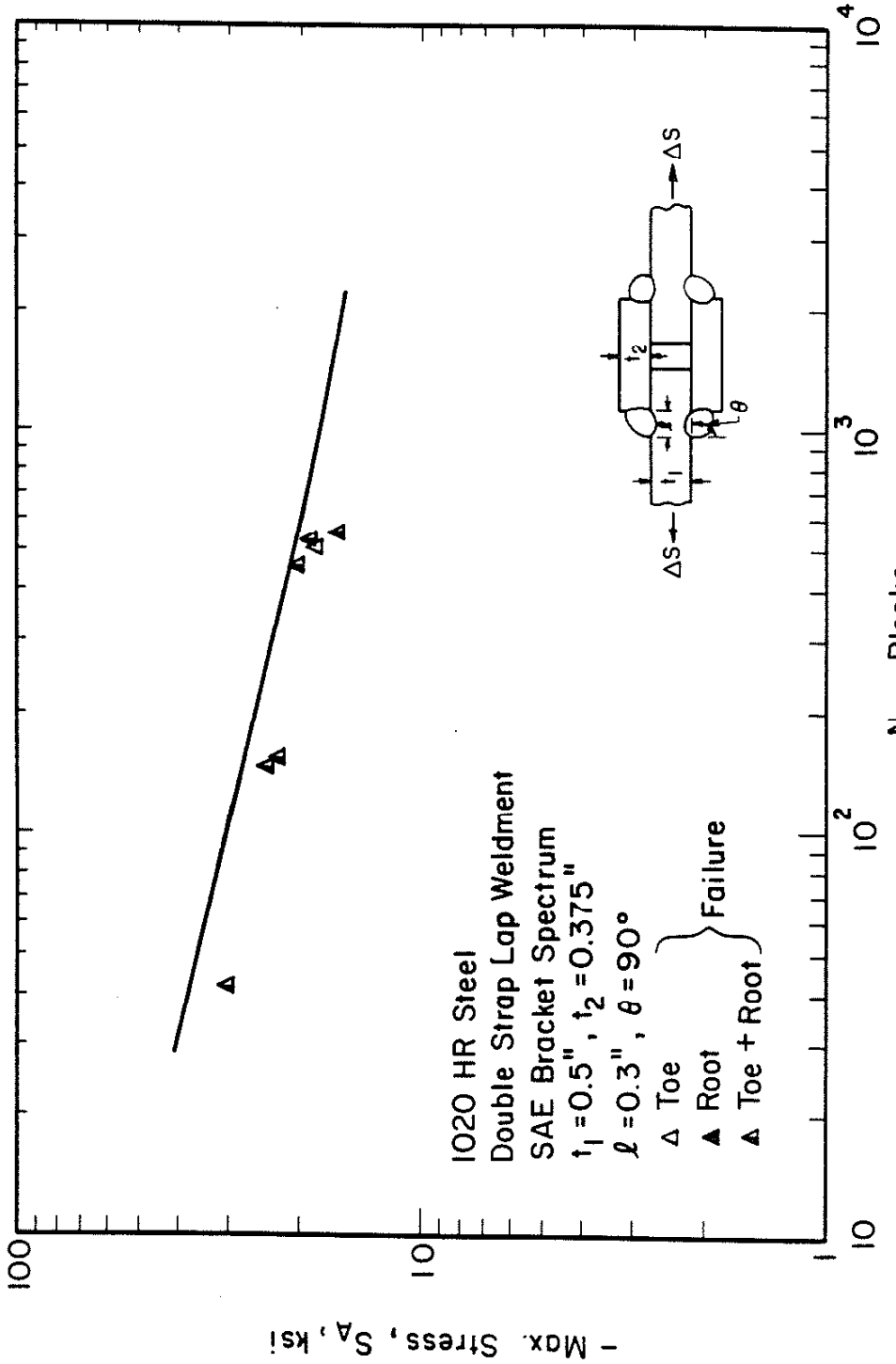

Fig. 33 TOTAL FATIGUE LIFE PREDICTIONS AND EXPERIMENTAL RESULTS FOR 1020 HR DOUBLE STRAP LAP WELDMENTS UNDER SAE BRACKET LOADING HISTORY.

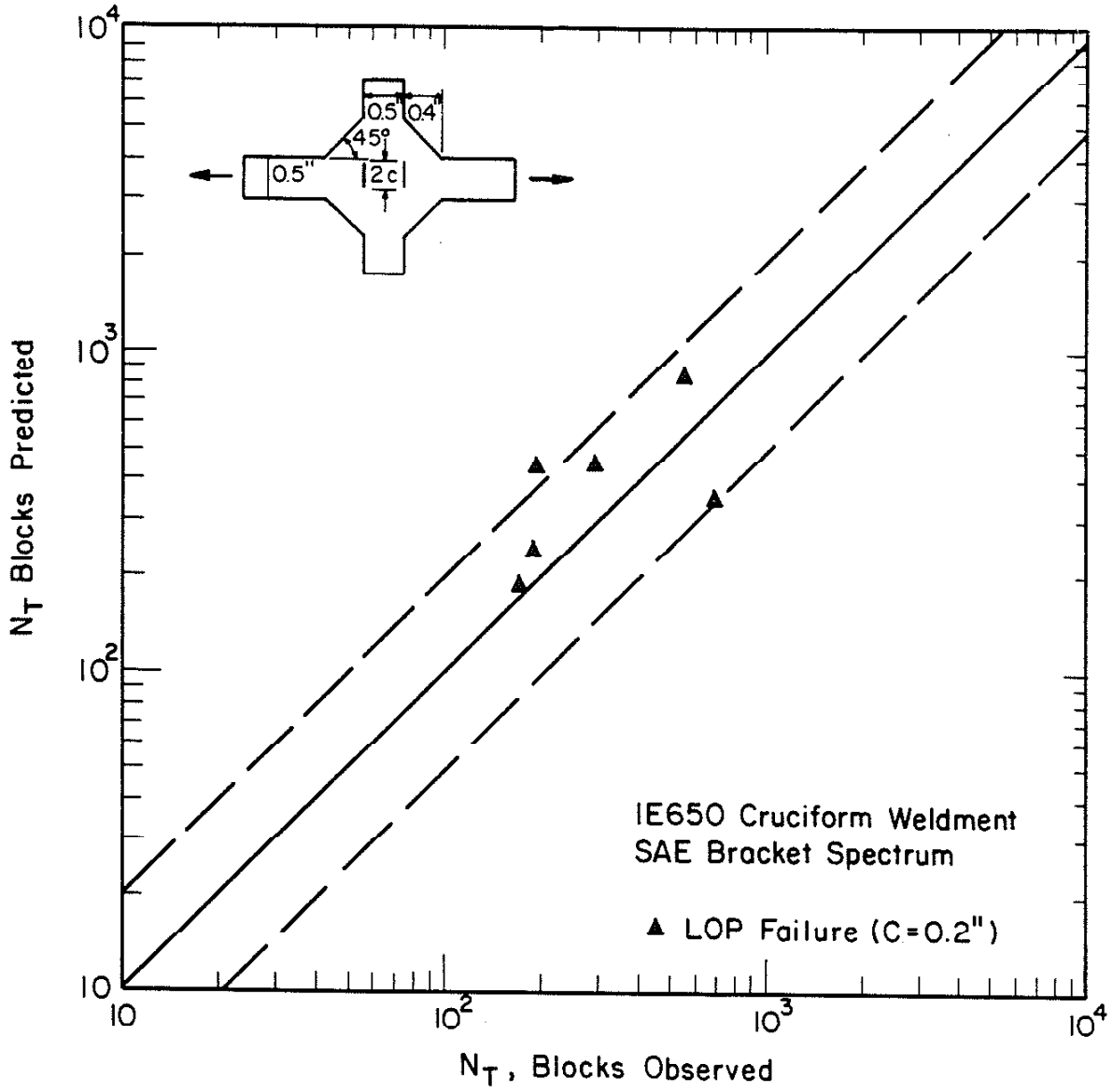

Fig. 34 COMPARISON OF PREDICTED AND OBSERVED TOTAL FATIGUE LIFE FOR 1E650 CRUCIFORM WELDMENTS (GROUP B) UNDER SAE BRACKET LOADING HISTORY.

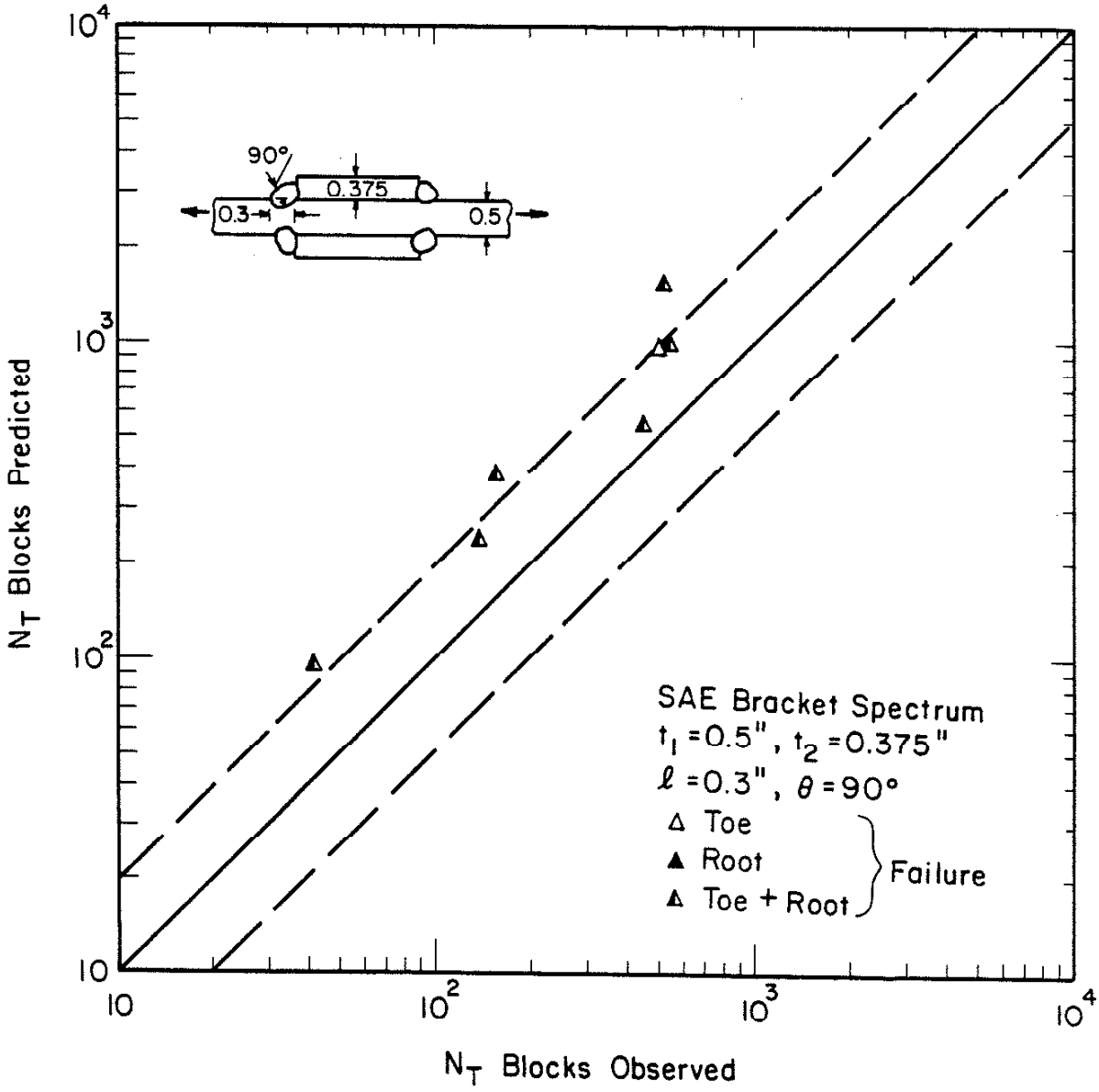

Fig. 35 COMPARISON OF PREDICTED AND OBSERVED TOTAL FATIGUE LIFE FOR 1020 HR DOUBLE STRAP LAP WELDMENTS UNDER SAE BRACKET LOADING HISTORY.

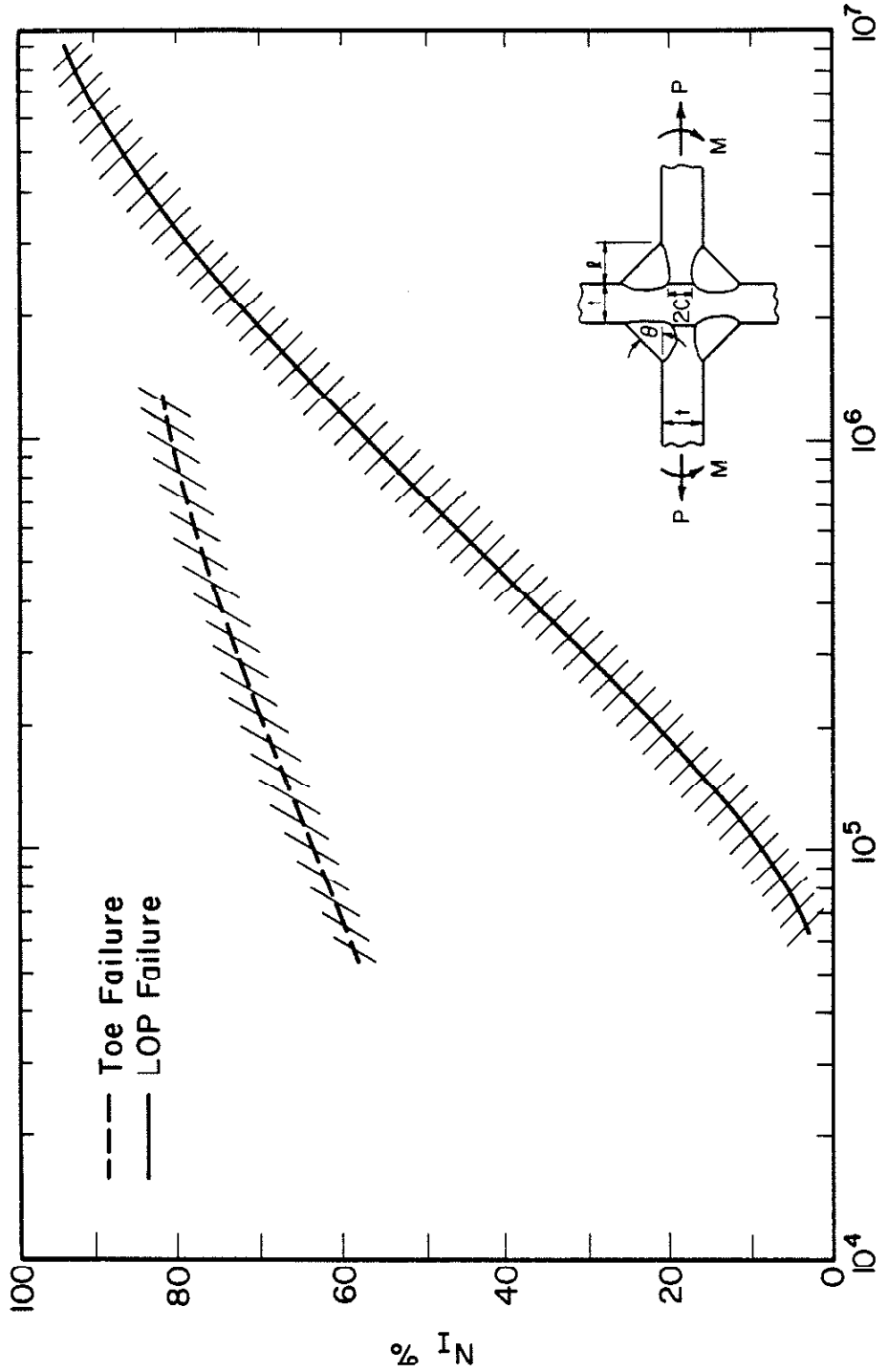

Fig. 36 PREDICTED VARIATION OF PERCENT OF LIFE DEVOTED TO CRACK INITIATION (N_I) VERSUS TOTAL LIFE (N_T) FOR CRUCIFORM WELDMENTS.

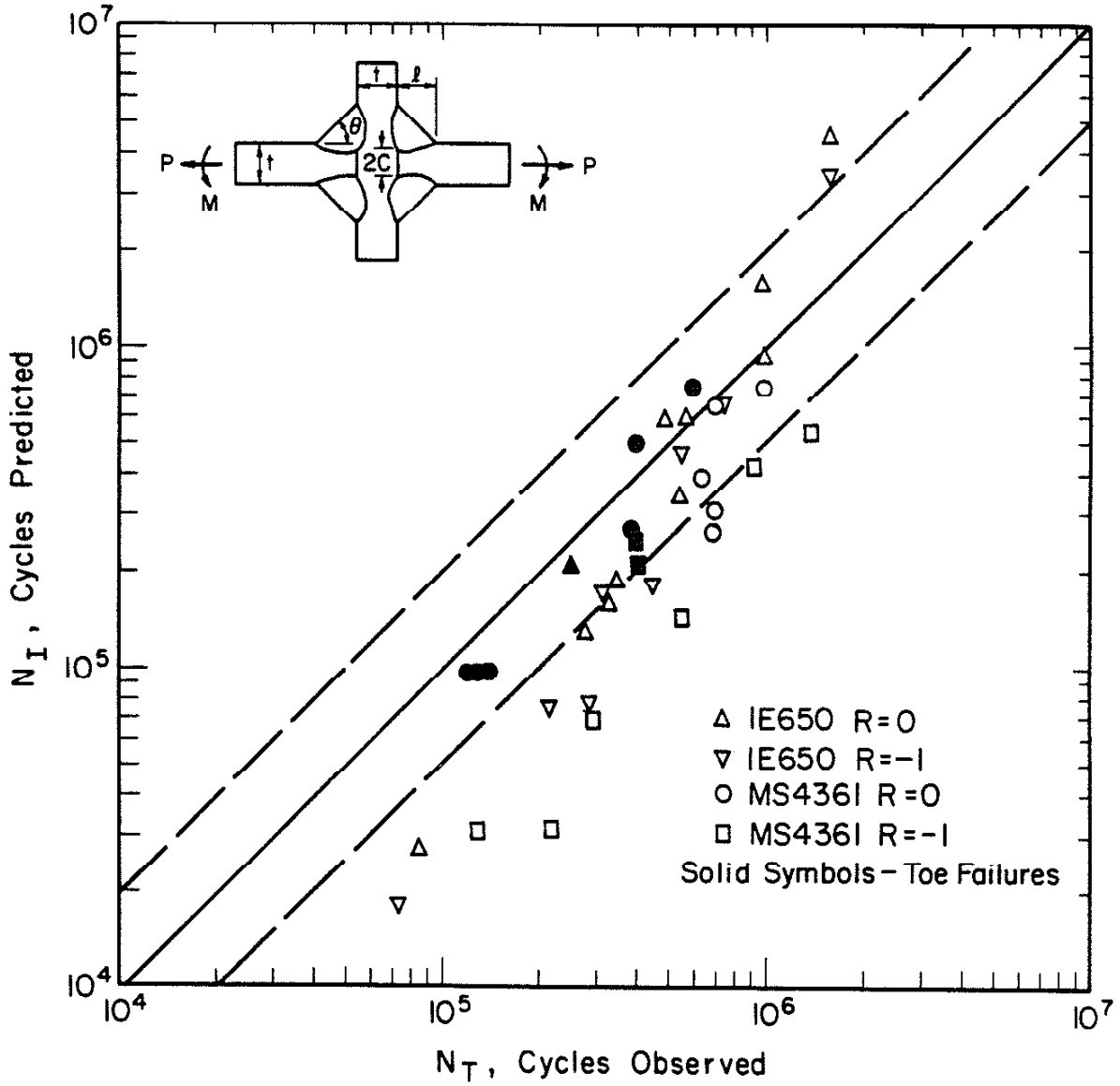

Fig. 37 COMPARISON OF PREDICTED INITIATION LIFE (N_I) AND OBSERVED TOTAL FATIGUE LIFE (N_T) FOR VARIOUS CRUCIFORM WELDMENTS AT VARIOUS STRESS RATIOS.

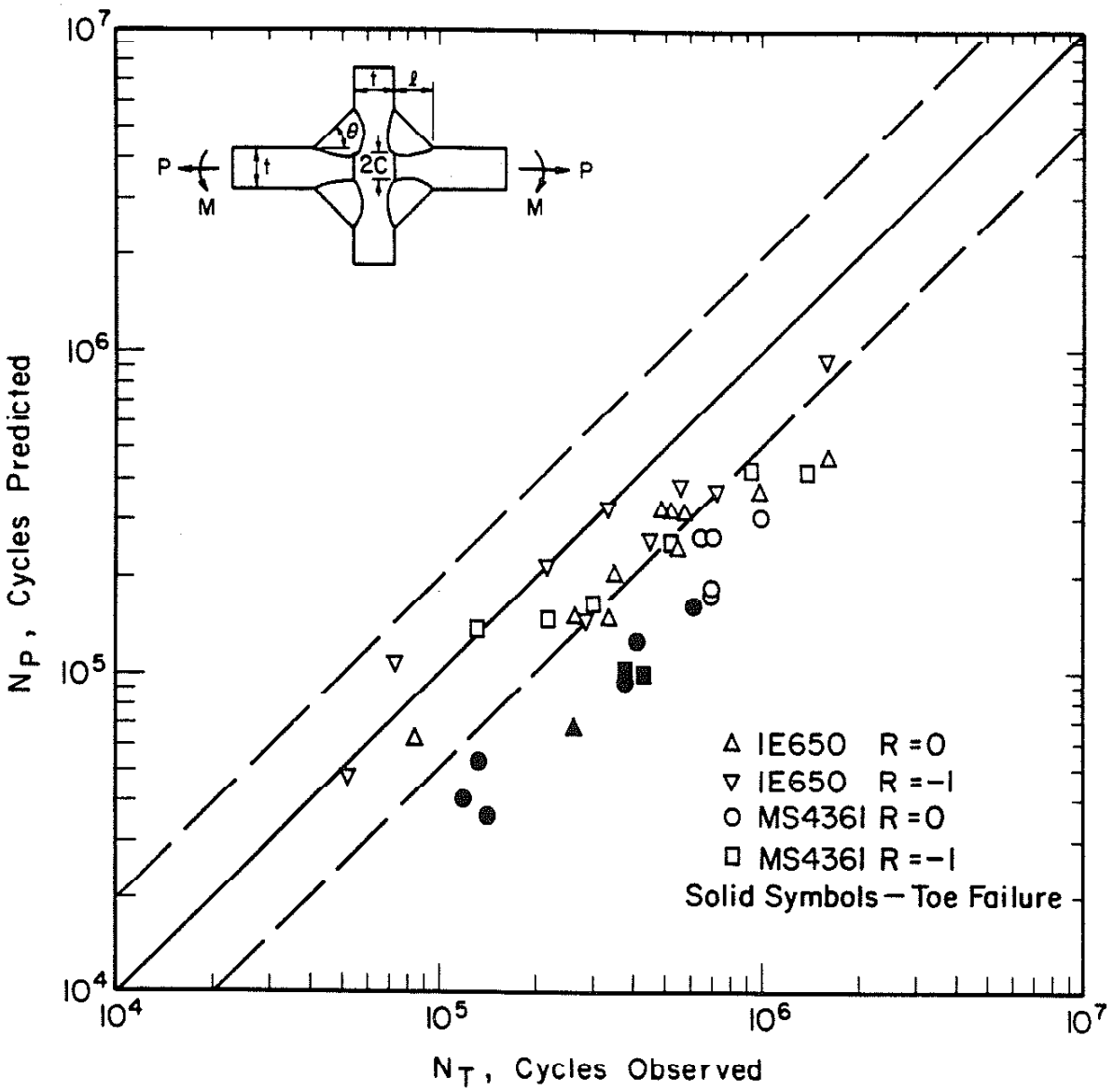

Fig. 38 COMPARISON OF PREDICTED CRACK PROPAGATION LIFE (N_P) AND OBSERVED TOTAL FATIGUE LIFE (N_T) FOR VARIOUS CRUCIFORM WELDMENTS AT VARIOUS STRESS RATIOS.

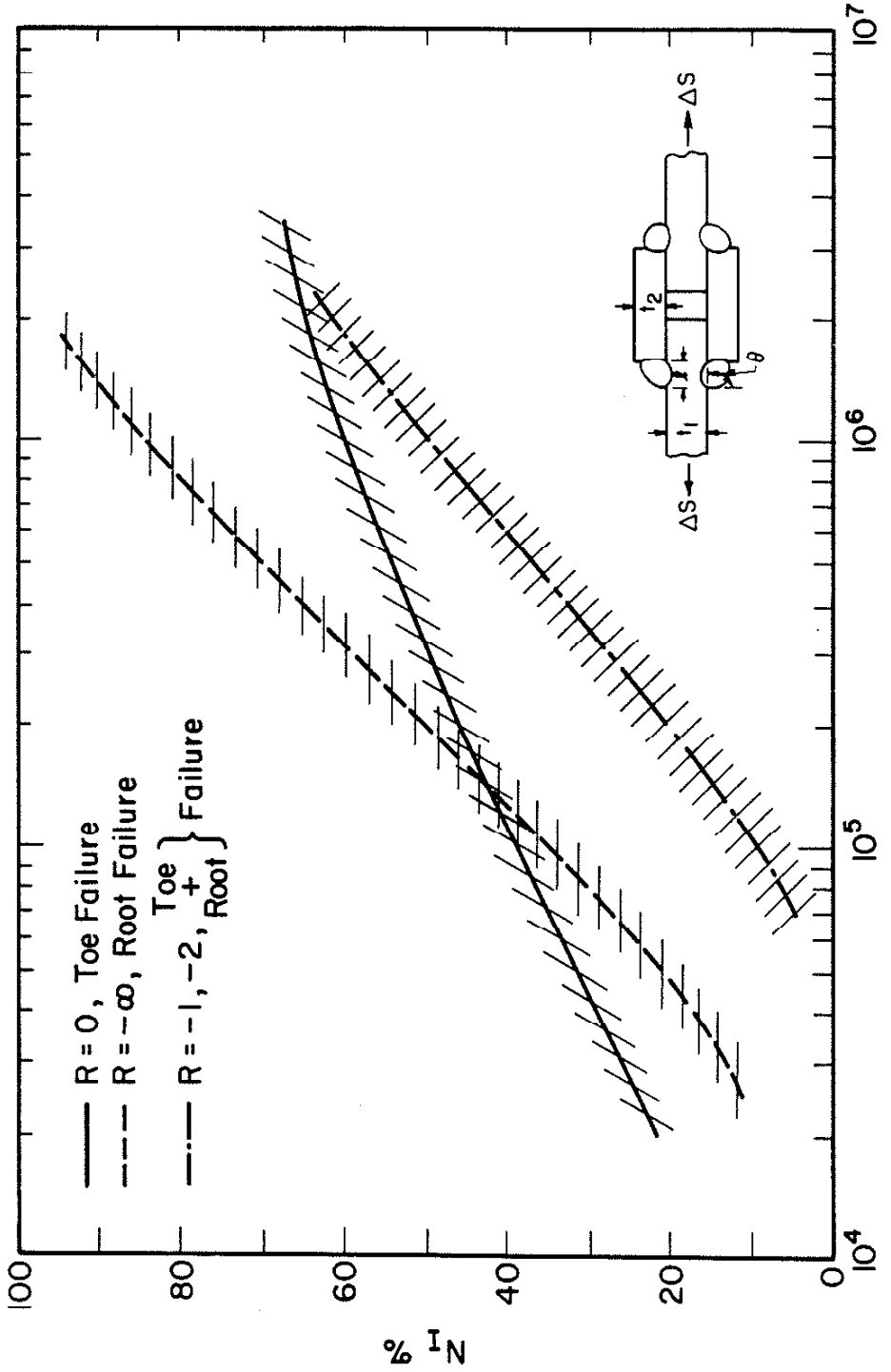

Fig. 39 PREDICTED VARIATION OF PERCENT OF LIFE DEVOTED TO CRACK INITIATION (N_I%) VERSUS TOTAL LIFE (N_T) FOR DOUBLE STRAP LAP WELDMENTS AT VARIOUS STRESS RATIOS

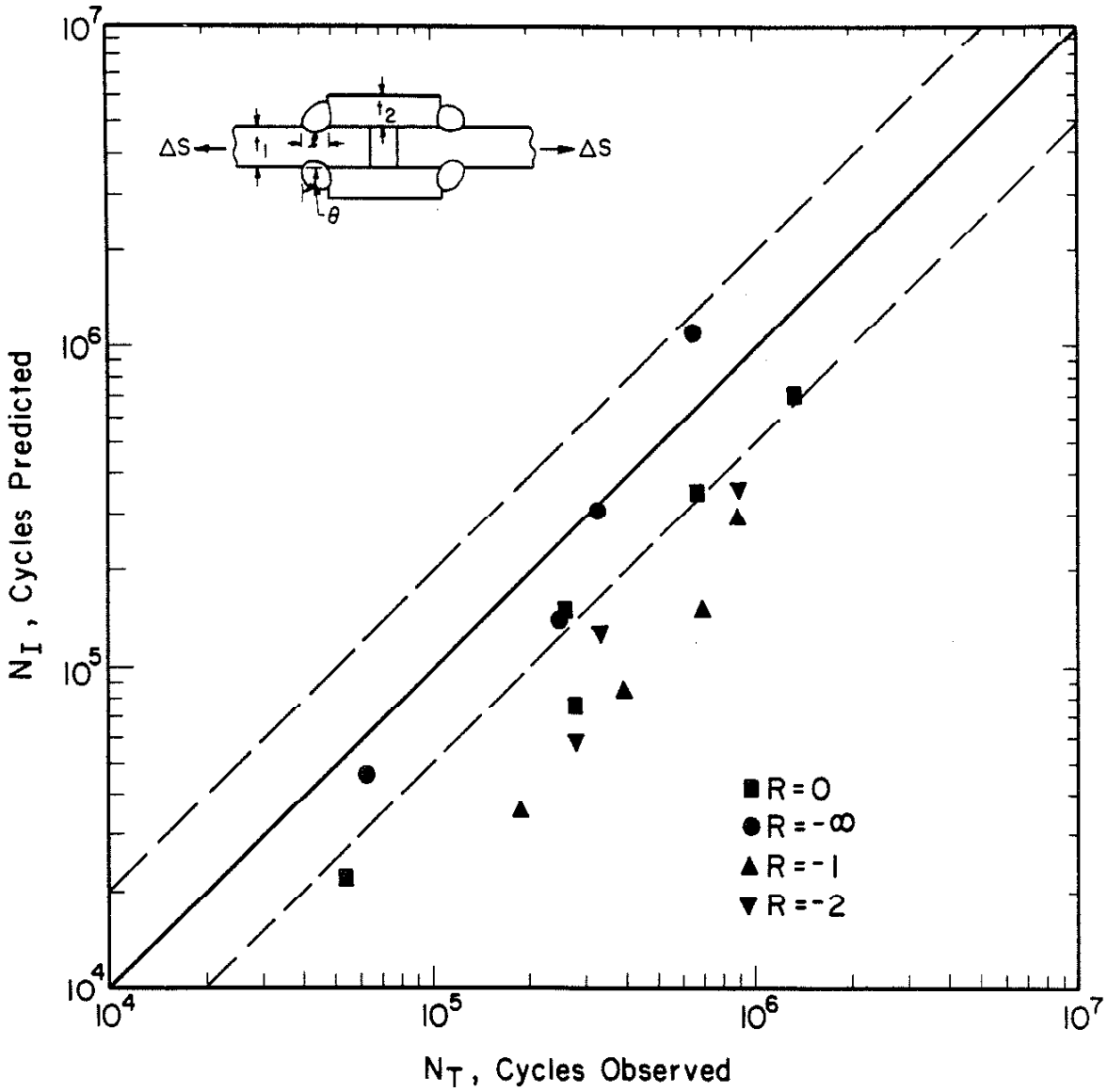

Fig. 40 COMPARISON OF PREDICTED CRACK INITIATION LIFE (N_I) AND OBSERVED TOTAL FATIGUE LIFE (N_T) OF 1020 HR DOUBLE STRAP LAP WELDMENTS AT VARIOUS STRESS RATIOS.

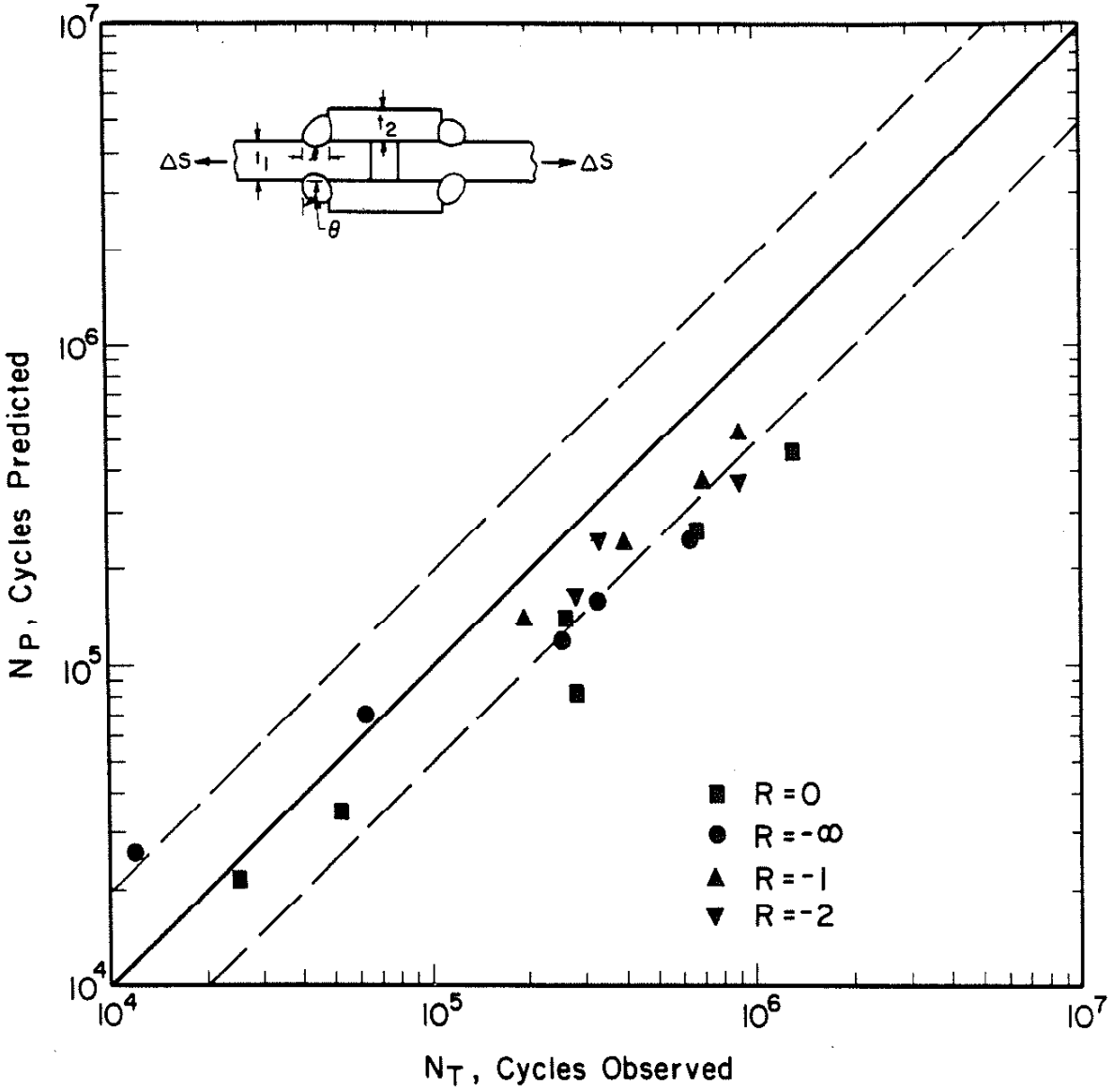

Fig. 41 COMPARISON OF CRACK PROPAGATION LIFE (N_p) AND OBSERVED TOTAL FATIGUE LIFE (N_T) FOR 1020 HR DOUBLE STRAP LAP WELDMENT AT VARIOUS STRESS RATIOS.

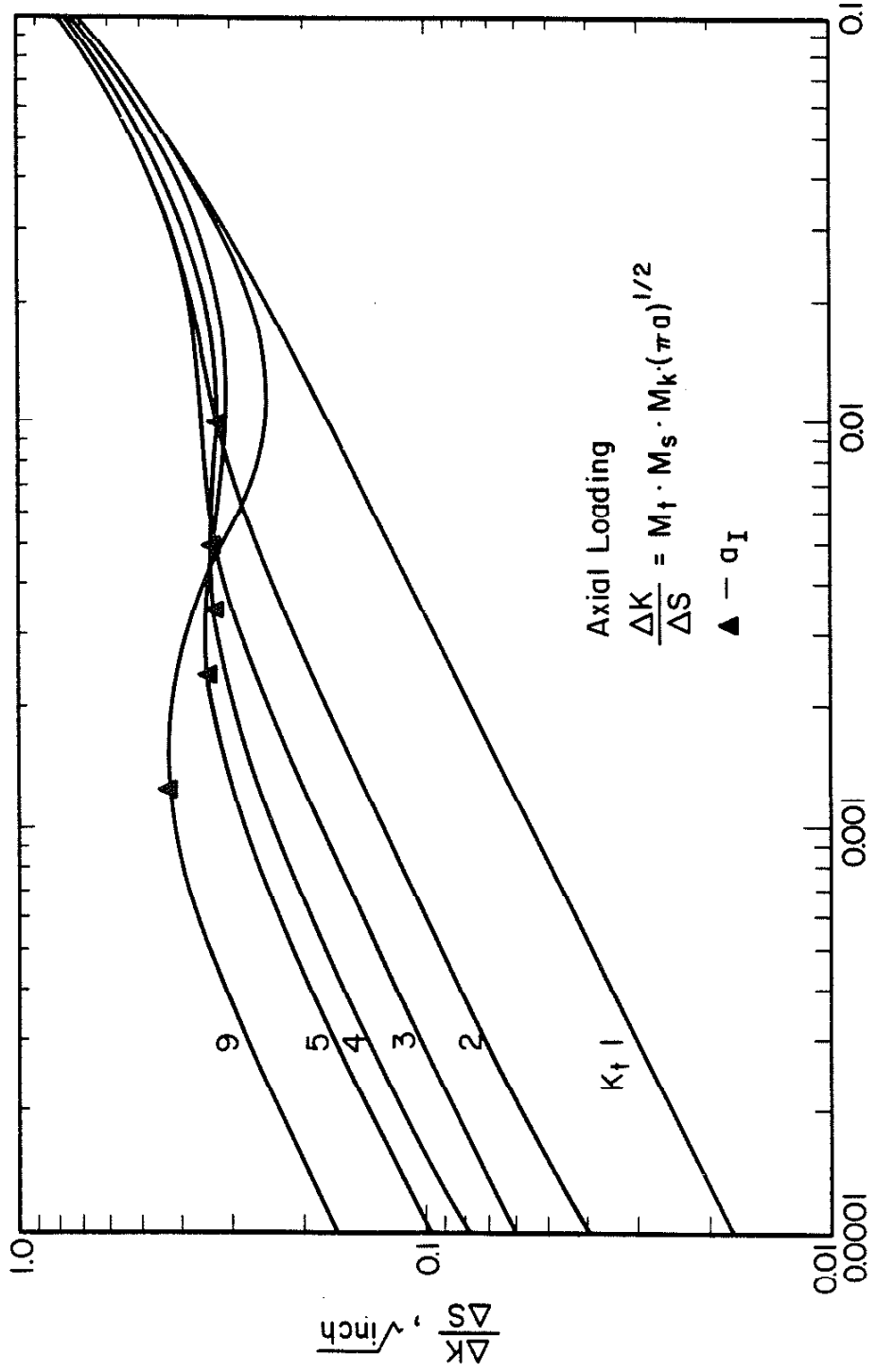

Fig. 42 VARIATION OF $\Delta K/S$ VERSUS CRACK LENGTH (a) AT DIFFERENT VALUES OF K_t UNDER AXIAL LOADING CONDITION.

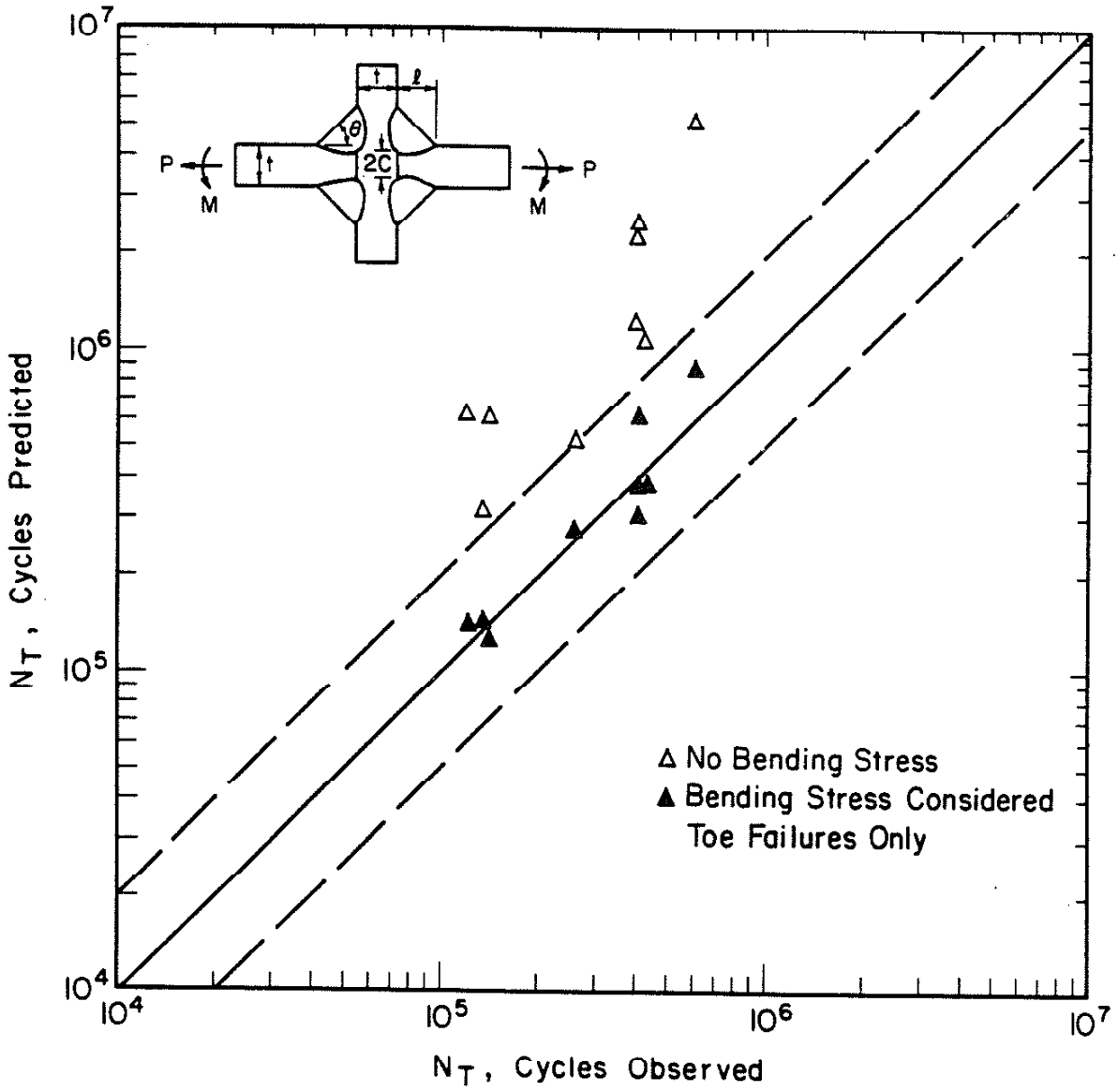

Fig. 43 COMPARISON OF PREDICTED AND OBSERVED TOTAL FATIGUE LIFE FOR FATIGUE FAILURE AT WELD TOE OF CRUCIFORM WELDMENTS WITH AND WITHOUT BENDING STRESSES INCLUDED IN THE PREDICTION.

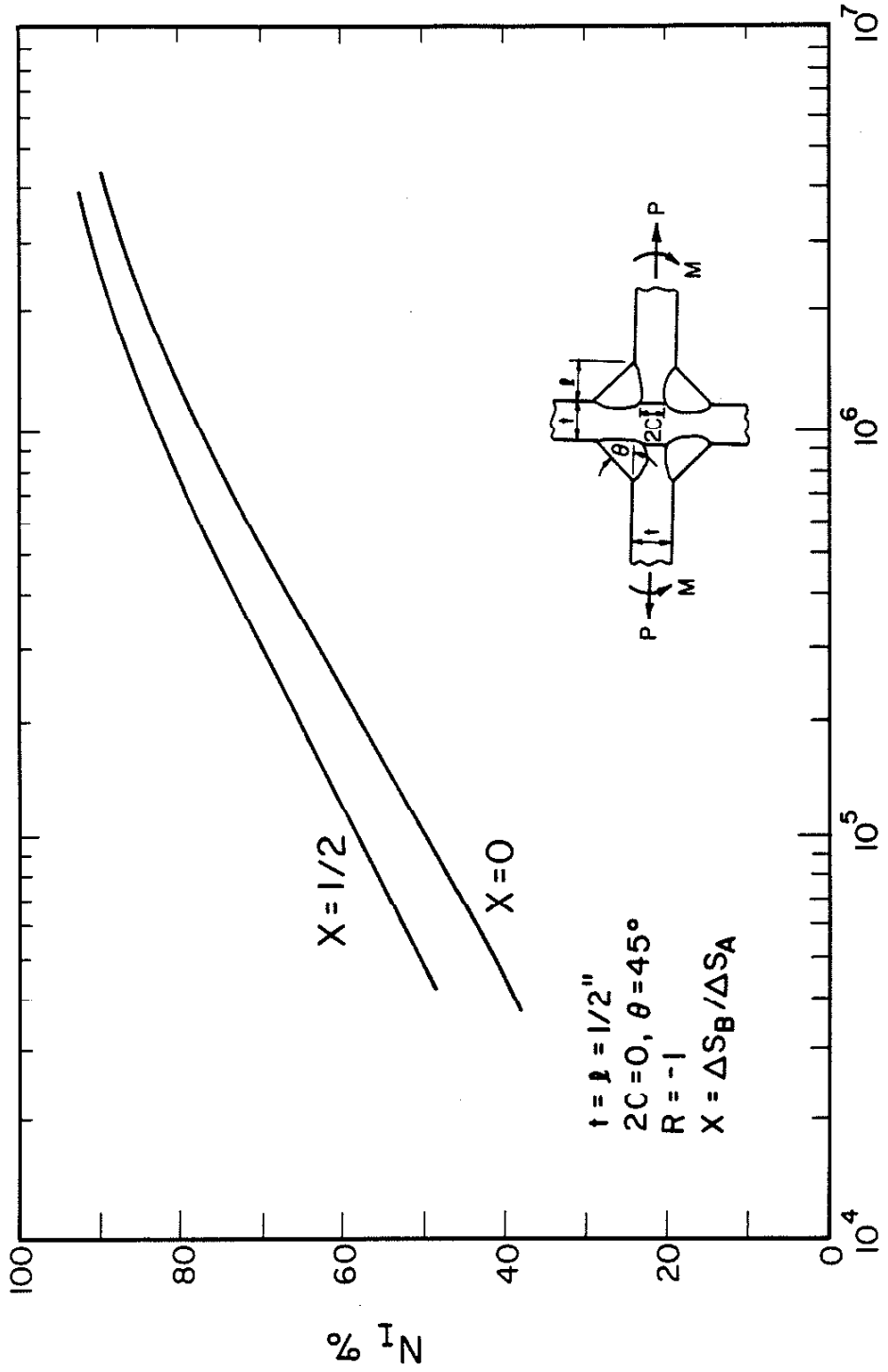

Fig. 44 PREDICTED VARIATION OF PERCENT OF LIFE DEVOTED TO CRACK INITIATION (N_I%) VERSUS TOTAL LIFE (N_T) FOR CRUCIFORM WELDMENT WITH ZERO AND 50% BENDING STRESSES.

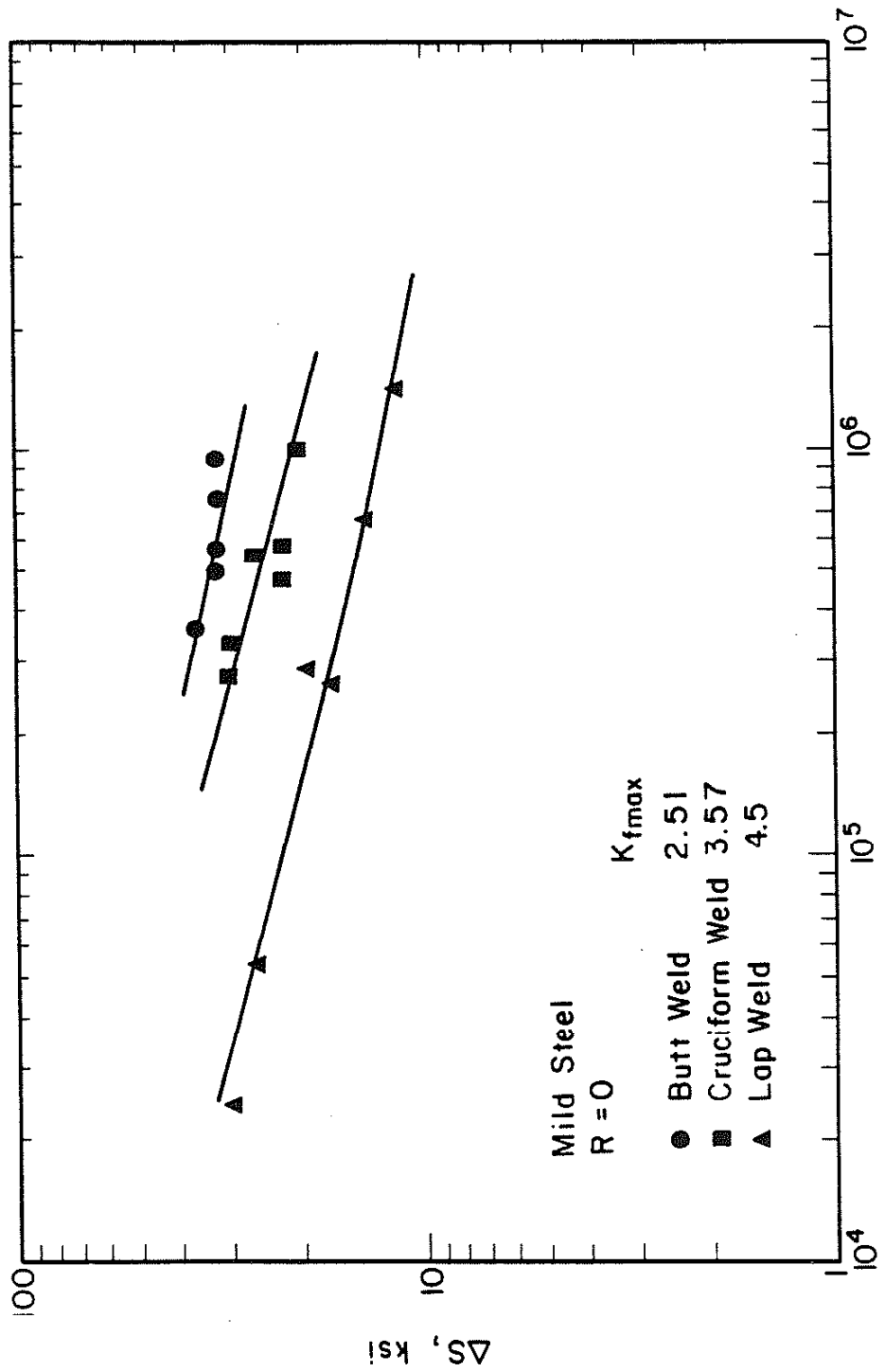

Fig. 45 COMPARISON OF TOTAL FATIGUE LIFE OF THREE TYPES OF WELDS.

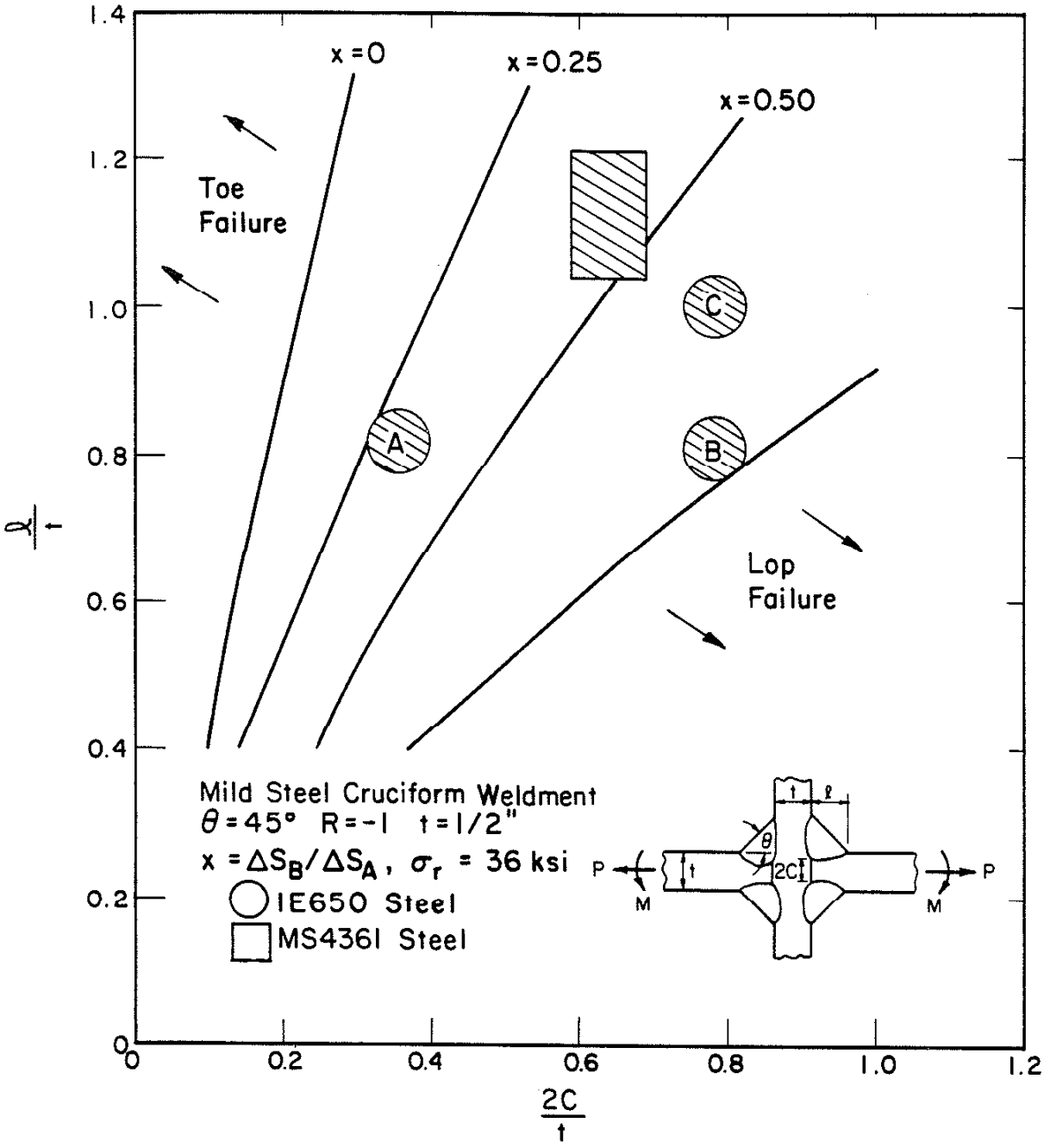

Fig. 46 PREDICTED CRITICAL WELD SIZE OF CRUCIFORM WELDMENT SUBJECTED TO COMBINED AXIAL AND BENDING STRESSES AT θ = 45°, t = 0.5", AND R = -1 CONDITION USING THE PRESENT METHOD.

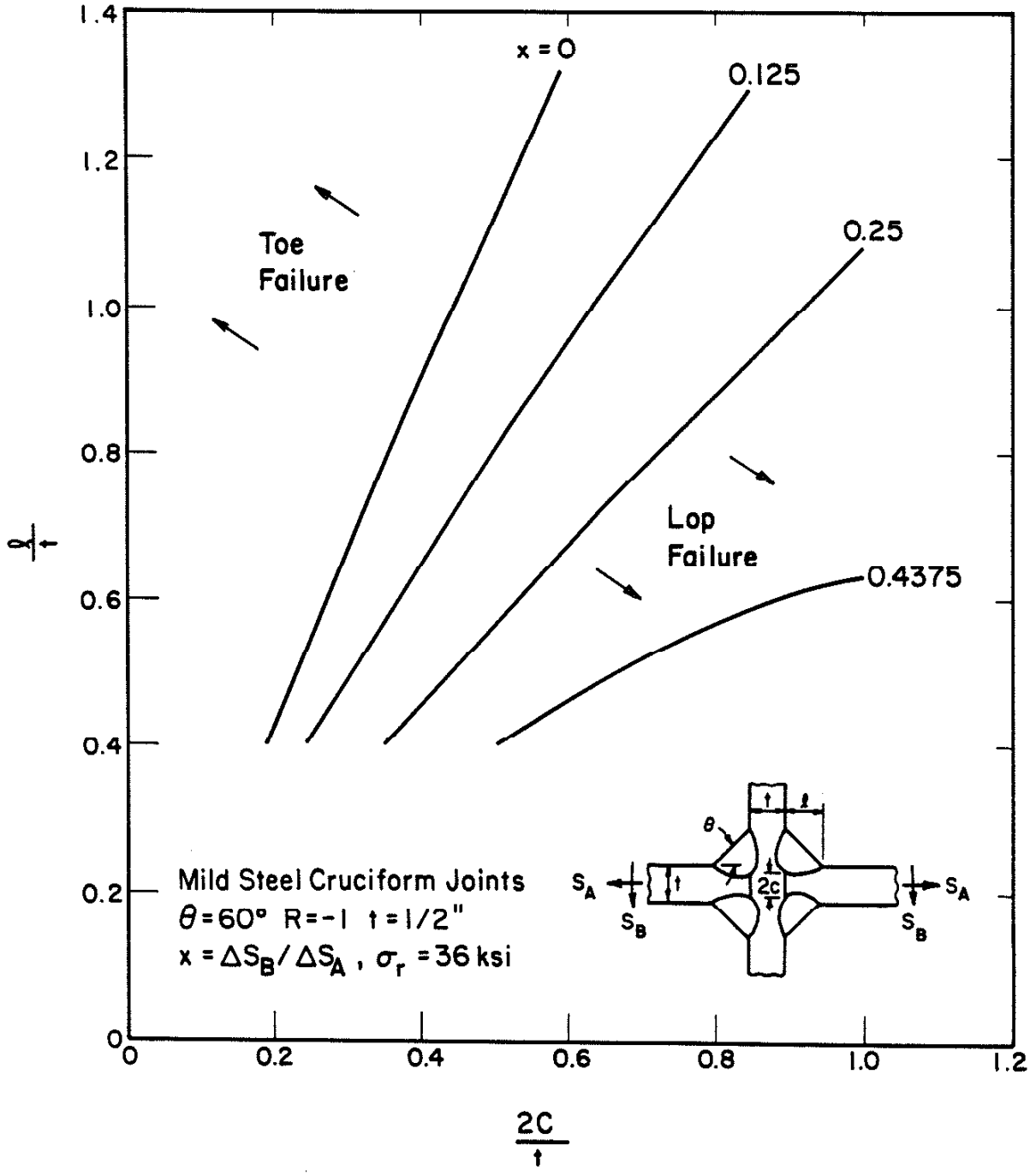

Fig. 47 PREDICTED CRITICAL WELD SIZE OF CRUCIFORM WELDMENTS SUBJECTED TO COMBINED AXIAL AND BENDING STRESSES AT θ =60°, R = -1 AND t =0.5" CONDITION USING THE PRESENT METHOD.

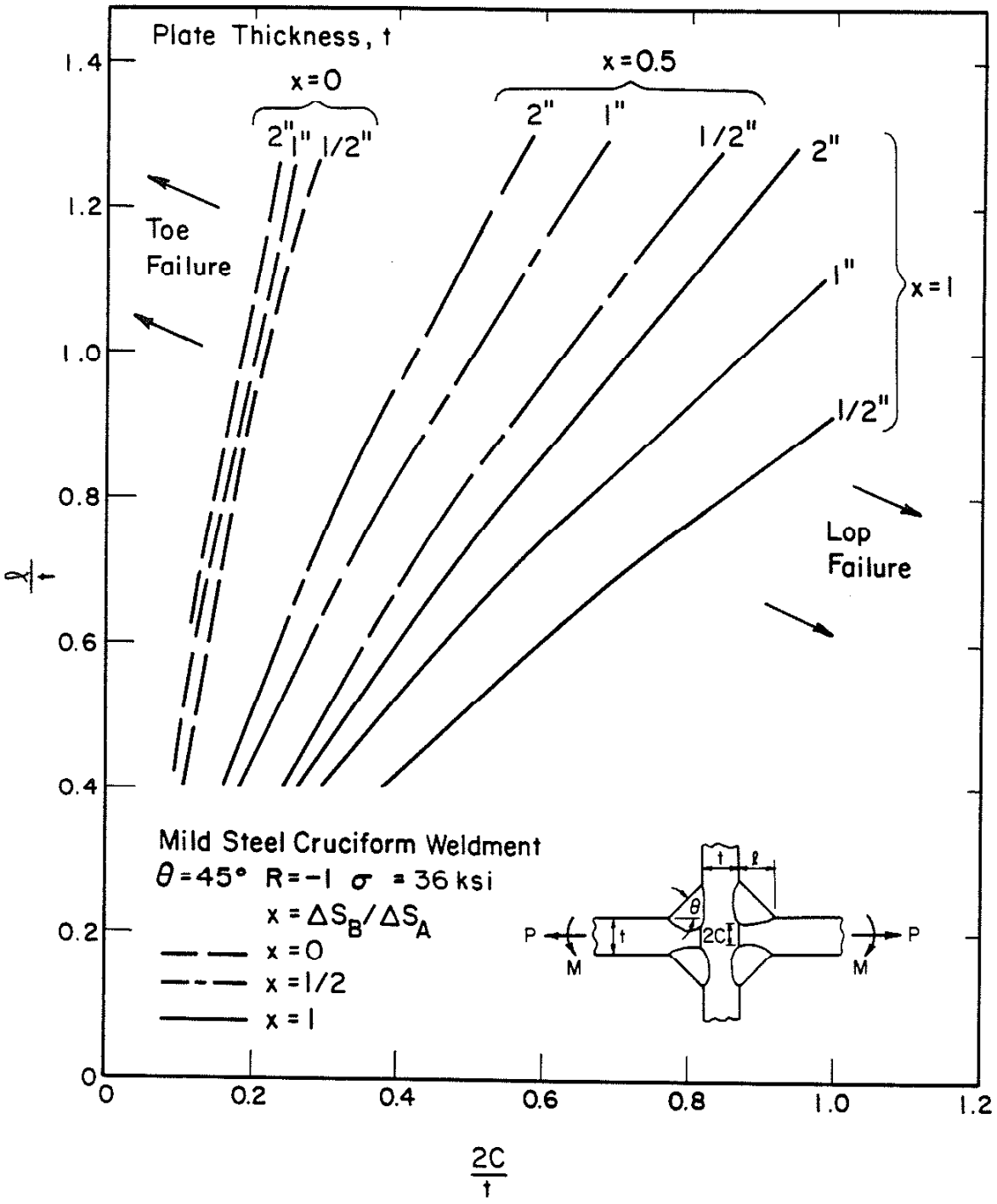

Fig. 48 PREDICTED CRITICAL WELD SIZE OF CRUCIFORM WELDMENTS SUBJECTED TO COMBINED AXIAL AND BENDING STRESSES FOR DIFFERENT PLATE THICKNESS (t) AT θ = 45° AND R = -1 CONDITION USING THE PRESENT METHOD.

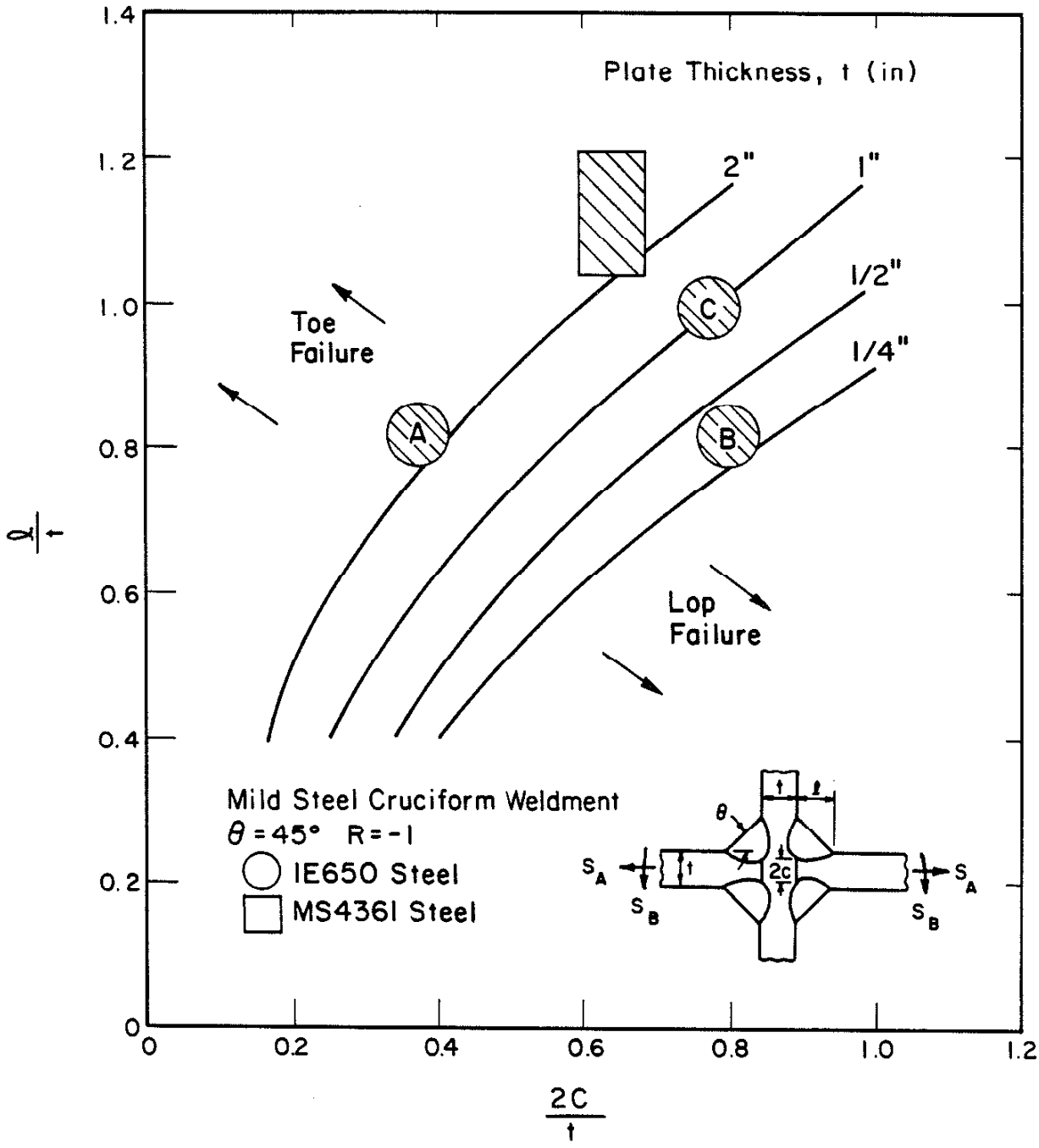

Fig. 49 PREDICTED CRITICAL WELD SIZE OF CRUCIFORM WELDMENT FOR DIFFERENT PLATE THICKNESSES (t) USING LEFM [54].

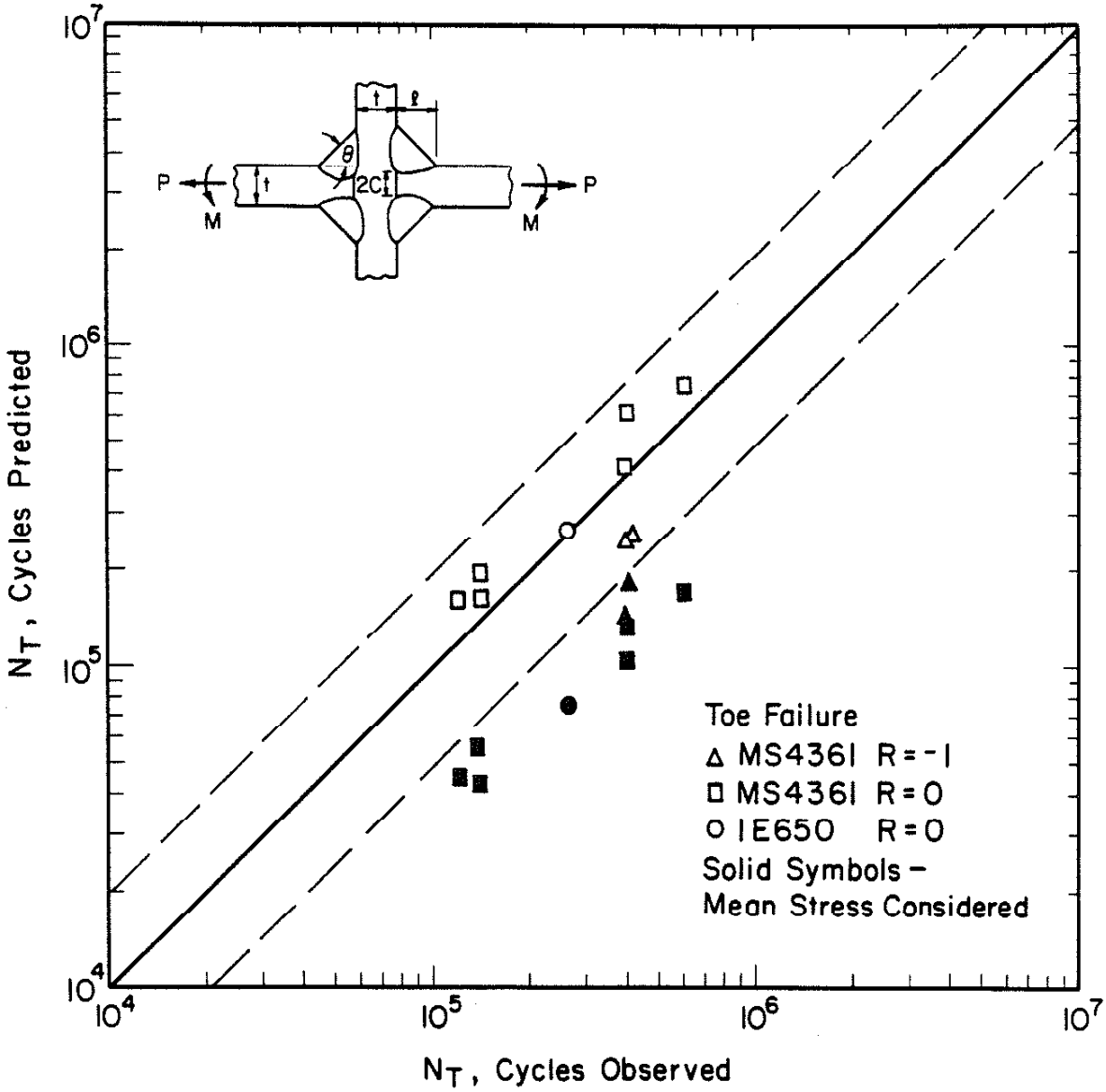

Fig. 50 COMPARISON OF PREDICTED TOTAL FATIGUE LIFE WITH BENDING STRESSES USING EL HADDAD, TOPPER AND SMITH METHOD AND OBSERVED TOTAL FATIGUE LIFE FOR FATIGUE FAILURE AT THE WELD TOE OF CRUCIFORM WELDMENTS.

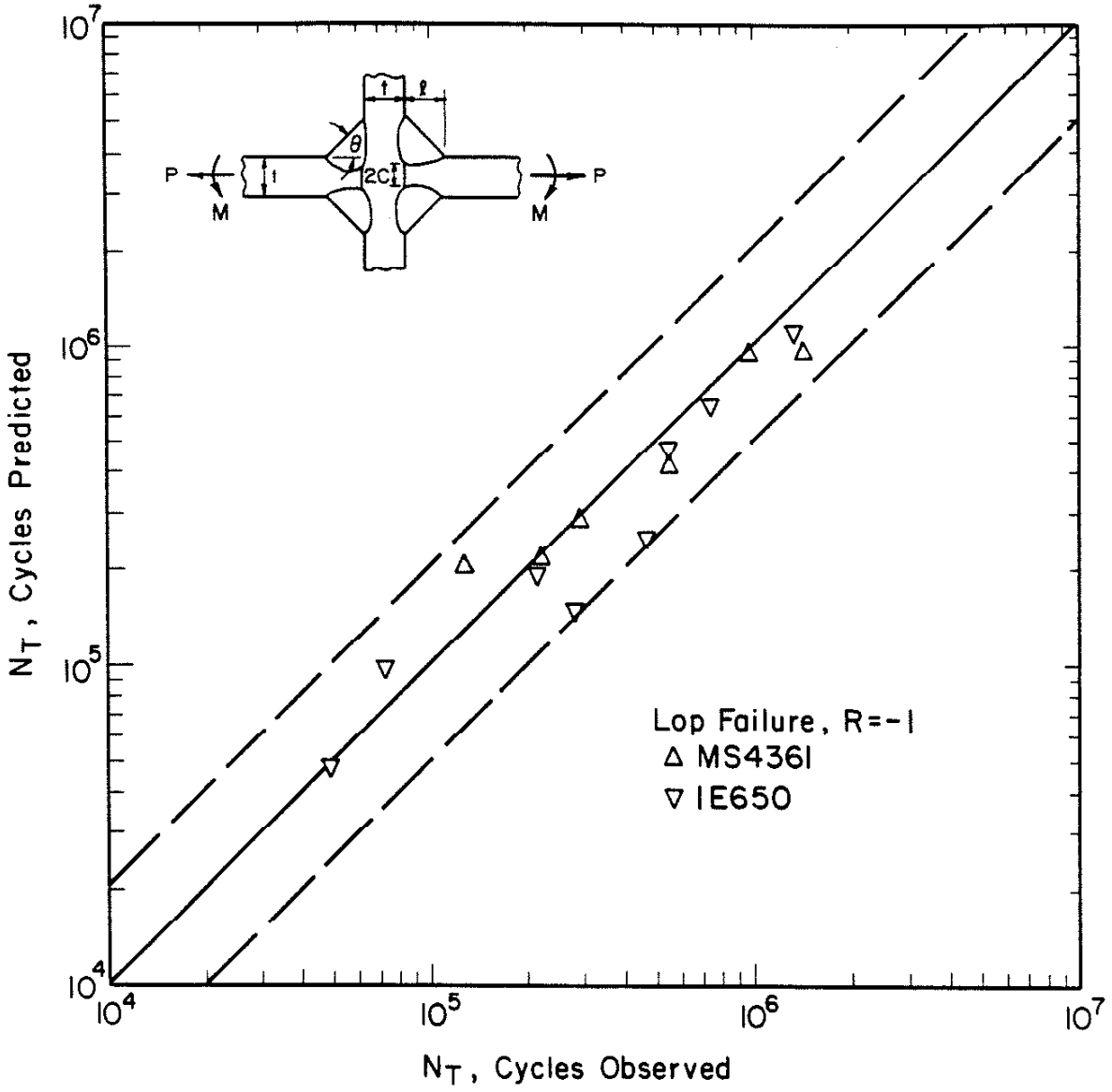

Fig. 51 COMPARISON OF PREDICTED TOTAL FATIGUE LIFE USING EL HADDAD, TOPPER AND SMITH METHOD AND OBSERVED TOTAL FATIGUE LIFE FOR FATIGUE FAILURE AT THE LOP OF CRUCIFORM WELDMENTS AT A STRESS RATIO OF R = -1.

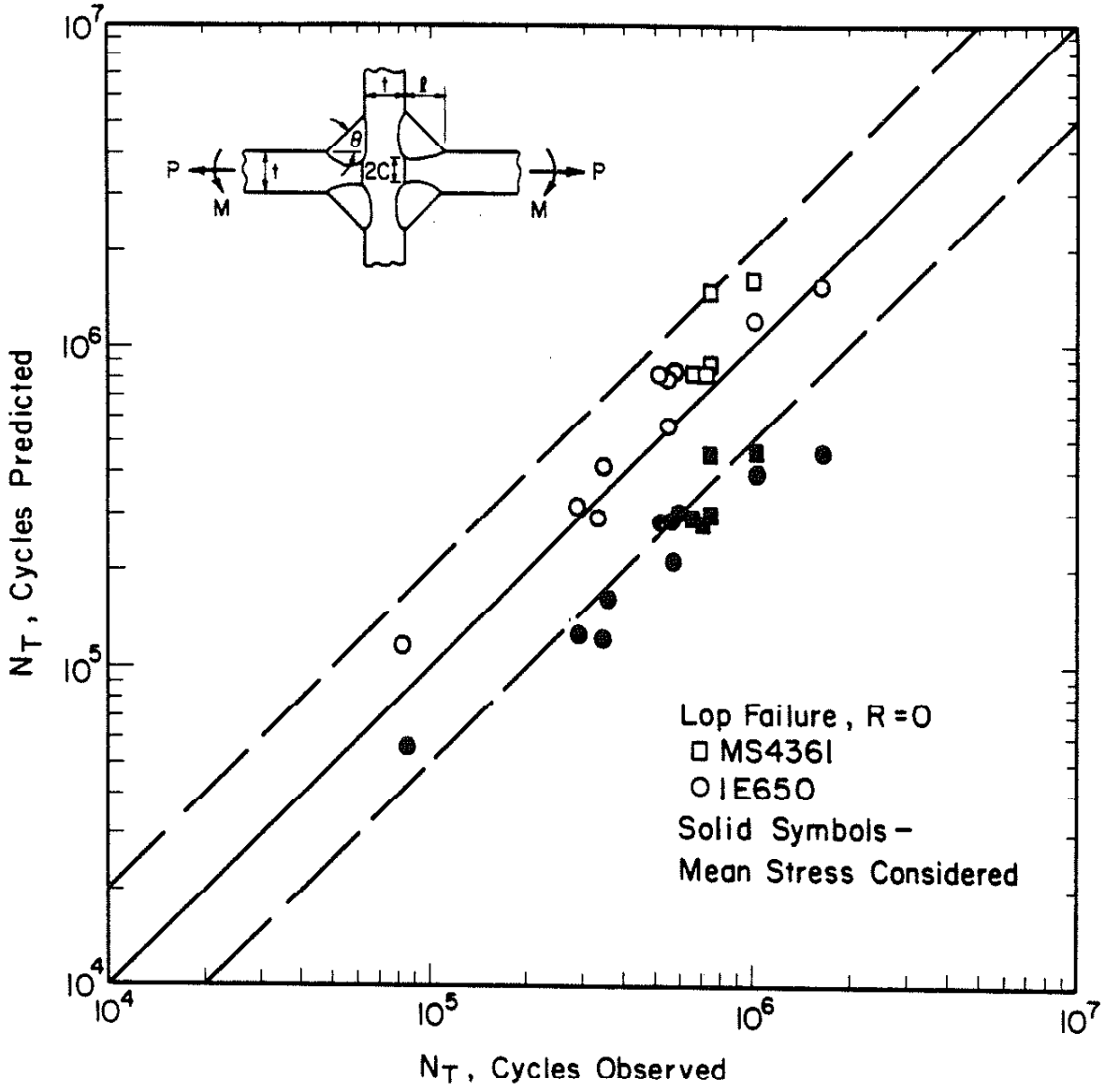

Fig. 52 COMPARISON OF PREDICTED TOTAL FATIGUE LIFE USING EL HADDAD, TOPPER AND SMITH METHOD AND OBSERVED TOTAL FATIGUE LIFE FOR FATIGUE FAILURE AT THE LOP OF CRUCIFORM WELDMENTS AT A STRESS RATIO OF R = 0.

APPENDIX

The computer program which was used to calculate the total fatigue life is listed in this appendix. The program was based on the method discussed in the Chapter 2 and was written in FORTRAN IV language and the computation was performed on a Cyber 175 computer. Most of the principal variables appearing in the program are easily understood by their names and by comparing the input data files. The program used free formatted input which need only blank(s) to separate the data. The input data were stored in two separated files. The material properties are stored in the first input file which is listed bellow:

```
"MATERIAL"  "MILD "    "MS4361 HAZ"  "CRUCI  "  "TOE"
"+++++"  "MONOTONIC" "PROPERTIES"  "++++++"
"YOUNG'S"  "MODULUS"  "CONST"  "E(KSI)" 28700.00
".2%OFFSET" "YIELD" "STRENGTH" "SY(KSI)" 60.00
"TENSILE" "STRENGTH" "-----" "UTS(KSI)"  90.50
"REDUCTION" "IN" "AREA" "RA%" 60.7
"TRUE" "FRACTURE" "STRENGTH" "SF(KSI)" 133.00
"TRUE" "FRACTURE" "DUCTILITY" "EF" 0.745
"STRAIN" "HARDENING" "EXPONENT" "N" 0.102
"STRENGTH" "COEFFT" "----" "K(KSI)" 142.0
"+++++" "CYCLIC" "PROPERTIES" "+++++"
"CYCLIC" "YIELD" "STRENGTH" "SY'(KSI)" 50.00
"CYCLIC" "STRENGTH" "COEFFT" "K'(KSI)" 148.00
"STRAIN" "HARDENING" "EXPONENT" "N'" 0.175
"FATIGUE" "STRENGTH" "COEFFT" "SF'(KSI)" 120.00
"FATIGUE" "DUCTILITY" "COEFFT" "EF'" 0.280
"FATIGUE" "STRENGTH" "EXPONENT" "B" -0.0820
"FATIGUE" "DUCTILITY" "EXPONENT" "C" -0.520
"TRANSITION" "   FATIGUE" "  STRAIN" "  ETR" 0.0050
"RESIDUAL " "STRESS  "  "------"   "SFR(KSI) "   34.0
"PROPAG. "  "CONST  "  " C "  "M"  1.00E-10   3.30  0.0  70.0  0.0
```

In the first line of the above input file, the forth and fifth data specify the type and location of a weld to be analysed. In the last line, crack growth rate constants correspond to the first two numbers, a_I corresponds to the third number (if zero, Eq. 31 will be used to

calculate a_I), and the forth and fifth numbers correspond to the fracture toughness and crack opening load, respectively.

the weld geometry and load history are stored in the second input file which is listed below:

For constant amplitude fatigue

```
"THICKNESS" "----------" "--------"  "T (IN.) "   0.50
"WELD "  "SIZE " "-----"   "L2(IN.)"  0.40
"WELD  "  "SIZE " "-----"   "L1(IN.) "  0.400
"LENGTH"  " OF LOP "   "-----"    "C(IN.) "  0.20
"LOAD" "HISTORY" " CONST" "    AMPT"
"NUMBER"  "OF  "  "REVERALS "  "-----"  3
"AXIAL"  25.00  -0.00   25.00
"BENDING"   10.0   2.00   10.0
```

For Variable amplidude fatigue

```
 "THICKNESS" "----------" "--------"  "T (KSI) "   0.50
 "WELD "  "SIZE " "-----"   "L2(IN.)"  0.4300
 "WELD  "  "SIZE " "-----"   "L1(IN.) "  0.450
 "LENGTH"  " OF LOP "   "-----"    "C(IN.) "  0.200
 "LOAD  "  "SAE   "   "VARIABLE"  " BRACKET"
 "NUMBER "   "   OF  "  "REVERSALS"  " ----"  5936
 "MAXIMUM "  "ABSOLUTE"  "  STRESS"   "-- KSI  "   30
 "NUMBER "  "OF "  "MONITOR "  "NET"   3
 "PRINT "  "ONE "  "RESULT "  "FOR EVERY "  1000
 "BENDING" " FACTOR, " " RANGE  "   "MEAN "   0.2   5.0
  -999  255 -875  201 -177  433 -487 -172 -708  182 -201  295 -196   63
  -354  113 -167   63 -191   44 -172   34 -177   34 -246  137 -226  177
  -506  191 -142  314 -388  108 -113  334 -433  113 -329  359 -305   88
  -585  113 -344   24 -221  319 -413   19 -324  285 -108  388 -191  216
  -600  118 -162  177 -757  236  -29  408 -374  359 -226  177 -403  275
  -255   34 -442   88 -226  275 -472  -88 -447  196 -369  265 -177   34
  -383  226 -314  103 -290  231 -467   44 -275  260 -433  211 -285  329
  -310  211 -398   68 -255  118 -383  206  -39  157 -285   73 -167  354
  -565  260 -270    9 -290  433 -132   93 -492  -59 -433  123 -157   59
  -447  241 -290  738 -280  364 -679  260   29  310 -556  255  -14  201
  -452  -83 -324  295 -354  206 -501  132 -216   49 -201  177 -349  108
  -447  241 -383  167 -275   54 -182  285 -275   24 -378  201 -462  127
  -442  319 -196  172 -551  270 -211  201 -428  290 -442  241 -344  152
  -359   -9 -664  403  -49  285 -467   54 -324  182 -201   88 -511   73
  -437  472    9  329 -374  236 -516  383 -172  295 -280  329 -639  314
  -314  -24 -595  280 -191  147 -580  167 -280  255 -226  329 -393    0
  -703  265 -255  211 -442  285  -29  383 -172  246 -570  172 -605  344
  -442  324 -354    0 -442  265 -452  167  -34  265 -679  290 -206  250
   -78  241 -359  123 -467  182 -187  221 -314  295 -314   88 -127  226
  -285  398 -521  393 -142  285 -250   24 -265  275 -344  177 -644 -275
  ------ CONTINUED BUT NOT LISTED HERE --------------
```

The out for constant amplitude fatigue is

MATERIAL MILD MS4361 HAZ CRUCI TOE

+++++ MONOTONIC PROPERTIES++++++

YOUNG'S	MODULUS	CONST	E(KSI)	28700.00000
.2%OFFSET	YIELD	STRENGTH	SY(KSI)	60.00000
TENSILE	STRENGTH	-----	UTS(KSI)	90.50000
REDUCTION	IN	AREA	RA%	60.70000
TRUE	FRACTURE	STRENGTH	SF(KSI)	133.00000
TRUE	FRACTURE	DUCTILITY	EF	.74500
STRAIN	HARDENING	EXPONENT	N	.10200
STRENGTH	COEFFT	----	K(KSI)	142.00000

+++++ CYCLIC PROPERTIES+++++

CYCLIC	YIELD	STRENGTH	SY'(KSI)	50.00000
CYCLIC	STRENGTH	COEFFT	K'(KSI)	148.00000
STRAIN	HARDENING	EXPONENT	N'	.17500
FATIGUE	STRENGTH	COEFFT	SF'(KSI)	120.00000
FATIGUE	DUCTILITY	COEFFT	EF'	.28000
FATIGUE	STRENGTH	EXPONENT	B	-.08200
FATIGUE	DUCTILITY	EXPONENT	C	-.52000
TRANSITION	FATIGUE	STRAIN	ETR	.00500
RESIDUAL	STRESS	------	SFR(KSI)	34.00000
PROPAG.	CONST	C	M	.1000E-09 3.300

GEOMETRY OF CRUCI TOE

THICKNESS	----------		T (IN.)	.50000
WELD	SIZE	-----	L2(IN.)	.40000
WELD	SIZE	-----	L1(IN.)	.40000

LENGTH OF LOP ----- C(IN.) .20000

FATIGUE NOTCH FACTOR OF TOE

AXIAL	BENDING
2.729	1.760

LOAD HISTORY CONST AMPT

NUMBER OF REVERALS ----- 3

NOMINAL AXIAL STRESS 25.00 0.00 25.00

NOMINAL BENDING STRESS 10.00 2.00 10.00

REVS.	AXIAL LOAD	BENDING LOAD	LOCAL STRESS	LOCAL STRAIN
0	0.00	0.00	0.00	0.000000
1	25.00	10.00	60.77	.008297
2	0.00	2.00	-12.38	.005069
3	25.00	10.00	60.77	.008297

MEAN STRESS RELAXED*2NI= .419E+06 XK=-.043792

NO MEAN STRESS *****2NI= .196E+07

FULL MEAN STRESS*** 2NI= .126E+06

PROPAGATION LIFE** NP = .158E+06 AF= .2984

TOTAL LIFE ***** NT = .367E+06

The output for variable amplitude fatigue is:

NUMBER OF REVERSALS 5936

LOAD SCALE 30.00

MONITOR NET 3

PRINT EVERY 1000 POINTS
BENDING FACTOR .20 5.00

PEAKS	AXIAL LOAD	BENDING LOAD	STRESS	STRAIN	DAMAGE	LOOP
0	0.000	0.000	0.00	0.000000	0.	0
1	22.162	9.432	59.06	.007306	0.	0
1000	-13.003	2.399	-23.28	.002503	.771E-04	499
2000	-9.429	3.114	-8.67	.002586	.104E-03	999
3000	-11.952	2.610	-18.66	.002541	.182E-03	1499
4000	-5.736	3.853	-5.52	.003385	.315E-03	2008
5000	-9.429	3.114	-14.85	.002912	.351E-03	2508
5937	22.162	9.432	59.23	.007357	.390E-03	2978

INITIATION LIFE = .128E+04 BLOCK

PROPAGATION LIFE = .508E+03 BLOCK

TOTAL LIFE = .179E+04 BLOCK

Program listing for constant amplitude fatigue:

```
      COMMON/ONE/SL,EL,PS(100),PB(100),YKC,YNC,SFC,EFC,NSIGN
      COMMON/TWO/TPS(100),TPN(100),XKFA,XKFB,T,E
      COMMON/THREE/CC,XM,XPN,CK,A,OPX
C
C  *****  THE FOLLOWING DATA ARE MATERIAL PROPERTIES ****
C
      READ(5,*)M1,MAT,M2,NSHAPE,NPOSI
      WRITE(6,100)M1,MAT,M2,NSHAPE,NPOSI
  100 FORMAT(1H1,///,5X,3A10,3X,2A10)
      READ(5,*)M1,M2,M3,M4
      WRITE(6,101)M1,M2,M3,M4
  101 FORMAT(///,5X,4A10)
      READ(5,*)M1,M2,M3,M4,E
      WRITE(6,102)M1,M2,M3,M4,E
  102 FORMAT(/,10X,4A10,3X,F12.5)
      READ(5,*)M1,M2,M3,M4,SY
      WRITE(6,102)M1,M2,M3,M4,SY
      READ(5,*)M1,M2,M3,M4,UTS
      WRITE(6,102)M1,M2,M3,M4,UTS
      READ(5,*)M1,M2,M3,M4,RA
      WRITE(6,102)M1,M2,M3,M4,RA
      READ(5,*)M1,M2,M3,M4,SF
      WRITE(6,102)M1,M2,M3,M4,SF
      READ(5,*)M1,M2,M3,M4,EF
      WRITE(6,102)M1,M2,M3,M4,EF
      READ(5,*)M1,M2,M3,M4,YN
      WRITE(6,102)M1,M2,M3,M4,YN
      READ(5,*)M1,M2,M3,M4,YK
      WRITE(6,102)M1,M2,M3,M4,YK
      READ(5,*)M1,M2,M3,M4
      WRITE(6,101)M1,M2,M3,M4
      READ(5,*)M1,M2,M3,M4,SYC
      WRITE(6,102)M1,M2,M3,M4,SYC
      READ(5,*)M1,M2,M3,M4,YKC
      WRITE(6,102)M1,M2,M3,M4,YKC
      READ(5,*)M1,M2,M3,M4,YNC
      WRITE(6,102)M1,M2,M3,M4,YNC
      READ(5,*)M1,M2,M3,M4,SFC
      WRITE(6,102)M1,M2,M3,M4,SFC
      READ(5,*)M1,M2,M3,M4,EFC
      WRITE(6,102)M1,M2,M3,M4,EFC
      READ(5,*)M1,M2,M3,M4,B
      WRITE(6,102)M1,M2,M3,M4,B
      READ(5,*)M1,M2,M3,M4,C
      WRITE(6,102)M1,M2,M3,M4,C
      READ(5,*)M1,M2,M3,M4,ETR
      WRITE(6,102)M1,M2,M3,M4,ETR
      READ(5,*)M1,M2,M3,M4,SFR
      WRITE(6,102)M1,M2,M3,M4,SFR
      READ(5,*)M1,M2,M4,M5,CC,XM,AI,CK,OPX
      WRITE(6,110)M1,M2,M4,M5,CC,XM
```

```
  110 FORMAT(/,10X,4A10,E10.4,5X,F6.3)
C
C****** THE GEOMETRIC FACTOR DATA *****
C
      AM=0.001*((300.0/UTS)**1.8)
      IF(NSHAPE.EQ.4HBUTT) GO TO 300
      IF(NSHAPE.EQ.3HLAP)GO TO 400
  112 FORMAT(//,5X,11HGEOMETRY OF,3X,2A10)
      WRITE(6,112)NSHAPE,NPOSI
C
C  *** CRUCIFORM JOINT  *******
C
      READ(4,*)M1,M2,M3,M4,T
      WRITE(6,102)M1,M2,M3,M4,T
      READ(4,*)M1,M2,M3,M4,XLC
      WRITE(6,102)M1,M2,M3,M4,XLC
      READ(4,*)M1,M2,M3,M4,XLS
      WRITE(6,102)M1,M2,M3,M4,XLS
      READ(4,*)M1,M2,M3,M4,XLOP
      WRITE(6,102)M1,M2,M3,M4,XLOP
C
      IF(NPOSI .EQ. 3HLOP) GO TO 10
C
      XTH=(XLC/XLS)**0.25
      XKFA=1.0+0.5*0.340*(1.0+1.06*((XLOP/XLS)**1.65))*SQRT(T/AM)*XTH
      XKFB=1.0+.20/2.0*SQRT(T/AM)*XTH
      GO TO 14
   10 XKFA=1.+.5*1.15*SQRT(XLOP*T/AM/XLS)*((XLC/XLS)**(-.2))
      XKFB=1.0+0.5*3.22*((XLOP/XLS)**.150)*SQRT(T/AM)
      BFACT=1./(((XLC+T/2.)**3.0)/XLOP/T/T-(XLOP/T)**2.0)/4.0
      XKFB=XKFB*BFACT
      GO TO 14
C
C **** BUTT WELD
C
  300 READ(5,*)M1,M2,M3,M4,T
      WRITE(6,102)M1,M2,M3,M4,T
      READ(5,*)M1,M2,M3,M4,XTHETA
      WRITE(6,102)M1,M2,M3,M4,XTHETA
      XKFA=1+0.135*(TAN(XTHETA))**0.25*(T/AM)**0.5
      XKFB=1+0.83*(TAN(XTHETA))**(1./6.)*(T/AM)**0.5
      AFACT=1.
      BFACT=1.
      GO TO 14
C
C  *** DOUBLE STRAP LAP WELD *****
C
  400 READ(4,*)M1,M2,M3,M4,T1
      WRITE(6,102)M1,M2,M3,M4,T1
      READ(4,*)M1,M2,M3,M4,T2
      WRITE(6,102)M1,M2,M3,M4,T2
      READ(4,*)M1,M2,M3,M4,XL1
```

```
      WRITE(6,102)M1,M2,M3,M4,XL1
      READ(4,*)M1,M2,M3,M4,XL2
      WRITE(6,102)M1,M2,M3,M4,XL2
      READ(4,*)M1,M2,M3,M4,XTHETA
      WRITE(6,102)M1,M2,M3,M4,XTHETA
C
      IF(NPOSI.NE.3HTOE) GO TO 401
C
      XKFA=1.+0.3*(XTHETA**.25)*(T1*T1/AM/XL1)**.5
      XKFB=1.+.008*(XTHETA**.25)*(T1*T1/AM/XL1)**.5
      BFACT=1.0
      AFACT=1.0
      T=XL1
      GO TO 14
C  *** BELOW IS FOR ROOTX
  401 IF(NPOSI.NE.5HROOTX) GO TO 402
      XKFA=1.+.152*((XL2/AM)**.5)*((T1/XL2)**.59)*((XL2/XL1)**.1)
      XKFB=1.+.084*(XL2/AM)**.5
      BFACT=.5*((XL2/XL1)**(-.43))*((T1/XL1)**1.3)*((XL2/T1)**.73)
      AFACT=T1/XL2/2.
      T=XL2
      GO TO 14
C *** BELOW IS FOR ROOTY
  402 XKFB=1.+.25*((T1/AM)**.5)*((XL2/XL1)**.12)
      BFACT=1.35*((T1/XL1)**.45)*((T1/XL2)**0.20)
      AFACT=0.0
      XKFA=1.0
      T=XL1
C
   14 WRITE(6,99)NPOSI
   99 FORMAT(1H1,//,5X,24HFATIGUE NOTCH FACTOR OF ,A10)
      WRITE(6,98)
   98 FORMAT(/,7X,17HAXIAL     BENDING)
      WRITE(6,97)XKFA,XKFB
   97 FORMAT(/,5X,F7.3,5X,F7.3)
C
C*******THE FOLLOWING BLOCK IS LOAD HISTORY********
C
  301 READ(4,*)M1,M2,M3,M4
      WRITE(6,101)M1,M2,M3,M4
      READ(4,*)M1,M2,M3,M4,NPEAK
      WRITE(6,106)M1,M2,M3,M4,NPEAK
  106 FORMAT(/,10X,4A10,I5)
      READ(4,*)M1,(PS(I),I=1,NPEAK)
      READ(4,*)M1,(PB(I),I=1,NPEAK)
      WRITE(6,103)(PS(I),I=1,NPEAK)
      WRITE(6,104)(PB(I),I=1,NPEAK)
  103 FORMAT(/,10X,20HNOMINAL AXIAL STRESS,5X,10F8.2)
  104 FORMAT(/,10X,22HNOMINAL BENDING STRESS,3X,10F8.2)
      IF(NSHAPE.NE.3HLAP) GO TO 330
      DO 320 I=1,NPEAK
      PB(I)=PS(I)*BFACT
```

```
      PS(I)=PS(I)*AFACT
  320 CONTINUE
C
C  ***** INITIATION LIFE CALCULATION *******
C
  330 IF((SFR*(XKFA*PS(1)+XKFB*PB(1))).GE.0.0) GO TO 201
      TPS(1)=SFR
      TPN(1)=0.0
      PSO=0.0
      PBO=0.0
      NREV=1
      GO TO 202
  201 TPS(1)=0.0
      TPN(1)=0.0
      PSO=0.0
      PSI=PS(1)
      PBO=0.0
      PBI=PB(1)
      XNEU=YNEUB(SFR,PSO,PSI,XKFA,PBO,PBI,XKFB,E)
      NREV=1
      CALL COUNT(NREV,1.0,PSO,PSI,PBO,PBI,XNEU)
      PSO=PSI
      PBO=PBI
      NREV=2
  202 DO 203 I=NREV,NPEAK
      PSI=PS(I)
      PBI=PB(I)
      XNEU=YNEUB(0.0,PSO,PSI,XKFA,PBO,PBI,XKFB,E)
      CALL COUNT(I,2.0,PSO,PSI,PBO,PBI,XNEU)
      PSO=PSI
      PBO=PBI
  203 CONTINUE
      WRITE(6,108)
  108 FORMAT(/,17X,5HAXIAL,7X,7HBENDING,5X,5HLOCAL,7X,5HLOCAL,/,
     *7X,5HREVS.,5X,4HLOAD,8X,4HLOAD,8X,6HSTRESS,6X,6HSTRAIN)
      PSO=0.0
      PBO=0.0
      I=0
      WRITE(6,105)I,PSO,PBO,TPS(I+1),TPN(I+1)
      DO 30 I=1,NPEAK
      WRITE(6,105)I,PS(I),PB(I),TPS(I+1),TPN(I+1)
  105 FORMAT(/10X,I2,5X,F7.2,5X,F7.2,5X,F7.2,5X,F8.6)
   30 CONTINUE
      XK=0.0
      XNI=0.0
      SMN=TPS(NPEAK)+SL*NSIGN/2.0
      XK=-4625.*(EL-SL/E)/E/ETR
      IF(EL .LT. 0.0080) XK=XK*2.0
      X=(10.0-ALOG10(50.0))/150.0
      F=0.0
      DO 500 K=1,50
      G=((SFC-SMN*(K**XK))/SL*2.0)**(1.0/B)
```

```
      F=F+G
  500 CONTINUE
      XNI=K
      DO 510 J=1,150
      XNN=50.0*10**((J-1)*X)*(10**X-1)
      IF(F.GT.0.70) XNN=XNN/2.0
      XNI=XNI+XNN
      G1=((SFC-SMN*(XNI**XK))/SL*2.0)**(1/B)
      F=F+(G+G1)*XNN/2.0
      G=G1
C     WRITE(6,505)F,XNI
  505 FORMAT(2X,F8.6,2X,E9.3)
      IF(F.GE.1.0) GO TO 520
  510 CONTINUE
  520 WRITE(6,502)XNI,XK
  502 FORMAT(//5X,24HMEAN STRESS RELAXED*2NI=,E9.3,10X,3HXK=,F8.6)
      XI=(SL/2.0/SFC)**(1/B)
      WRITE(6,503)XI
  503 FORMAT(/5X,24HNO MEAN STRESS *****2NI=,E9.3)
      XI=(SL/2.0/(SFC-SMN))**(1/B)
      WRITE(6,540)XI
  540 FORMAT(/5X,25HFULL MEAN STRESS*** 2NI= ,E9.3)
C
C******** PROPAGATION LIFE AND TOTAL LIFE *********
C
      XPN=0.0
      CC=CC/(0.7**XM)
      PSI=PS(NPEAK)
      PSO=PS(NPEAK-1)
      PBI=PB(NPEAK)
      PBO=PB(NPEAK-1)
  125 IF(NPOSI .EQ. 3HLOP) GO TO 131
      IF(NSHAPE.EQ.3HLAP) 132,133
  132 IF(NPOSI.EQ.3HTOE)GO TO 135
      CALL TOELIFE(PSI,PSO,PBI,PBO,AI)
      GO TO 140
  135 PBO=PSO
      PBI=PSI
      CALL TOELIFE(PSI,PSO,PBI,PBO,AI)
      GO TO 140
  133 CALL TOELIFE(PSI,PSO,PBI,PBO,AI)
      GO TO 140
  131 X=ABS(PS(NPEAK)+PB(NPEAK)*BFACT)*T/0.707/UTS
      CA=XLC+T/2.-X
      CALL LOPLIFE(PSI,PSO,PBI,PBO,XLOP,XLC)
  140 WRITE(6,111)XPN,A
  111 FORMAT(/,5X,25HPROPAGATION LIFE** NP  = ,E10.3,10X,3HAF=,F7.4)
      TN=XPN+XNI/2.0
      WRITE(6,530)TN
  530 FORMAT(/,5X,25HTOTAL LIFE     ***** NT = ,E9.3)
      STOP
      END
```

```
C
C*******************************
      FUNCTION YNEUB(SFR,PSO,PSI,XKFA,PBO,PBI,XKFB,E)
      YNEUB=((SFR+XKFA*(PSI-PSO)+XKFB*(PBI-PBO))**2)/E
      RETURN
      END
C
C*****************************
      SUBROUTINE COUNT(I,COF,PSO,PSI,PBO,PBI,XNEU)
      COMMON/TWO/TPS(100),TPN(100),XKFA,XKFB,T,E
      COMMON/ONE/SL,EL,PS(100),PB(100),YKC,YNC,SFC,EFC,NSIGN
      DRSN=0.0
      SL=0.0
      EL=0.0
      IF(XKFA*(PSI-PSO)+XKFB*(PBI-PBO) .GT. 0.0) GO TO 20
       NSIGN=-1
      GO TO 30
   20 NSIGN=1
   30 SL=SFC
      EL=EFC
   40 Y1=SL*EL-XNEU
      IF(ABS(Y1/XNEU).LE.0.01) GO TO 50
      Y2=EL+SL*(1./E+1./YNC/YKC*(SL/COF/YKC)**(1./YNC-1.))
      SL=SL-Y1/Y2
      EL=SL/E+COF*(SL/COF/YKC)**(1./YNC)
      GO TO 40
   50 TPS(I+1)=TPS(I)+NSIGN*SL
      TPN(I+1)=TPN(I)+NSIGN*EL
   75 RETURN
      END
C
C
      SUBROUTINE TOELIFE(SAI,SAO,SBI,SBO,AI)
      COMMON/TWO/TPS(100),TPN(100),XKFA,XKFB,T,E
      COMMON/THREE/CC,XM,XPN,CK,A,OPX
      COMMON/FIVE/XKTA,XKTB
      XKTA=1.0+(XKFA-1)*2.0
      XKTB=1.0+(XKFB-1.0)*2.0
      IF(AI.NE.0.0) GO TO 20
      IF (XKTA.EQ. 1.0) GO TO 10
      AI=0.0198*T/(XKTA-1.0)
      GO TO 20
   10 AI=0.0154*T/(XKTB-1.0)
   20 FF=ALOG10(T/AI)/100.0
      SKA1=FW(AI,T)*FMA(AI,T)*SQRT(3.14159*AI)
      SKB1=FMB(AI,T)*SQRT(3.14159*AI)*(1.122-1.4*(AI/T)+7.33*(AI/T)**2.0
     *     -13.08*(AI/T)**3.0+14.0*(AI/T)**4.0)
      A=AI
      SK1=SKA1*SAI+SKB1*SBI
      SKMN=SKA1*SAO+SKB1*SBO
      IF (SKMN .GT.(SK1*0.3)) 30,40
   30 SA=SAI-SAO
```

```
      SB=SBI-SBO
      GO TO 45
   40 IF (SKMN .GE. 0.) 43,42
   42 SA=SAI-OPX*SAO
      SB=SBI-OPX*SBO
      GO TO 45
   43 SA=0.7*SAI
      SB=0.7*SBI
   45 SK1=SKA1*SA+SKB1*SB
      FK1=1.0/(CC*(SK1**XM))
      DO 100 I=1,99
      AA=A*(10**FF)-A
      A=A+AA
      SKA2=FW(A,T)*FMA(A,T)*SQRT(3.14159*A)*SA
      SKB2=FMB(A,T)*SQRT(3.14159*A)*(1.122-1.4*(A/T)+7.33*(A/T)**2.0
     *-13.08*(A/T)**3.0+14.0*(A/T)**4.0)*SB
C     XK12=FS*FM(A)*SQRT(3.14159*A)
      SK2=SKA2+SKB2
      IF((SK2.GT.CK).OR.(A.GT.T))GO TO 101
      FK2=1.0/(CC*(SK2**XM))
      XPN=XPN+(FK1+FK2)*AA/2.0
      FK1=FK2
  100 CONTINUE
  101 RETURN
      END
C
C
      FUNCTION FW(A,T)
      COMMON/FIVE/XKTA,XKTB
      W=3.14159*A/T
      ST=SIN(W/2.0)
      CT=COS(W/2.0)
      PI=SQRT(3.14159)
      FW=2.0/PI*((ST**2.0)+(CT**(-2.0)))
C     TT=1.0/COS(T)
C     FW=SQRT(TT)
C     FW=1.1
      RETURN
      END
C
C
      FUNCTION FMA(A,T)
      COMMON/FIVE/XKTA,XKTB
      FMA=1+(XKTA-1.0)*EXP(-22.5*(XKTA-1.0)*A/T)
C     FMA=1.0
      RETURN
      END
C
C
      FUNCTION FMB(A,T)
      COMMON/FIVE/XKTA,XKTB
      FMB=1+(XKTB-1.0)*EXP(-45.0*(XKTB-1.0)*A/T)
```

```
      RETURN
      END
C
C
      SUBROUTINE LOPLIFE(SAI,SAO,SBI,SBO,AI,XL)
      COMMON/TWO/TPS(100),TPN(100),XKFA,XKFB,T,E
      COMMON/THREE/CC,XM,XPN,CK,A,OPX
      A=AI
      BFACT=1./(((XL+T/2.)**3.0)/A/T/T-(A/T)**2.0)/4.0
      FF=ALOG10((XL+T/2.)/AI)/100.0
      XA1=PW(AI,T,XL)*FM(AI,XL,T)*SQRT(3.14159*AI)
      XB1=PMB(A,T)*SQRT(3.14159*A)*BFACT
      XK1=XA1*SAI+XB1*SBI
      SKMN=XA1*SAO+XB1*SBO
      IF (SKMN .GT. 0.3*XK1) 10,20
   10 SA=SAI-SAO
      SB=SBI-SBO
      GO TO 30
   20 IF (SKMN .LT. 0.0) 25,26
   25 SA=SAI
      SB=SBI
      GO TO 30
   26 SA=SAI*0.7
      SB=SBI*0.7
   30 XK1=SA*XA1+SB*XB1
      FK1=1.0/(CC*(XK1**XM))
      DO 100 I=1,99
      AA=A*(10**FF)-A
      A=A+AA
      BFACT=1./(((XL+T/2.)**3.0)/A/T/T-(A/T)**2.0)/4.0
      XA2=PW(A,T,XL)*FM(A,XL,T)*SQRT(3.14159*A)*SA
      XB2=SB*PMB(A,T)*SQRT(3.14159*A)*BFACT
      XK12=XB2+XA2
      FK2=1.0/(CC*(XK12**XM))
      IF((A.GE.T).OR.(XK12.GE.CK))GO TO 101
      XPN=XPN+(FK1+FK2)*AA/2.0
      FK1=FK2
  100 CONTINUE
  101 RETURN
      END
C
C
      FUNCTION PW(A,T,XL)
      W=3.14159*A/(2.0*XL+T)
      CT=COS(W)
      PW=CT**(-0.5)
      RETURN
      END
C
C
      FUNCTION FM(A,XL,T)
      A1=.528+3.287*(XL/T)-4.361*(XL/T)**2.+3.696*(XL/T)**3.-1.874*
```

```
     *(XL/T)**4.+.415*(XL/T)**5.
      A2=.218+2.717*(XL/T)-10.171*(XL/T)**2.+13.122*(XL/T)**3.-7.755*
     *(XL/T)**4.+1.785*(XL/T)**5.
      FM=(A1+A2*(A/(2*XL+T)))/(1+(2*XL/T))
      RETURN
      END
C
      FUNCTION PMB(A,T)
      PMB=0.5*(1+0.417*(A/1.5/T)**4+0.146*(A/1.5/T)**6.0)
      RETURN
      END
```

Program listing for variable amplitude fatigue:

```
      DIMENSION PS(6002),PMAX(10),PMIN(10),TSMX(11),TSMN(11),TNMX(11)
      DIMENSION TNMN(11),BMIN(11),BMAX(11),PB(6002)
      COMMON /ZERO/ SEGS(150),SEGN(150)
      COMMON/ONE/ NAV(151),NC
      COMMON/TWO/TPS,TPN,XKFA,XKFB,XNI,CC,XM,PN,T,E,ISTOP
      COMMON/THREE/ SFC,B,C,DAM,LOOP,ETR,M3,SAM,OPX,AF,CK
      COMMON/FOUR/YNC,YKC,NSIGN,SL,EL,NPOSI,XB,XXB
C
      READ(5,*)M1,M2,M3,M4,NPEAK
      READ(5,*)M1,M2,M3,M4,XMF
      READ(5,*)M1,M2,M3,M4,NN
      READ(5,*)M1,M2,M3,M4,N
      READ(5,*)M1,M2,M3,M4,XB,XXB
    1 WRITE(6,107)NPEAK,XMF,NN,N,XB,XXB
  107 FORMAT(/10X,20HNUMBER OF REVERSALS ,I5,//10X,11HLOAD  SCALE,
     *F7.2,//10X,11HMONITOR NET,I4,//10X,11HPRINT EVERY,I5,2X,
     *6HPOINTS,/,10X,14HBENDING FACTOR,F7.2,10X,F5.2)
      READ(5,*)(PS(I),I=1,NPEAK)
C     READ(5,*)(PB(I),I=1,NPEAK)
      XMF=XMF/999.0
      XMX=0.0
      SAM=0.0
C
C **** FIND STARTING POINT *****
C
      DO 220 I=1,NPEAK
      PS(I)=PS(I)*XMF
      PB(I)=(PS(I)*XB+XXB)*BFACT
      PS(I)=PS(I)*AFACT
      PX=PS(I)*XKFA+PB(I)*XKFB+SFR
      IF(ABS(PX).GT.XMX)221,220
  221 XMX=PX
      MAX=I
  220 CONTINUE
      OPX=OPX*(PS(MAX)+PB(MAX))
      WRITE(6,106)
  106 FORMAT(//,23X,5HAXIAL,5X,7HBENDING,/,10X,5HPEAKS,8X,4HLOAD,6X,
     *4HLOAD,5X,6HSTRESS,6X,6HSTRAIN,5X,6HDAMAGE,5X,4HLOOP)
      LOOP=0
      DAM=0.0
      ISTOP=NPEAK+1
      CALL SIMU(.10,YKC,YNC,E)
      DO 200 I=1,151
      NAV(I)=0
  200 CONTINUE
C
C **** STRATING CYCLE COUNTING
C
      PBO=PB(MAX)
```

```
      IF((SFR+XKFA*PS(MAX)+XKFB*PBO).GE.0.0) GO TO 201
      TPS=SFR
      TPN=0.0
      PSO=0.0
      PBO=0.0
      NREV=1
      M=0
      WRITE(6,105)M,PBO,TPS,TPN,DAM,LOOP
      GO TO 202
  201 TPS=0.0
      TPN=0.0
      PSO=0.0
      PSI=PS(MAX)
      PBO=0.0
      PBI=PB(MAX)
      XNEU=YNEUB(SFR,PSO,PSI,XKFA,PBO,PBI,XKFB,E)
      NREV=1
      M=0
      WRITE(6,105)M,PSO,PBO,TPS,TPN,DAM,LOOP
      CALL COUNT(NREV,PSO,PSI,PBO,PBI,XNEU)
      PSO=PSI
      PBO=PBI
      PMAX(1)=PSI
      PMIN(1)=PSI
      BMAX(1)=PBI
      BMIN(1)=PBI
      TSMX(1)=TPS
      TNMX(1)=TPN
      NREV=2
      M=1
      WRITE(6,105)M,PSI,PBI,TPS,TPN,DAM,LOOP
  202 DO 203 I=NREV,NPEAK
      J=I+MAX-1
      IF(J.GT.NPEAK) J=J-NPEAK
      PSI=PS(J)
      PBI=PB(J)
      XNEU=YNEUB(0.0,PSO,PSI,XKFA,PBO,PBI,XKFB,E)
      CALL COUNT(I,PSO,PSI,PBO,PBI,XNEU)
      IF(I.NE.1) GO TO 206
      M=1
      WRITE(6,105)M,PSI,PBI,TPS,TPN,DAM,LOOP
      PMIN(1)=PSI
C
C **** MODIFY THE LOOP PATH
C
      PMAX(2)=PSI
      BMIN(1)=PBI
      BMAX(2)=PBI
      TSMN(1)=TPS
      TNMN(1)=TPN
      GO TO 203
  206 DO 210 K=1,NN
```

```
      IF((PSI.LT.PMIN(K)).OR.(PBI.LT.BMIN(K)))211,212
  211 CALL PEAK(PSI,PMAX(K),PBI,BMAX(K))
      PMIN(K)=PSI
      PMAX(K+1)=PSI
      BMIN(K)=PBI
      BMAX(K+1)=PBI
      TPS=TSMX(K)-SL
      TPN=TNMX(K)-EL
      TSMN(K)=TPS
      TNMN(K)=TPN
      GO TO 215
  212 IF((PSI.GT.PMAX(K+1)).OR.(PBI.GT.BMAX(K+1)))213,210
  213 CALL PEAK(PSI,PMIN(K),PBI,BMIN(K))
      PMAX(K+1)=PSI
      PMIN(K+1)=PSI
      BMAX(K+1)=PBI
      BMIN(K+1)=PBI
      TPS=TSMN(K)+SL
      TPN=TNMN(K)+EL
      TSMX(K+1)=TPS
      TNMX(K+1)=TPN
      GO TO 215
  210 CONTINUE
  215 PSO=PSI
      PBO=PBI
      IF(I.NE.(I/N*N)) GO TO 203
  205 WRITE(6,105)I,PSI,PBI,TPS,TPN,DAM,LOOP
  105 FORMAT(/10X,I5,5X,F7.3,4X,F7.3,4X,F7.2,2X,F10.6,5X,E9.3,2X,I4)
      IF(DAM.GT. 1.0) GO TO 204
  203 CONTINUE
      XNEU=YNEUB(0.0,PSI,PS(MAX),XKFA,PBI,PB(MAX),XKFB,E)
      CALL COUNT(ISTOP,PSI,PS(MAX),PBI,PB(MAX),XNEU)
      WRITE(6,105)ISTOP,PS(MAX),PB(MAX),TPS,TPN,DAM,LOOP
  204 XNI=0.5/DAM
      WRITE(6,108)XNI
  108 FORMAT(/,10X,18HINITIATION LIFE = ,E9.3,3X,5HBLOCK)
C
C **** PROPAGATION LIFE CALCULATION ********
C
      PN=0.0
      IF(NPOSI.EQ.3HLOP)500,501
  500 CALL LOPLIFE(SAM,XLOP,XLC)
      GO TO 510
  501 IF(NSHAPE.NE.3HLAP)GO TO 506
      IF(NPOSI.EQ.5HROOTY)GO TO 505
      XB=BFACT
      CALL TOELIFE(SAM)
      GO TO 510
  505 CALL TOELIFE(SAM)
      GO TO 510
  506 CALL TOELIFE(SAM)
  510 WRITE(6,503)PN
```

```
  503 FORMAT(//10X,19HPROPAGATION LIFE = ,E9.3,3X,5HBLOCK)
      TN=XNI+PN
      WRITE(6,504)TN
  504 FORMAT(//10X,13HTOTAL LIFE = ,E9.3,3X,5HBLOCK)
      STOP
      END
C
C
      FUNCTION YNEUB(SFR,PSO,PSI,XKFA,PBO,PBI,XKFB,E)
      YNEUB=((SFR+XKFA*(PSI-PSO)+XKFB*(PBI-PBO))**2)/E
      RETURN
      END
C
C
      SUBROUTINE SIMU(F,XK,XN,XE)
      COMMON /ZERO/ SEGS(150),SEGN(150)
      DE=ALOG10(F/.0001)/75.0
      SL=XK*(0.0001)**XN
      DS=SL/75.0
      EL1=0.0
      DO 10 I=1,75
      SEGS(I)=DS
      EL=DS*I/XE+(DS*I/XK)**(1./XN)
      SEGN(I)=EL-EL1
      EL1=EL
   10 CONTINUE
      SL1=SL
      DO 20 I=76,150
      EP=0.0001*(10.0**((I-75.0)*DE))
      SL=XK*(EP)**XN
      EL=SL/XE+EP
      SEGS(I)=SL-SL1
      SEGN(I)=EL-EL1
      SL1=SL
      EL1=EL
   20 CONTINUE
      RETURN
      END
C
C
      SUBROUTINE COUNT(I,PSO,PSI,PBO,PBI,XNEU)
      COMMON/TWO/TPS,TPN,XKFA,XKFB,XNI,CC,XM,PN,T,E,ISTOP
      COMMON/ZERO/ SEGS(150),SEGN(150)
      COMMON/ONE/ NAV(151),NC
      COMMON/FOUR/YNC,YKC,NSIGN,SL,EL,NPOSI,XB,XXB
      SKS=0.0
      SKN=0.0
      SL=0.0
      EL=0.0
      SLX=0.0
      J=1
      IF(XKFA*(PSI-PSO)+XKFB*(PBI-PBO) .GT. 0.0) GO TO 20
```

```
      NSIGN=-1
      GO TO 30
   20 NSIGN=1
   30 IF(NSIGN*NAV(J).GT. 0) GO TO 40
      IF(NAV(J).EQ.0) GO TO 31
      COF=2.0
      GO TO 32
   31 COF=1.0
   32 NFLAG=1
      NAV(J)=NSIGN
      SL=COF*SEGS(J)+SL
      EL=COF*SEGN(J)+EL
      IF(SL*EL.GE.XNEU) GO TO 53
      J=J+1
      GO TO 30
   53 IF(NAV(J)*NAV(J+1).LT. 0) GO TO 55
      CALL DAMP(PSO,PBO)
      CALL DAMAGE(I,SL,EL,NSIGN)
   55 TPS=TPS+SL*NSIGN
      TPN=TPN+EL*NSIGN
      GO TO 75
   40 NAV(J)=NSIGN*2
C     WRITE(6,41)J,SL,EL,NPOSI,XB,XXB,NAV(J)
      SKS=SKS+COF*SEGS(J)
      SKN=SKN+COF*SEGN(J)
      J=J+1
      IF(NFLAG.NE.1) GO TO 30
      NFLAG=2
      CALL DAMP(PSO,PBO)
   45 CALL DAMAGE(I,SL,EL,NSIGN)
      GO TO 30
   75 RETURN
      END
C
C
      SUBROUTINE DAMAGE(I,DRSS,DRSN,NSIGN)
      COMMON/TWO/TPS,TPN,XKFA,XKFB,XNI,CC,XM,PN,T,E,ISTOP
      COMMON/THREE/SFC,B,C,DAM,LOOP,ETR,M3,SAM,OPX,AF,CK
      IF(I.NE. 1) GO TO 6
      DAM=0.0
      XK=0.0
      XNI=0.0
      GO TO 12
    6 SMN=TPS+DRSS*NSIGN/2.0
   20 DAM=DAM+(DRSS/(2*(SFC-SMN)))**(-1/B)
      LOOP=LOOP+1
   12 RETURN
      END
C
C
      SUBROUTINE PEAK(A,B,C,D)
      COMMON/TWO/TPS,TPN,XKFA,XKFB,XNI,CC,XM,PN,T,E,ISTOP
```

```
      COMMON/FOUR/YNC,YKC,NSIGN,SL,EL,NPOSI,XB,XXB
      XNEU=YNEUB(0.0,A,B,XKFA,C,D,XKFB,E)
    1 EL=SL/E+2.0*(SL/2./YKC)**(1./YNC)
      Y1=SL*EL-XNEU
      IF(ABS(Y1/XNEU).LE.0.01) GO TO 10
      Y2=EL+SL*(1./E+1./YNC/YKC*(SL/2./YKC)**(1./YNC-1.))
      SL=SL-Y1/Y2
      GO TO 1
   10 RETURN
      END
C
C
      SUBROUTINE DAMP(SO,SB)
      COMMON/TWO/TPS,TPN,XKFA,XKFB,XNI,CC,XM,PN,T,E,ISTOP
      COMMON/THREE/ SFC,D,C,DAM,LOOP,ETR,M3,SAM,OPX,AF,CK
      COMMON/FOUR/YNC,YKC,NSIGN,SL,EL,NPOSI,XB,XXB
      IF(XKFA.NE.1.0)GO TO 10
      SI=SQRT(SL*EL*E)/XKFB
      SO=SB
      GO TO 30
   10 SI=SQRT(SL*EL*E)/(XKFA)
   30 SI=SO+SI*NSIGN
      IF(SI.GT.SO)1,2
    1 SMAX=SI
      SMIN=SO
      GO TO 3
    2 SMAX=SO
      SMIN=SI
    3 IF(SMIN.GE.OPX)5,6
    5 SAM=SAM+(SMAX-SMIN)**XM
      GO TO 4
    6 IF(SMAX.LT.OPX) GO TO 4
      SAM=SAM+(SMAX-OPX)**XM
    4 RETURN
      END
C
C
      SUBROUTINE LOPLIFE(SA,AI,XL)
      COMMON/TWO/TPS,TPN,XKFA,XKFB,XNI,CC,XM,PN,T,E,ISTOP
      COMMON/THREE/ SFC,B,C,DAM,LOOP,ETR,M3,SAM,OPX,AF,CK
      A=AI
      AF=XL+T/2.
      AA=(XL+T/2.)/100.
      XA1=PW(AI,T,XL)*FM(AI,XL,T)*SQRT(3.14159*AI)
      FK1=1.0/(CC*(XA1**XM)*SA)
      DO 100 I=1,99
      A=A+AA
      XA2=PW(A,T,XL)*FM(A,XL,T)*SQRT(3.14159*A)
      FK2=1.0/(CC*(XA2**XM)*SA)
      IF((A.GT.AF))GO TO 101
      PN=PN+(FK1+FK2)*AA/2.0
      FK1=FK2
```

```
  100 CONTINUE
  101 RETURN
      END
C
C
      FUNCTION PW(A,T,XL)
      W=3.14159*A/(2.0*XL+T)
      CT=COS(W)
      PW=CT**(-0.5)
      RETURN
      END
C
C
      FUNCTION FM(A,XL,T)
      A1=.528+3.287*(XL/T)-4.361*(XL/T)**2.+3.696*(XL/T)**3.-1.874*
     *(XL/T)**4.+.415*(XL/T)**5.
      A2=.218+2.717*(XL/T)-10.171*(XL/T)**2.+13.122*(XL/T)**3.-7.755*
     *(XL/T)**4.+1.785*(XL/T)**5.
      FM=(A1+A2*(A/(2*XL+T)))/(1+(2*XL/T))
      RETURN
      END
C
C
      SUBROUTINE TOELIFE(SA)
      COMMON/TWO/TPS,TPN,XKFA,XKFB,XNI,CC,XM,PN,T,E,ISTOP
      COMMON/THREE/ SFC,B,C,DAM,LOOP,ETR,M3,SAM,OPX,AF,CK
      COMMON/FOUR/YNC,YKC,NSIGN,SL,EL,NPOSI,XB,XXB
      COMMON/FIVE/XKTA,XKTB
      XKTA=1.0+(XKFA-1)*2.0
      XKTB=1.0+(XKFB-1.0)*2.0
      AI=0.01
C     GO TO 20
C     IF (XKTA.EQ. 1.0) GO TO 10
C     AI=0.0198*T/(XKTA-1.0)
C     GO TO 20
C  10 AI=0.0154*T/(XKTB-1.0)
   20 FF=ALOG10(T/AI)/100.0
      SKA1=FW(AI,T)*FMA(AI,T)*SQRT(3.14159*AI)
      SKB1=FMB(AI,T)*SQRT(3.14159*AI)*(1.122-1.4*(AI/T)+7.33*(AI/T)**2.0
     *     -13.08*(AI/T)**3.0+14.0*(AI/T)**4.0)
      A=AI
AF=T
      IF(XKFA .NE.1.0) GO TO 30
      FK1=1.0/(CC*(SKB1**XM)*SA)
      GO TO 40
   30 SK1=(SKA1+SKB1*XB)
      FK1=1.0/(CC*SA*(SK1**XM))
   40 DO 100 I=1,99
      AA=A*(10**FF)-A
      A=A+AA
      SKA2=FW(A,T)*FMA(A,T)*SQRT(3.14159*A)
      SKB2=FMB(A,T)*SQRT(3.14159*A)*(1.122-1.4*(A/T)+7.33*(A/T)**2.0
```

```
     *-13.08*(A/T)**3.0+14.0*(A/T)**4.0)
      IF(XKFA.NE.1.0) GO TO 50
      FK2=1.0/(CC*SA*(SKB2**XM))
      GO TO 60
   50 SK2=(SKA2+SKB2*XB)
      FK2=1.0/(CC*SA*(SK2**XM))
   60 IF(A.GE.AF) GO TO 101
      PN=PN+(FK1+FK2)*AA/2.0
      FK1=FK2
  100 CONTINUE
  101 RETURN
      END
C
C
      FUNCTION FW(A,T)
      COMMON/FIVE/XKTA,XKTB
      W=3.14159*A/T
      ST=SIN(W/2.0)
      CT=COS(W/2.0)
      PI=SQRT(3.14159)
      FW=2.0/PI*((ST**2.0)+(CT**(-2.0)))
C     TT=1.0/COS(T)
C     FW=SQRT(TT)
C     FW=1.1
      RETURN
      END
C
C
      FUNCTION FMA(A,T)
      COMMON/FIVE/XKTA,XKTB
      FMA=1+(XKTA-1.0)*EXP(-22.5*(XKTA-1.0)*A/T)
C     FMA=1.0
      RETURN
      END
C
C
      FUNCTION FMB(A,T)
      COMMON/FIVE/XKTA,XKTB
      FMB=1+(XKTB-1.0)*EXP(-45.0*(XKTB-1.0)*A/T)
      RETURN
      END
```

REFERENCES

1. Harrison, J. D., "An Analysis of the Fatigue Behavior of Cruciform Joints," Brit. Weld. Inst., Report No. E/21/12/68, 1968.

2. Gurney, T. R., "A revised Analysis of the Influence of Toe Defects on the Fatigue Strength of Transverse Non-Load-Carrying Fillet Welds," Weld. Res. Intl., Vol. 9, No. 3, p. 43, 1979.

3. Maddox, S. J., "Fracture Mechainos Applied to Fatigue in Welded Structure," Brit. Weld. Inst. Report No. E/36/70, 1970.

4. Frank, K, H., " The Fatigue Strength of Fillet Welded Connections," Ph.D. Thesis, Leighi University, 1971

5. Lawrence, F. V. Jr., and Munse, W. H., "Fatigue Crack Propagation in Butt Welds Containing Joint Penetration Defects," Weld. J. Vol. 52, p. 221s, 1973

6. Burk, J. D., and Lawrence, F. V., Jr., "Effects of Lack of Penetration and Lack of Fusion on the Fatigue Properties of 5083 Aluminum Alloy welds", Weld. Res. Council Bull. Vol. 4 No. 4, 1979.

7. Lawrence, F. V., "Estimation of Fatigue Crack Propagation Life in Butt Weld," Weld. J. vol. 52 212s-220s, 1973.

8. Burk, J. D. and Lawrence, F. V. Jr., "Influence of Bending stresses on Fatigue Crack Propagation LIfe in Butt Joint Welds," Weld. J. vol. 56, p. 43s, 1977

9. Smith, I. F. C. and Smith, R. A., "Measurement of Fatigue Crack in Welded Joints," Int. J. Fatigue, Vol. 4, No. 1, p. 42, 1981.

10. Higashida, Y., " Strain Controlled Fatigue Behavior of Weld Metal and Heat-Affected Base Metal in A36, A514 Steel Welds," Ph.D. Thesis, Univer. Ill., 1976.

11. Langaraf, R. W., "Cyclic Deformation and Fatigue Behavior of Hardened Steels," Ph.D. Thesis, Univer. Ill., 1969

12. Berge, S. and Myhre, H., "Fatigue Strength of Misaligned Cruciform and Butt Joints," Norwagian Maritime Research, vol. 15, No. 1, p. 29-39, 1977

13. Lohne, W., "Joints in Offshore Structure," Norwagian Maritime Research, vol. 7, No. 3, p. 12-20, 1979

14. Morrow, JoDean, Ross, A. S., and Sinclair, G. M., "Relaxation of Residual Stresses Due to Fatigue Loading", TAM Reoprt No. 568, Univeristy of Illinois, Urbana, Ill., 1959.

15. Mattos, R. J., "Estimation Fatigue Initiation Life of Weld", Ph.D. Thesis, Univer. Ill., 1973

16. Lomacky, O., Ellingwood, B. and Figgord, L. N., "Analysis of Low Cycle Fatigue Performacne of Welded Structural Joints", Trans. 3rd Int. Conf. on Strucural Mechanics in Reactor Technology, Vol. 5 Part L, L6/6, 1976.

17. Smith, K. N., El Haddad, M. and Martin, J. F., " Fatigue Life and Crack Propagation Analyses of Welded Components Containing Residual Stresses", J. Mat. and Eval., Vol.,5, No. 4, p. 327, 1977.

18. Burk, J. D., "Effect of Residual Stresses on Weld Fatigue Life," Ph.D. Thesis, Univ. Ill., Urbana, Ill., 1978.

19. Munse, W. H., Fatigue of Welded Steel Structure, Weld. Res. Council, New York, 1964.

20. Gurney, T. R., "Some Factor Affecting Design Stresses", Fatigue of Welded Structure, Chap. 14, Cambridge Press, Cambridge, England, 1979.

21. Pollard, B. and Cover, R. J., "Fatigue of Steel Weldments", Weld. J., Vol. 51, No. 11, p. 544s, 1972.

22. Kelsey, R. A., "Fatigue and Fracture Characteristics of Al Mg Butt Welds", Alcoa Lab., Report No. 57-77-18, 1977.

23. Reemsnyder H. S., "Evaluating the Effect of Residual Stress on Notch Fatigue Resistance", Symposium on Residual Stress, ASTM, Phionex, 1981.

24. Ho, N.-J. and Lawrence, F. V., Unpublished results, Dept. of Metallurgical Engineering, University of Illinois, 1979.

25. Booth, G. S., "The Fatigue Life of Ground or Peened Fillet Weld Steel Joints - the Effect of Mean Stress," Metal Constru., vol. 13, No. 2, p. 38-42, 1981

26. Palmgren, A., "Die lebensdauer von Kygellagorn," Verein Deutscher Ingenieure Zeitschrift, Vol. 68, p. 339, 1924

27. Miner, M. A., "Cumulative Damage in Fatigue," J. Appl. Mech., vol. 12, No. 3, p. a159 1945.

28. Maddox, S. J., "A Fracture Mechanics Approach to Service Load Fatigue in Welded Structure", Weld. Res. Int. Vol. 4, No. 2, p. 1-30, 1974.

29. Munse, W. H., " Predicting the Fatigue Behavior of Weldments for for Random Loads," 10th Annual Offshore Technology Conf. in Houston, 1978

30. Barsom, J., "Fatigue Crack Growth Under Variable Amplitude Loading in ASTM A514 Grade B STeel," ASTM STP 536, 1973

31 Dowling, N. E., "FAtigue Failure Prediction for Complicated Stress Strain History", J. Materials, JMSLA, Vol. 7, No. 1, 1972.

32. Socie, D. F., "Estimation Fatigue Crack Initiation and Propagation lives in Notched Plates under Variable Loading History," Ph.D. Thesis, Univer. Ill., 1977

33. Lawrence, F. V., Mattos, R. J., Higashida, Y., Burk, J. D., "Estimation of Fatigue Crack Initiation Life of Weld," ASTM STP 648, p. 420 American Society of Testing and Materials, 1978.

34. Lopes, L. A., Dodds, R. H., Rehak, D. R. and Urzua, J., "POLO FINITE, A Structural Mechanics System for Linear and Nonlinear Analysis", Technical Report, CESL of U. of I., Urbana, Ill., 1977

35. Lawrence, F. V. Jr., Ho, N.-J., Mazumdar, P. k., " Predicting Fatigue Resistance of Welds," Annual Review of Materials Science, vol. 11, p. 402-425, 1981,

36. Topper, T. H., Wetzel, R. M., and Morrow, JoDean, " Neuber's Rule Applied to Fatigue Notched Specimens," J. Materials, vol. 4, p. 200, 1969.

37. Peterson, R. E., "Notch Sensitivity," Metal Fatigue, Chap. 13, Sines and Waisman (ed.) McGraw-Hill, New York, 1959.

38. Wetzel, R. M., "A Method of Fatigue Damage Analysis," Ph.D. Thesis, Univer. Waterloo, Ontario, Canada, 1971

39. Paris, P. C., and Erdogan, "A critical Analysis of Crack Propagation Law," J. Basic Eng. vol. 85, p. 528, 1963

40. Maddox, S. J., "An Analysis of Fatigue Crack in Fillet Welded Joints," Brit. Weld. Inst. Report No. E/49/72, 1972

41. Emery, A. F., "Stress Intenstiy Factor for Thermal Stress in Thick Hollow Cyclinder," J. Basic Eng., ASME Trans. Series D, vol. 88, p. 45, 1966.

42. Albrecht, P. and Yamada, K., "Rapid Calculation of Stress Intensity Factors," J. Str. Div. of ASCE, vol. 2, p. 377-389, 1977.

43. Testin, R. A.,"Material Properties of a Mild Steel (MS4361) Weld Heat Affected Zone", General Motors Eletro Motive Division, Engineering Report No. 81-76, 1981.

44. Tupek, G. F., "Analysis of the Thermal Cycle at the Toe of a Fillet Weld", General Motors Electro Motive Division, Welding Engineering Report No. 874-78-5, 1978.

45. Testin, R. A., Private Communication, General Motors Electro Motive Division, 1981.

46. Barsom, J. M., "Fatigue-Crack Propagation in Steel of Various Yield Strengths", J. Eng. Ind., Vol. 93, No. 4, 1971

47. Maddox, S. J., " Fatigue Crack Propagation Data Obtained from Parent Plate, Weld Metal and HAZ in Structure Steel," Brit. Weld. Inst. Report No. E/37/70, 1970

48. Chen, W.-C., and Lawrence, F. V., "A Model for Jointing the Fatigue Crack Initiation and Propagation Analysis," Report to Fracture Control Program, Report No. 32, University of Illinois, Urbana, Ill. 1979.

49. Chang, S. T., Private Communication, Dept. of Metallurgical Engineering, University of Illinois, 1982,

50. Usami, S., Kusumoto, S., Kimoto, H. and Kawakami, M., "Effects of Crack Length and Flank Angle Size on Fatigue Strength at Toes of Mild steel Welded Joint", Trans. Japan Weld. Society Vol. No. 1 1978.

51. BS153, Design and Construction, Part 4. Stress, Part 3B, British Standard Institution.

52. BS5400, British Standard Institution. Also, Gurney, T. R. "Some Factors Affecting Design Stress", Chap. 14, Fatigue of Welded Structure, Camgridge University Press, Cambridge, England, 1978.

53. Ho, N.-J., Lawrence, F. V. and Altstetter, C. J.," Fatigue Resistance of Plasma and Oxygen Cut Steel", Weld. J. Vol. 60 No. 11, p213s, 1981.

54. Maddox, S. J., "Assessing the Significance of Flaws in Welds subjec to Fatigue," Weld. J. vol. 53, p. 401s-409s, 1974

55. El Haddad, M. H., Topper, T. H. and Smith, I. F. C., "Fatigue life Prediction of Welded Components Based on Fracture Mechanics", J. of Testing and Eval., Vol. 8, No. 6, p. 301, 1980.

56. El Haddad, M. H., Dowling, N. E. and Smith, K. N., "J Integral Applications for Short Fatigue Cracks at Notches", Int. J. of Fracture, Vol. 16, No. 1, p. 15, 1980.

57. El Haddad, M. H., Smith, K. N. and Topper, T. H. "A Strain Based Intensity Factor Solution for Short Fatigue Crack Initiating from Notches", ASTM STP 677, American Society for Testing and Materials, 1979.

58. McEvily, A. J., "Current Aspects of Fatigue", presented at Fatigue, 1977 Conference, Unversity of Cambridge, p. 1, 1977.

59. Smith, I. F. C. and Smith, R. A., "Fatigue Crack Growth in a Fillet Welded Joint", Eng. Frac. Mech., to be published.

60. Hartman, A. and Schjive, J., "The Effects of Environment and Load Frequency on the Crack Propagation Law for Macrofatigue Crack Growth in Aluminum Alloys", Eng. Frac. Mech. Vol. 1. No. 4, p. 615-631, 1970.

61. Smith, R. A. and Miller, K. J., "Fatigue Cracks at Notches", Intl. J. Mech. Sci. Vol. 19, p. 11-12, 1977.

62 Smith, I. F. C. and Smith, R. A., "Defects and Crack Shape Development in Fillet Welded Joints", Fatigue of Eng. Matl. and Struc., to be published.